
Electronic Thesis and Dissertation Repository

11-13-2018 8:00 AM

Revision Total Knee Arthroplasty using a Novel 3D Printed Titanium Augment: A Cadaveric Biomechanical Study

Charles-Antoine Dion, *The University of Western Ontario*

Supervisor: Lanting, Brent, *The University of Western Ontario*

Co-Supervisor: Willing, Ryan, *The University of Western Ontario*

Co-Supervisor: Howard, James L., *The University of Western Ontario*

A thesis submitted in partial fulfillment of the requirements for the Master of Science degree in Surgery

© Charles-Antoine Dion 2018

Follow this and additional works at: <https://ir.lib.uwo.ca/etd>



Part of the [Orthopedics Commons](#)

Recommended Citation

Dion, Charles-Antoine, "Revision Total Knee Arthroplasty using a Novel 3D Printed Titanium Augment: A Cadaveric Biomechanical Study" (2018). *Electronic Thesis and Dissertation Repository*. 5842. <https://ir.lib.uwo.ca/etd/5842>

This Dissertation/Thesis is brought to you for free and open access by Scholarship@Western. It has been accepted for inclusion in Electronic Thesis and Dissertation Repository by an authorized administrator of Scholarship@Western. For more information, please contact wlsadmin@uwo.ca.

Abstract

During revision total knee arthroplasty (rTKA), proximal tibial bone loss is frequently encountered and can result in a less-stable bone-implant fixation. A 3D printed titanium augment that conforms to the irregular shape of the proximal tibia was recently developed. The purpose of this study was to evaluate the fixation stability of rTKA with this augment in comparison to conventional cemented rTKA.

Fixation stability testing was conducted on eleven pairs of thawed fresh-frozen cadaveric tibias (22 tibias) after primary and revision TKA. During the loading protocol, the bone-implant micromotion was measured using a high-resolution optical system.

There was significantly less micromotion in the experimental rTKA in comparison to the standard fully cemented rTKA ($p= 0.04$). The novel 3D printed titanium augment offers better fixation in rTKA that would be sufficient for bony ingrowth of the augment in vivo.

Keywords

3D printed, additive manufacturing, titanium, total knee arthroplasty, total knee replacement, revision, surgery, orthopaedic, micromotion, fixation stability, biomechanics, cadaveric, anatomy, press-fit, optical system, digital image correlation, FARO Gage arm, VIVO AMTI, porous, novel, augment, tibia, loosening, cement, cementless.

Co-Authorship Statement

Dr. Brent Lanting: Designed the novel 3D printed augment, supervised day-to-day activities, contributed to study design, reviewed and revised manuscript.

Dr. Ryan Willing: Supervised day-to-day activities, contributed to study design, data analysis, reviewed and revised manuscript.

Dr. James Howard: Designed the novel 3D printed augment, contributed to study design, reviewed and revised manuscript.

Dr. Matthew Teeter: Contributed to study design and assisted with implant retrieval required for primary and revision surgery.

Mr. Michael Pollock: Contributed to data collection for the systematic review in chapter 2.

Dr. Lyndsay Somerville: Contributed to data analysis for the systematic review in chapter 2.

Mr. Geoffrey Yamomo: Provided assistance with day-to-day activities, data collection, data analysis and interpretation of micromotion measurements.

Acknowledgments

I would like to sincerely thank a number of individuals that were key contributors to my success throughout my graduate studies. First and foremost, I'd like to show my deepest gratitude towards **Dr. Brent Lanting**. You have devoted numerous hours away from family to teach me and support me as a scientist and as a surgical resident. Even with your busy schedule, you made time to guide me and make sure I was on the right path. Thank you for challenging me and believing in me. I will cherish the lessons I have learned from you. I am very fortunate to have you as a mentor.

Furthermore, I'd like to acknowledge my research committee members. **Dr. Ryan Willing**, your support was crucial to my success. You were always available during testing and had a solution to every problem. Thank you for teaching me how to think critically and making me a better researcher and presenter. **Dr. Teeter and Dr. Howard**, your overall support and advice during my studies helped me immensely.

I would also like to acknowledge my amazing lab partner, **Geoffrey Yamomo**. It was a daily occurrence to spend over 16 hours in the University Hospital Orthopaedic Biomechanics Laboratory (UHOB-L) during the testing period. Your devotion and perseverance are exemplary.

I'd like to thank **my brother, Pierre-Marc Dion and my parents** for supporting me during my endless studying and academia. Your love and support have made me overcome every obstacle I have encountered in life.

Finally, I'd like to thank anyone that wasn't mentioned that supported me and helped me achieve my goals.

Dedication

To Jean-Pierre Dion and Danielle Courtemanche,

You have supported me my entire life and helped me pursue my dreams.

Table of Contents

Abstract	i
Co-Authorship Statement	ii
Acknowledgments	iii
Dedication	iv
Table of Contents	v
List of Abbreviations	ix
List of Tables	x
List of Figures	xi
List of Appendices	xiv
CHAPTER 1	1
1 Introduction	1
1.1 Osteoarthritis of the Knee	1
1.2 Anatomy and Biomechanics of the Knee	6
1.2.1 Anatomy of proximal tibia	10
1.2.2 Knee joint kinematics and alignment	11
1.3 Total Knee Arthroplasty	17
1.3.1 Description of procedure	18
1.3.2 Implantation Techniques	21
1.3.3 Implant Loading	23
1.4 Revision Total Knee Arthroplasty and 3D Printing	23
1.5 Study Rationale	24
1.6 Specific Objectives and Hypotheses	25
1.7 Thesis Overview	26
1.8 References	28

2	Surgical outcomes of 3D printed musculoskeletal metal implants: A systematic review	36
2.1	Introduction	36
2.2	Materials and Methods	39
2.3	Results and Discussion	42
2.4	Conclusion	50
2.5	References	51
CHAPTER 3		57
3	Measuring micromotion: A comparative study between the FARO arm and the digital image correlation system	57
3.1	Introduction	57
3.2	Materials and Methods	59
3.2.1	FARO Gage Arm Measurements	60
3.2.2	DIC System Measurements	61
3.3	Results	62
3.4	Discussion	65
3.5	Conclusions	67
3.6	References	67
CHAPTER 4		70
4	Quantifying the magnitude and direction of micromotion in primary total knee arthroplasty	70
4.1	Introduction	70
4.2	Materials and Methods	71
4.2.1	Primary TKA technique	72
4.2.2	Testing protocol	73
4.3	Results	74
4.3.1	Vertical (Axial) micromotion	74
4.3.2	Horizontal or transverse micromotion	75

4.4	Discussion	76
4.4.1	Limitations	78
4.5	Conclusions	79
4.6	References	79
CHAPTER 5		83
5	Revision total knee arthroplasty using a novel 3D printed titanium augment: A biomechanical cadaveric study.	83
5.1	Introduction	83
5.1.1	Revision total knee arthroplasty and tibial bone loss	86
5.1.2	Purpose and hypothesis	90
5.2	Materials and Methods	90
5.2.1	Novel augment design and printing	90
5.2.2	Experimental method	91
5.2.3	Description of the equipment	94
5.2.4	Surgical techniques	101
5.3	Results	105
5.3.1	Comparison of specimens prior to rTKA	106
5.3.2	Comparison of specimens after revision TKA	107
5.4	Discussion	112
5.4.1	Limitations of the study	115
5.5	Conclusions	117
5.6	References	117
CHAPTER 6		126
6	Conclusion	126
6.1	Conclusion	126
6.2	Future Directions	126

Bibliography	128
Appendices	149
Curriculum Vitae	158

List of Abbreviations

3D	Three dimensional
μ	micro
μm	micrometer
ANOVA	analysis of variance
CAD	computer-aided design
DIC	digital image correlation
EBM	Electron Beam Melting
g	grams
Hz	Hertz (unit of frequency)
N	Newton (unit of force)
p	Probability value
PMMA	Polymethylmethacrylate
pixel	pixel element
pTKA	Primary Total Knee Arthroplasty
rTKA	Revision Total Knee Arthroplasty
SD	Standard deviation
SLM	Selective Laser Melting
TKA	Total Knee Arthroplasty

List of Tables

Table 2.1. Inclusion and Exclusion Criteria.....	40
Table 2.2. Data extraction.....	42
Table 2.3. Study characteristics	48
Table 3.1. Mean axial micromotion measurements of the tibial component bone-implant interface in primary TKA (rTKA) and revision TKA (rTKA) using the FARO Gage Arm and the digital image correlation system (DIC).....	62
Table 4.1. Significance of differences in vertical micromotion between anterior, medial and posterior-lateral micromotion. <i>Post hoc</i> Mann-Whitney U test with Bonferroni correction.....	75
Table 4.2. Vertical and horizontal micromotion (μm) pre and post-cycle.....	76
Table 5.1. Eleven fresh-frozen cadaveric pairs of tibias (22 tibias) used for biomechanical testing.	105
Table 5.2. Vertical micromotion (Post-cycle).....	110
Table 5.3. Transverse micromotion (Post-cycle).....	111

List of Figures

Figure 1.1. Radiographic representation of knee OA.	2
Figure 1.2. X-ray of a total knee replacement.	6
Figure 1.3. Extensor lever arm created by the extensor mechanism (patellar tendon, patellar and quadriceps tendon/muscle). “J” shaped curve of the center of rotation of the knee. Original drawing by author.	7
Figure 1.4. Anatomy of the knee. Image obtained from: Drake, R., Vogle, A., Mitchell, A. (2015). Gray’s Anatomy for Students, 3 rd Edition. (<i>Copyright approval license number: 4396780051808</i>)	9
Figure 1.5. Six degrees of freedom of the knee joint. Image modified from original obtained from: Drake, R., Vogle, A., Mitchell, A. (2015). Gray’s Anatomy for Students, 3 rd Edition. (<i>Copyright approval license number: 4396780051808</i>)	11
Figure 1.6. Mechanical, anatomic and vertical axis of the lower extremity. Mechanical Axis of Femur (MAF); Mechanical Axis of Tibia (MAT). Image modified from original obtained from: Drake, R., Vogle, A., Mitchell, A. (2015). Gray’s Anatomy for Students, 3 rd Edition. (<i>Copyright approval license number: 4396780051808</i>)	14
Figure 1.7. Components and bone cuts of a total knee arthroplasty. Reproduced with permission from (Leopold, 2009), Copyright Massachusetts Medical Society.	17
Figure 1.8. Mechanical, anatomic and joint surface angle after total knee replacement. Image modified from original obtained from: Drake, R., Vogle, A., Mitchell, A. (2015). Gray’s Anatomy for Students, 3 rd Edition. (<i>Copyright approval license number: 4396780051808</i>)	19
Figure 1.9. Posterior condylar axis (red), posterior femoral cut (orange) and proximal tibial cut (blue). This creates a box cut during total knee arthroplasty resulting in 3 degrees of external rotation prior to the insertion of the femoral implant. Original drawing by author.....	20
Figure 2.1. Schematic representation of electron beam melting, a type of Metal-based additive manufacturing (Prabhakar, Sames, Dehoff, & Babu, 2015).....	37

Figure 2.2. Workflow of 3D printing	38
Figure 2.3. Flow diagram summarizing the identification, screening and data collection of relevant articles.	41
Figure 2.4. Picture and x-ray of 3D printed glenoid metal augment implanted during revision total shoulder arthroplasty with severe glenoid bone defect (Stoffelen, Eraly, & Debeer, 2015)	43
Figure 2.5. Picture and x-ray of 3D printed acetabular metal augment implanted during revision total hip (Wong et al., 2015)	50
Figure 5.1. Example of TKA removal with failure of the cement-bone interface (left) vs. the cement-implant interface (right). Image taken from (Schlegel, Bishop, Püschel, Morlock, & Nagel, 2014): copyright SICOT-J under the Creative Commons license.	84
Figure 5.2. Anderson Orthopaedic Research Institute (AORI) tibia bone defect classification. Image taken from (Panegrossi et al., 2014): copyright SICOT-J under the Creative Commons license. ...	85
Figure 5.3. Zones of fixation during revision TKA.	86
Figure 5.7. Optical tracking system hardware	97
Figure 5.9. Volumetric measurement of bone defect after removal of primary TKA. Illustration of sawbones used during preliminary testing.....	99
Figure 5.12. Tools used for shaping and insertion of 3D printed revision tibial augment	104
Figure 5.14. Bone-implant vertical micromotion during post-cycle loading of primary and revision TKAs. Error bars represent standard error.....	108
Figure 5.15. Bone-implant transverse micromotion during post-cycle loading of primary and revision TKAs. Error bars represent standard error.....	109
Figure 5.16. Volume of the proximal tibial bone defect after explantation of the primary and revision TKAs. Error bars represent standard error.....	110

Figure 5.18. Photographs of the proximal tibial fracture during isolated augment loading (left) and resultant open reduction internal fixation. 116

List of Appendices

Appendix 1. REB approval..... 150

Appendix 2. Chapter 2 Search Strategy	151
Appendix 3. Chapter 2 Article Summary	154

CHAPTER 1

1 Introduction

Overview: This chapter familiarizes the reader with basic concepts that are needed to fully understand and appreciate this thesis. It goes over degenerative joint disease, knee anatomy, biomechanics, and joint replacement principles. It also goes over the study rational and an overview of the thesis.

1.1 Osteoarthritis of the Knee

Osteoarthritis (OA) is the irreversible and progressive degeneration of the articular surface of joints. It is the most common form of arthritis and a leading cause of chronic disability in the world. It is characterized by joint pain and stiffness leading to functional decline and loss of quality of life (F. Xie, Thumboo, & Li, 2007). The hip and knee are amongst the most symptomatic joints affected by OA (Bierma-Zeinstra & Koes, 2007). The risk of mobility impairments from knee arthritis is greater than any other medical condition in people over 65 years old (Guccione et al., 1994). The lifetime risk of developing symptomatic knee OA is 45%, rising to over 60% in obese individuals (Murphy et al., 2015) with an estimated 43 million people affected in the United States alone. The estimated prevalence of knee OA in Canada is proportionally similar to the United States with a prevalence of 48.7% of Canadians 65 years and older affected by knee OA (Macdonald, Sanmartin, Langlois, & Marshall, 2014). Moreover, recent studies are predicting a substantial increase in the incidence of OA secondary to demographic changes, which will lead to increased socioeconomic and personal burden

(Egloff, Hügle, & Valderrabano, 2012). Therefore, an understanding of the pathophysiology, diagnosis and treatment of this disease is required to do further research in this domain in the hope of decreasing its burden on society.

The pathology behind OA varies and can include focal damage and loss of articular cartilage, abnormal remodeling, sclerosis of subarticular bone, osteophytes (bone spurs), ligamentous laxity, weakening of muscles and synovial hyperplasia (Arden & Nevitt, 2006). Radiographically, it is described as joint space narrowing, osteophytes, subchondral sclerosis and the presence of subchondral cysts called geodes. Histologically, it is depicted by early fragmentation of the joint surface, cloning of chondrocytes, variable crystal deposition, remodeling and eventually violation of the chondral surface by blood vessels (Pereira, Ramos, & Branco, 2015).

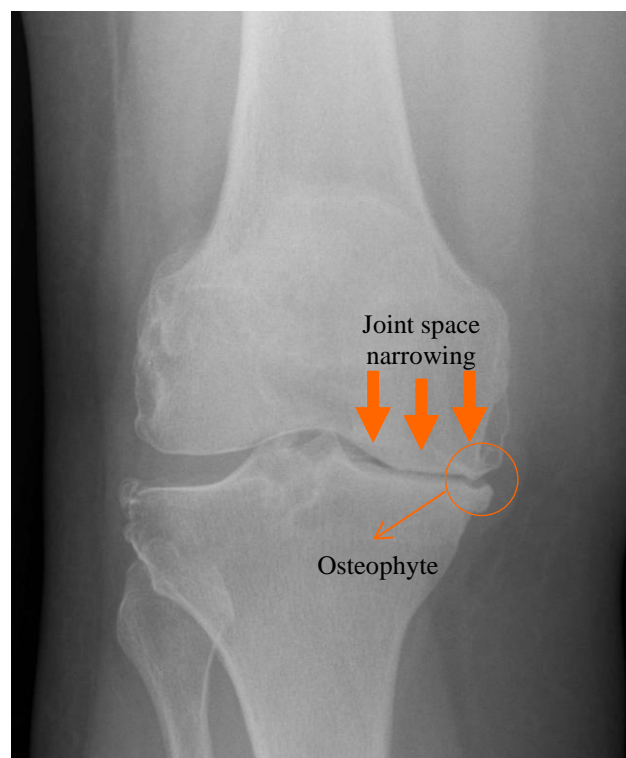


Figure 1.1. Radiographic representation of knee OA.

The etiology of OA is fairly complex and multi-factorial. OA is thought to be secondary to structural, mechanical and biological processes. It may evolve as a consequence of intraarticular fractures, ligament lesions, systemic diseases like rheumatoid arthritis and

haemophilia, post infectious arthritis, osteochondritis dissecans or anatomic abnormalities (Egloff et al., 2012). Normal adult articular cartilage is made up of extracellular matrix (water, collagen, proteoglycans) and chondrocytes (Goldring & Marcu, 2009). Chondrocytes mediate the turnover of the extracellular matrix. OA is a consequence of chondrocytes failing to maintain homeostasis between the synthesis and degradation of these extracellular matrix components (Man & Mologhianu, 2014). Chondrocytes are influenced by a number of chemical and physical stimuli. Therefore, any stimuli causing disruption of chondrocyte activity can cause or accelerate the rate of osteoarthritis. Blasioli et al. described the OA disease perpetuation catabolic cycle. First, pro-inflammatory cytokines (IL-1, IL-6, TNF-alpha) are released secondary to an intraarticular insult. Second, pro-inflammatory cytokines bind to chondrocyte receptors leading to release of degradative enzymes (metalloproteinases) and inhibition of chondrocyte activity resulting in decrease collagen production and increase in extracellular matrix degeneration. Third, matrix fragments are engulfed by macrophages that release further pro-inflammatory cytokines. This creates a vicious cycle resulting in cartilage degradation. (Blasioli & Kaplan, 2014).

The risk factors for OA may vary for different joints. Twin studies have established that OA is largely determined by genetic predisposition and newer studies have yielded the discovery of genes containing OA-associated variants (Loughlin, 2005). Nevertheless, age is the strongest predictor of OA progression and development. OA affects mostly the middle-aged and older population demographic. Prior to the age of 40, the incidence is lower and occurs mostly secondary to trauma (Arden & Nevitt, 2006). The physiologic changes seen with aging makes the joint vulnerable to joint damage and degradation. Histologic studies have shown age-related decrease in chondrocytes' ability to maintain and repair tissue; decrease in mitotic and synthetic activity (Abramson & Attur, 2009). With age, the water content of cartilage increases and the proteoglycan content decreases. This weakens the collagen network and makes cartilage prone to degradation. Other risk factors that have been identified and include obesity, female sex, high intensity sporting activities, menopause, occupational risk factors such as repetitive joint loading and knee bending and joint incongruity (ie dysplasia) or malalignment (Bierma-Zeinstra & Koes, 2007).

The diagnosis of symptomatic OA is made when both clinical and radiographic evidence of OA are present. Nevertheless, there is discordance between knee pain and the radiographic severity of OA. Radiographic knee OA is an imprecise guide to the likelihood of knee pain and therefore should not be used in isolation when assessing and treating patients with knee OA (Bedson & Croft, 2008).

After diagnosing symptomatic OA, the first step in treating it is to educate the patient about modifiable risk factors that can be changed in order to slow down the progression of OA. The Osteoarthritis Research Society International (OARSI) (Zhang et al., 2010) and the American Academy of Orthopaedic Surgery (AAOS) (Jevsevar, 2013) summarized the treatment strategies for hip and knee OA in their evidence-based guidelines. The goal of treatment is to reduce pain, improve function and quality of life. The AAOS treatment recommendations with strength of recommendations (SOR) are summarized below:

- Recommended:
 - Self-management programs, strengthening and low-impact aerobic exercises and neuromuscular education, nonsteroidal anti-inflammatory drugs (NSAIDs) (oral or topical) and tramadol. (SOR strong)
 - Weight loss for patients with symptomatic knee OA and a body mass index (BMI) > 25 (SOR moderate)
- Not recommended:
 - Acupuncture, glucosamine, chondroitin, Intra-articular injection of hyaluronic acid (HA)/ viscosupplementation (SOR strong)
 - Lateral wedge insoles (SOR moderate)
- In-conclusive:
 - Electrotherapy, manual therapy, valgus-directing force brace, acetaminophen, opioids, intra-articular injection of corticosteroids and for knee OA, growth factor and platelet rich plasma (PRP) injections in knee OA

Again, there are conflicts between the AAOS and the OARSI guidelines. OARSI recommends acetaminophen and opioids for effective pain relief of OA. They also mention that intra-articular injections of corticosteroids are highly effective for pain relief for a four-week period. A single injection was not effective after 4 weeks and multiple repeated injections stopped being effective after 2 years. It would nevertheless be appropriate during OA flare-ups to give a corticosteroid injection to achieve adequate pain relief (Zhang et al., 2010). Furthermore, while current AAOS guidelines do not recommend it, more recent systematic reviews have shown that viscosupplementation, also known as intra-articular injections of HA, may be an effective treatment or adjunct to recommended non-operative treatments of OA. The concept behind viscosupplementation is that HA is a major component of synovial fluid and helps facilitate lubrication and shock absorption in joints. In OA, there is a decrease in molecular weight (MW) of HA leading to a reduction in its viscoelastic properties (Leighton et al., 2018). By injecting high MW HA into the joint, one would theoretically replenish these viscoelastic properties.

As for surgical treatments prior to joint replacement, there is evidence that a valgus high tibial osteotomy reduces pain and improves knee function in patients with medial compartmental OA of the knee (Brouwer et al., 2005). Conversely, arthroscopic debridement in knee OA has been shown to have no benefits (Kirkley et al., 2017; I. Wong et al., 2018; Laupattarakasem, Laopaiboon, Laupattarakasem, & Sumananont, 2008).

Since OA is not reversible, the goal of early treatment is to delay the need for joint replacement surgery. Joint replacements have a limited implant survivorship and inevitably fail with time. Therefore, surgery needs to be delayed in order to make sure a joint replacement will last a patient's lifetime and thus preventing the need for revision surgery, which is known to have increased risks, have inferior post-operative outcomes and lower patient satisfaction (J. Cherian, Bhave, Harwin, & Mont, 2016).

In summary, osteoarthritis poses a substantial burden on society. One in two Canadians will develop knee OA in their lifetime (Macdonald et al., 2014). OA is associated with remarkable costs to both the patients and their community. The cost of illness (COI) is defined as the sum of direct (cost of treatment), indirect (productivity loss) and intangible (patient

suffering) costs. In Canada, the annual direct cost of OA per patient is \$2878. In contrast, the annual indirect cost of OA per patient is much higher at \$9847 (F. Xie et al., 2007). The only effective treatment that reduces pain and restores function for end-stage knee OA is total knee arthroplasty (TKA) (refer to figure 1.2). The high indirect cost of knee OA in Canada reflects the population's impaired ability to work or engage in usual activities secondary to OA. This might be a result of long waiting lists and delayed access to TKA in Canada. With the expected substantial increase in both the prevalence and incidence of OA secondary to the aging population, the increase in life expectancy, as well as the increased rate of obesity, it is imperative that we continue to improve the treatments of OA such as total knee arthroplasty.



Figure 1.2. X-ray of a total knee replacement.

1.2 Anatomy and Biomechanics of the Knee

The knee is the largest synovial joint in the human body. It is considered a trochoginglymos, meaning a gliding hinge joint (Hirschmann & Müller, 2015). Its main roles are to allow locomotion with minimum energy requirements and transmit, absorb and

redistribute forces experienced during activities of daily living (Masouros, Bull, & Amis, 2010). It comprises of two distinctly separate joints. First, it contains the articulation between the femur and tibia called the tibiofemoral joint (refer to figure 1.4), which is weight bearing. Second, the articulation between the patella and femur, called the patellofemoral joint, allows for the pull of the quadriceps to be anterior to the femur during knee extension. It is referred as the extensor mechanism and serves as a lever arm making knee extension more biomechanically efficient (refer to figure 1.3). The articular surface of the knee is covered with hyaline cartilage. In the orthopaedic literature, the knee is subdivided into three compartments in order to describe what parts of the knee are affected by osteoarthritis. The compartments include the patellofemoral joint, the medial part of the tibiofemoral joint (medial compartment) as well as the lateral part of the tibiofemoral joint (lateral compartment).

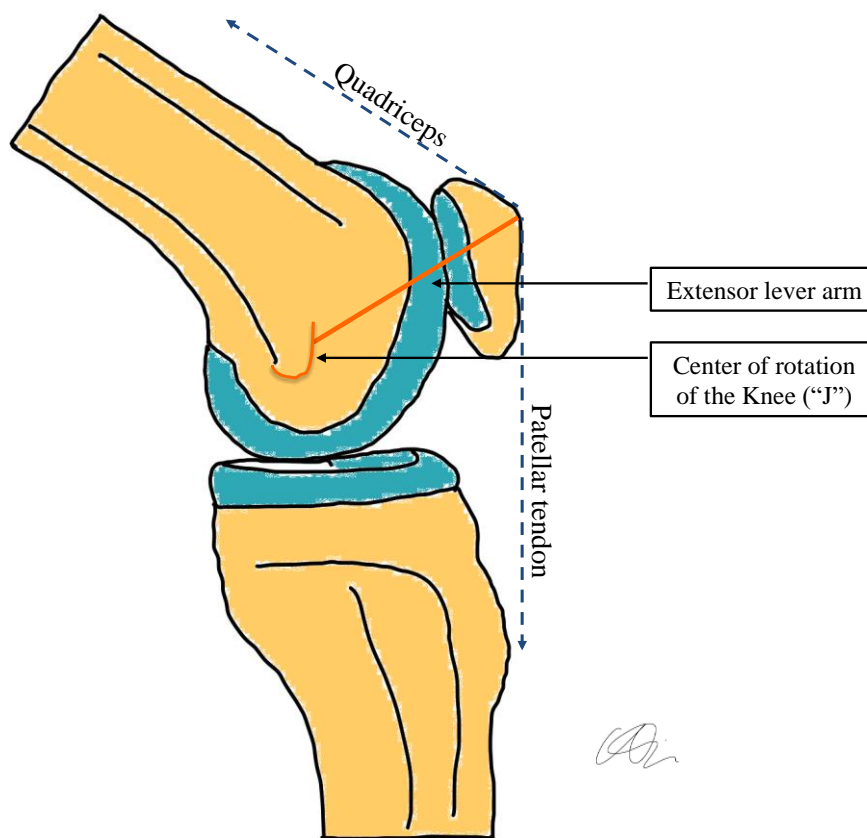


Figure 1.3. Extensor lever arm created by the extensor mechanism (patellar tendon, patellar and quadriceps tendon/muscle). “J” shaped curve of the center of rotation of the knee. Original drawing by author.

The overall stability of the knee is a result of the static stability created by the geometry and anatomy of the joint surface, the active stability produced by muscle contraction as well as the passive stability from the ligaments, menisci, capsule and retinacula (Masouros et al., 2010).

The four major ligaments of the knee are the two collateral ligaments present on each side of the knee called the medial (tibial) collateral ligament (MCL) and the lateral (fibular) collateral ligament (LCL) as well as the two cruciate ligaments, the anterior cruciate ligament (ACL) and the posterior cruciate ligament (PCL) found in the central inter-condylar notch (refer to figure 1.3). The LCL attaches to the lateral femoral epicondyle and the fibular head. The LCL is tight in extension and loose in flexion. It is a dynamized ligament meaning that the contraction of the biceps femoris muscle actively tightens the LCL for additional stability (Hirschmann & Müller, 2015). The MCL attaches to the medial femoral epicondyle and to the medial surface of the proximal tibia behind the pes anserinus (Drake, Vogl, & Mitchell, 2015). The MCL is tight in extension and external rotation, and loose in flexion and internal rotation. The collateral ligaments resist rotation, and valgus and varus stresses keeping the knee aligned in the coronal plane. The joint capsule is made up of an external fibrous layer and an internal synovial layer that covers the joint and serves as a barrier to keep the synovial fluid inside and everything else outside. It also contributes to passive stability of the joint such as valgus and varus stability.

The term “cruciate” means “shape of a cross” in latin; and describes the anatomy of the ACL and PCL, which cross in the middle of the knee. The ACL originates from the posteromedial corner of the lateral femoral condyle in the intercondylar notch and inserts into the medial tibial eminence just lateral to the anterior horn of the medial meniscus. The ACL prevents excessive anterior translation and rotation of the tibia relative to the femur. Furthermore, the ACL is composed of the anteromedial bundle, which is tight in flexion and the posterolateral bundle that is tight in extension. The PCL originates from the anterolateral aspect of the medial femoral condyle and inserts posteriorly and inferiorly to the posterior aspect of the tibial plateau (extra-articular). The PCL restrains the knee by limiting posterior translation of the tibia relative to the femur. The PCL’s anterolateral bundle is tight in flexion and its posteromedial bundle is tight in extension.

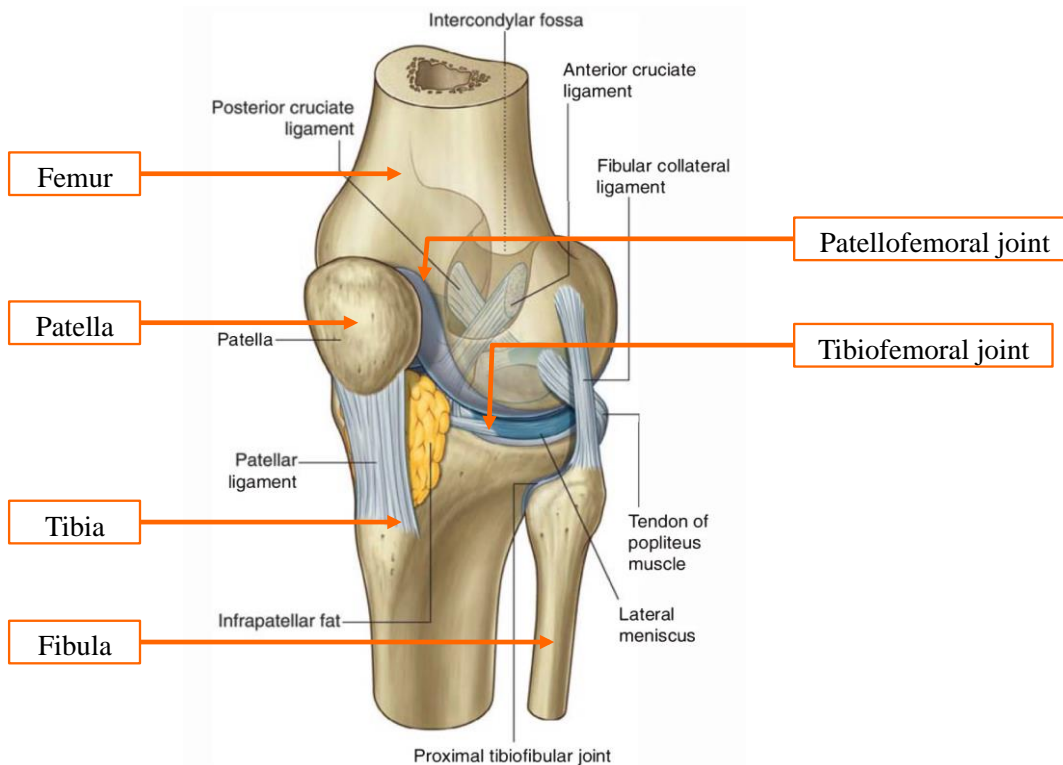


Figure 1.4. Anatomy of the knee. Image obtained from: Drake, R., Vogle, A., Mitchell, A. (2015). *Gray's Anatomy for Students*, 3rd Edition. (Copyright approval license number: 4396780051808)

Dynamic stability is achieved with 4 main muscle groups: the quadriceps, the hamstring, the adductors (gracilis) and the gastrocnemius. Furthermore, the popliteus is another muscle contributing to knee stability and is considered both a dynamic and passive stabilizer. It dynamically stabilizes the lateral knee compartment and its three tendon arms act as a static or passive stabilizer to external rotation (Hirschmann & Müller, 2015). Similarly, the iliotibial tract (IT band) is also a dynamic and passive stabilizer of the lateral knee compartment. It originates as a thickening of the lateral aspect of the tensor fascia latae that attaches to the iliac crest and inserts into the Gerdy's tubercle. It is an anterolateral stabilizer of the knee joint.

Two fibrocartilagenous menisci in the shape of crescentic pads, which lie on top of the tibial plateau, serve as shock absorbers and accommodate the shape of the articular surface of the femoral condyles. During articular movement of the tibiofemoral joint, the menisci make the joint more congruent. Both menisci are fixed to the joint capsule peripherally and the anterior/posterior roots are fixed to the tibial plateau. The anterior roots are connected by the transverse ligament. The medial meniscus is also connected to the medial collateral ligament and the posterior oblique ligament. The menisci move with the femoral condyles during knee flexion and extension. The lateral meniscus is more mobile than the medial meniscus based on the larger posterior translation of the lateral condyle during knee flexion. The posterior horn of the lateral meniscus is attached to the distal femur by the anterior menisiofemoral ligament (AMFL or ligament of Humphrey) and the posterior menisiofemoral ligament (PMFL or ligament of Wrisberg).

1.2.1 Anatomy of proximal tibia

The tibia is the medial and larger of the two bones in the lower leg. The structure of the tibia is made up of cancellous bone inside and cortical bone outside. The cancellous bone called the subchondral bone is strongest cancellous bone and is located under the chondral surface of the tibia. Its proximal end expands into two condyles called the medial and lateral tibial plateau. The two tibial plateaus overhang the shaft and are separated by an intercondylar region that contains tibial eminences that are sites of attachment of the cruciate ligaments and the menisci. The medial condyle is larger than the lateral condyle. The medial tibial plateau is concave, oval and lies on top of the the tibial shaft in comparison to the lateral plateau that is circular, more convex and overhangs laterally in relation to the tibial shaft. The tibial tubercle is an apophysis located on the anterior aspect of the tibia below the joint line and serves as an attachment for the patellar ligament or tendon, which is a continuation of the quadriceps tendon below the patella. The shaft of the tibia is triangular (cross section) with the anterior border being the tip of the triangle. The proximal tibia also articulates with the proximal fibula forming the proximal tibiofibular joint (refer to figure 1.3).

1.2.2 Knee joint kinematics and alignment

Knee joint kinematics is fairly complex. The tibiofemoral joint is simplified as a hinge-like joint that permits motion in the sagittal plane; however, it actually has 6 degrees of freedom described as 3 translations and 3 rotations. Translational movement of the tibia relative to the femur is possible in medial-lateral and anterior-posterior directions as well as by compression and distraction. Rotational movement of the tibia relative to the femur are achieved in the coronal (abduction/adduction), sagittal (flexion/extension) and vertical axes (refer to figure 1.5) (Mihalko, 2013).

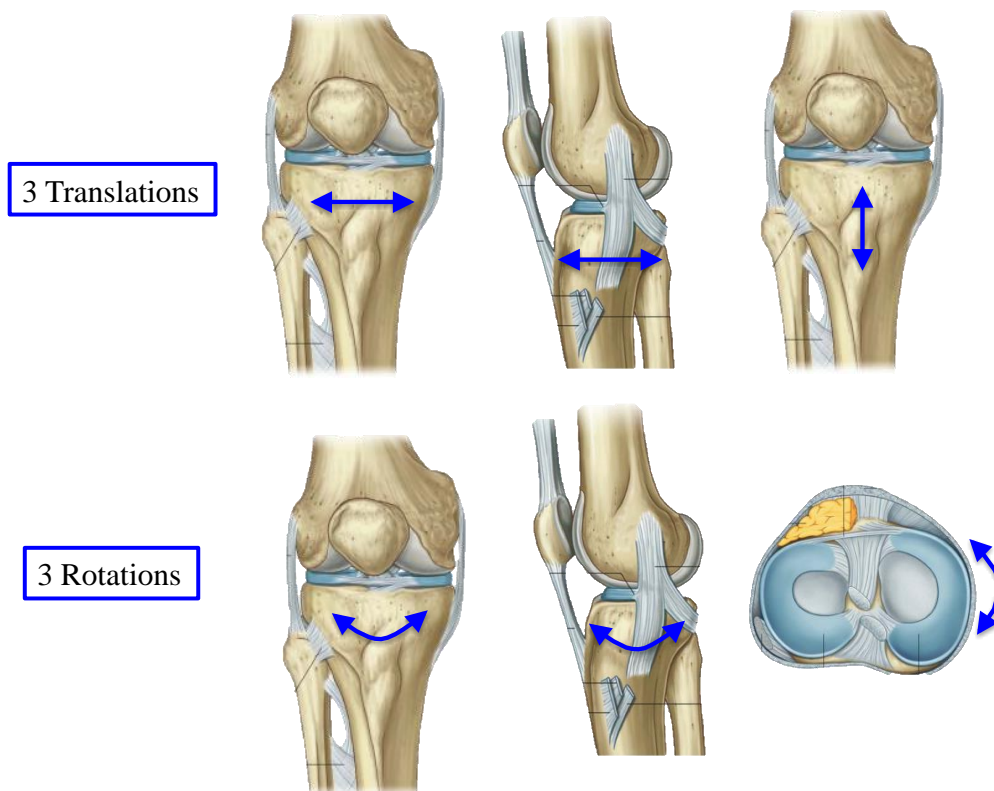


Figure 1.5. Six degrees of freedom of the knee joint. Image modified from original obtained from: Drake, R., Vogle, A., Mitchell, A. (2015). *Gray's Anatomy for Students*, 3rd Edition. (Copyright approval license number: 4396780051808)

1.2.2.1 Knee kinematics, femoral rollback and the screw home mechanism

The kinematics of the knee is sometimes described as tibial or femoral motion relative to the other. This depends on whether the knee is fixed due to weight bearing or free to move.

For simplicity's sake, we will always refer to knee kinematics in a weight-bearing scenario and will therefore be referring to femoral motion relative to the tibia. At full extension, the femur is internally rotated with respect to the tibia and is located anterior to the mid-point of the tibial plateau (Zingde & Slamin, 2017). As the knee flexes, both the lateral and medial femoral condyles translate posteriorly. This is called "femoral rollback" and is created partly by the action of the PCL. Femoral rollback moves the center of rotation of the femur posteriorly and allows for increased knee flexion. The center of rotation of the femur persistently moves during knee flexion secondary to the ellipsoidal shape of the femoral condyle and the translation/rotation of the condyles during knee flexion. The movement of the centre of rotation of the femur is described as a "J" shaped centre of rotation (refer to figure 1.3). Moreover, the longitudinal axis of rotation of the knee is based in the medial compartment; therefore, the medial compartment has much less movement (translation) than the lateral compartment resulting in femoral external rotation during knee flexion. Previous cadaveric and in-vivo studies have determined that the lateral femoral condyle rolls back an average of 21 mm during knee flexion while the medial femoral condyle rolls back only 1.9 mm (Zingde & Slamin, 2017). Therefore, this results in an axial rotation of approximately 21 degrees from full extension to full flexion of the knee (Zingde & Slamin, 2017). As the knee goes into full extension, the femur experiences internal rotation, which tightens up all associated ligaments and locks the knee in extension. This is referred as the "screw-home mechanism" and is particularly important during standing and prior to heel strike during gait (Masouros et al., 2010).

1.2.2.2 **Locking mechanism**

As mentioned, the knee has a locking mechanism in extension. This facilitates prolonged standing and conserves energy. When the knee is fully extended, the body's center of gravity is located anterior to the knee joint; therefore, acting to keep the knee extended. The popliteus muscle unlocks the knee by initiating flexion and external rotation of the femur on the tibia transferring the center of gravity posterior to the knee joint (Drake et al., 2015).

1.2.2.3 **Functional range of motion**

Studies of the knee have defined functional ranges of motion (ROM) at the knee needed for activities of daily living. Normal gait requires 67 degrees of knee flexion during the swing phase, 83 degrees for stair climbing, 90 degrees for going down stairs, and 93 degrees to rise from a chair. Sitting or standing from a standard toilet required 115 degrees and more than 115 degrees is needed for advanced functions such as gardening (Mihalko, 2013).

1.2.2.4 **Alignment of the knee**

The alignment of the knee is assessed with the help of 3 axes. The vertical axis is a straight vertical line that extends distally from the center of the pubic symphysis. The mechanical axis of the lower extremities, also known as the load-bearing axis (Iseki et al., 2009), is determined by drawing a line from the center of the femoral head to the centre of the ankle joint. There is a 3 degree difference between the vertical axis and the mechanical axis. It can be further subdivided into the mechanical axis of the femur (MAF) that is drawn from the centre of the femoral head to the intercondylar notch of the distal femur as well as the mechanical axis of the tibia (MAT), which is illustrated in figure 1.6 as a line from the centre of the proximal tibia to the centre of the ankle. The anatomic axis (AA) is the axis defined by the longitudinal axis of the intramedullary canals of the femur and tibia. There is a 5-7 degree difference between the anatomic axis of the femur (AAF) and the MAF. The anatomic axis of the tibia (AAT) and the MAT are usually fairly similar.

The medial angle formed by the MAF and the MAT is called the hip-knee-ankle angle (HKA). A negative HKA represents a varus and a positive HKA represents a valgus alignment. In normal knees, HKA is neutral and close to 180 degrees. Another way to assess alignment is the mechanical axis deviation (MAD) defined as the distance between the load-bearing axis and the centre of the knee where medial and lateral MADs are referred as varus and valgus alignment (J. J. Cherian et al., 2014).

Moreover, a study by Bellmans et al. noted that 32% of men and 17% of women had constitutional varus knees with a natural mechanical alignment of 3 degrees of varus or more

(Bellemans, Colyn, Vandenneucker, & Victor, 2012). Constitutional varus knees predisposes people to have arthritic knees with medial compartment wear, which progressively worsens their varus alignment (Vandekerckhove et al., 2017). Nevertheless, normal neutral knees have approximately 1 degree of varus (neutral alignment is considered to be between -3 degrees and +3 degrees). Constitutional varus is defined as having a HKA angle of 3 degrees or more of varus angulation and a constitutional valgus as having a HKA angle of 3 degrees or more of valgus angulation (Bellemans et al., 2012). Furthermore, note that the normal joint line is naturally in 3 degrees of varus so that when the leg is positioned under the centre of mass, the joint line is parallel to the ground. Therefore, it is not surprising that the proximal tibia has 3 degrees of varus (refer to figure 1.6).

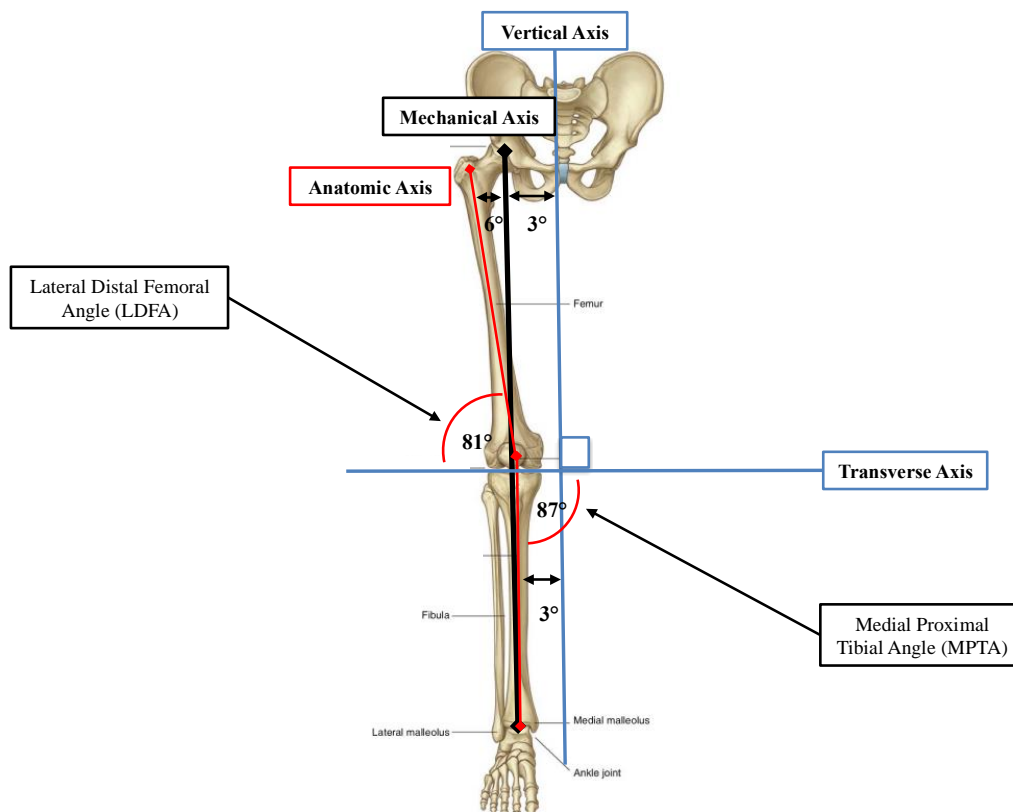


Figure 1.6. Mechanical, anatomic and vertical axis of the lower extremity. Mechanical Axis of Femur (MAF); Mechanical Axis of Tibia (MAT). Image modified from original obtained from: Drake, R., Vogle, A., Mitchell, A. (2015). Gray's Anatomy for Students, 3rd Edition. (Copyright approval license number: 4396780051808)

As for the sagittal alignment of the knee, both the posterior tibial slope (TS) and the distal femoral flexion angle (DFF) need to be considered. The tibial slope is defined as the angle between the proximal anatomic axis of the tibia and the tibial plateau in the sagittal plane (Helmy, Dao Trong, & Kühnel, 2014). Helmy et al. examined 113 knees and measured a tibial slope of 4.62 degrees +/- 2.76 with a range of -9 degrees to 10.5 degrees. The distal femoral flexion angle (DFF) is the distal femoral sagittal alignment in relation to the sagittal mechanical axis of the femur. A study by Hood et al. of nearly 2500 femurs found that the distal femoral flexion angle, was 2.90 degrees +/- 2 degrees (Hood et al., 2017).

1.2.2.5 **The gait cycle**

Bipedal walking is a repetition of a gait cycle that consists of 2 phases: the stance phase and the swing phase. The stance phase accounts for 60% of the gait cycle while the swing phase is 40% of the cycle. First, the stance phase starts off with heel strike, the initial contact where the foot touches the ground, and establishes double support (two feet on the ground). The ankle moves from neutral position to plantar flexion with an eccentric contraction of the tibialis anterior. Second, the flat foot or loading response phase starts as the body absorbs the impact of the foot by rolling in pronation. The knee flexes and the hip extends with the help of the adductor magnus (adductor moment) and gluteus maximus. Third, in the midstance phase, the knee reaches maximum flexion, the ankle dorsiflexes and supinates, with a single leg support. Fourth, heel off begins as the heel leaves the floor and the ankle plantar flexes and supinates. Then, toe off marks the beginning of the swing phase as the foot leaves the ground. During the swing phase, the knee flexes initially to clear the ground and goes into locked extension in the late swing in preparation for heel strike (Kharb, Saini, Jain, & Dhiman, 2011). During the gait cycle, the knee joint experiences dynamic loading conditions that affect both the tibiofemoral and patellofemoral joints.

1.2.2.6 **Knee joint loading**

One of the main functions of the knee joint is to transmit load. Three types of forces are present during joint loading: functional loads (gravity, inertia, ground-reaction forces and other external forces), muscle forces and joint forces (Eskandari, 1993). The ground-reaction force, that is part of the functional load, is defined as the force exerted against the foot during weight-bearing activities. As with all forces, it has a vector and creates a moment around the knee. When the functional load is applied, there is a muscle force produced to counter the applied force. The sum of these forces produces the joint-reaction forces, which is mainly composed of the joint-contact force and also includes forces in the soft tissues surrounding the joint (ie. ligaments, menisci, capsule). In order to counter the functional load's moment and achieve a desired movement, muscles have to create an antagonistic moment. The muscles have set anatomic origins and insertions and therefore have a set moment arm about a joint. The muscle force that is required to create an equivalent moment about the knee is usually much greater than the force exerted by the functional load due to the much smaller moment arm and biomechanical disadvantage of the muscle. Therefore, the muscle force is several times larger than the functional load and thus creates a substantial joint-contact force. The tibiofemoral joint-contact forces are 3.4 body weight (BW) when walking, 4.3 BW when going up stairs, and 8.5 BW when walking downhill. Not to mention the patellofemoral joint that also sustains incredible stresses that are both compressive and laterally oriented. These are defined by the amount of knee flexion and the Quadriceps- angle or Q-angle, the angle between the line of action of the patellar tendon (line from the patella to the tibial tubercle) and the line of action of the quadriceps muscle (line from the anterior superior iliac spine to the patella).

Furthermore, the medial compartment of the knee sustains 60-70% of the load (Egloff et al., 2012). This can be explained with a number of factors. First, the neutral knee is in slight varus meaning that load bearing will occur slightly medial. Second, hip adduction is needed to position the foot of the load bearing leg under the BW during the stance phase of gait and therefore creates an adductor moment compressing the medial compartment. Note that people that are more obese and/or older tend to walk slower and have a longer stance phase, which increases their total time weight bearing on the medial compartment (Egloff et al., 2012). This might be a factor contributing to accelerated OA in these populations. Third, because the

mechanical axis is 3 degrees from the vertical axis, the ground-reaction force is medial and contributes to compressive stress of the medial compartment.

1.3 Total Knee Arthroplasty

A total knee replacement or arthroplasty (TKA) is the removal and replacement of the entire articular cartilage of the knee. It is an effective treatment of end stage osteoarthritis, where the damage imposed by the degenerative disease is irreversible and replacement of the joint is needed. A TKA has 4 components: the femoral component, the tibial component, the polyethylene insert and the patella component (refer to figure 1.7).

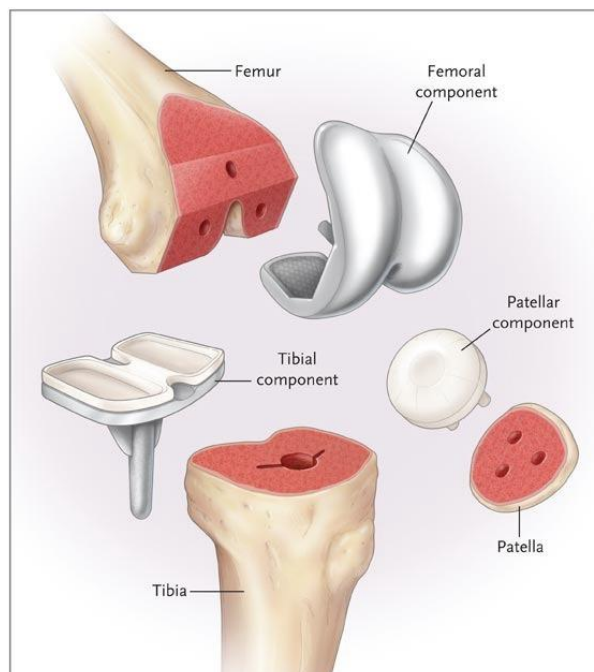


Figure 1.7. Components and bone cuts of a total knee arthroplasty. Reproduced with permission from (Leopold, 2009), Copyright Massachusetts Medical Society.

1.3.1 Description of procedure

The goal of TKA is to replicate the mechanical axis of the lower extremity by obtaining a neutral mechanical axis; thus, ensuring stability and durability of the implant by allowing for even distribution of joint stresses (J. J. Cherian et al., 2014). Historically, there were 2 alignment strategies to replicate the mechanical axis. The classical or mechanical alignment method (MaM) developed by John Insall and the anatomic alignment method (AaM) developed by Hungerford and Krackow. During the MaM, the distal femoral cut is made perpendicular to the mechanical axis of the femur and the proximal tibial cut is made perpendicular to the mechanical axis of the tibia; thus, insuring a neutral mechanical axis (Hungerford & Krackow, 1985; Insall, Hood, Flawn, & Sullivan, 1983). The distal femoral cut will be about 6 degrees in valgus relative to the AAF. The proximal tibial cut will be perpendicular to the AAT. Moreover, in order for the joint line to be parallel to the transverse axis and the ground, the load-bearing axis will need to be parallel to the vertical axis (refer to figure 1.8).

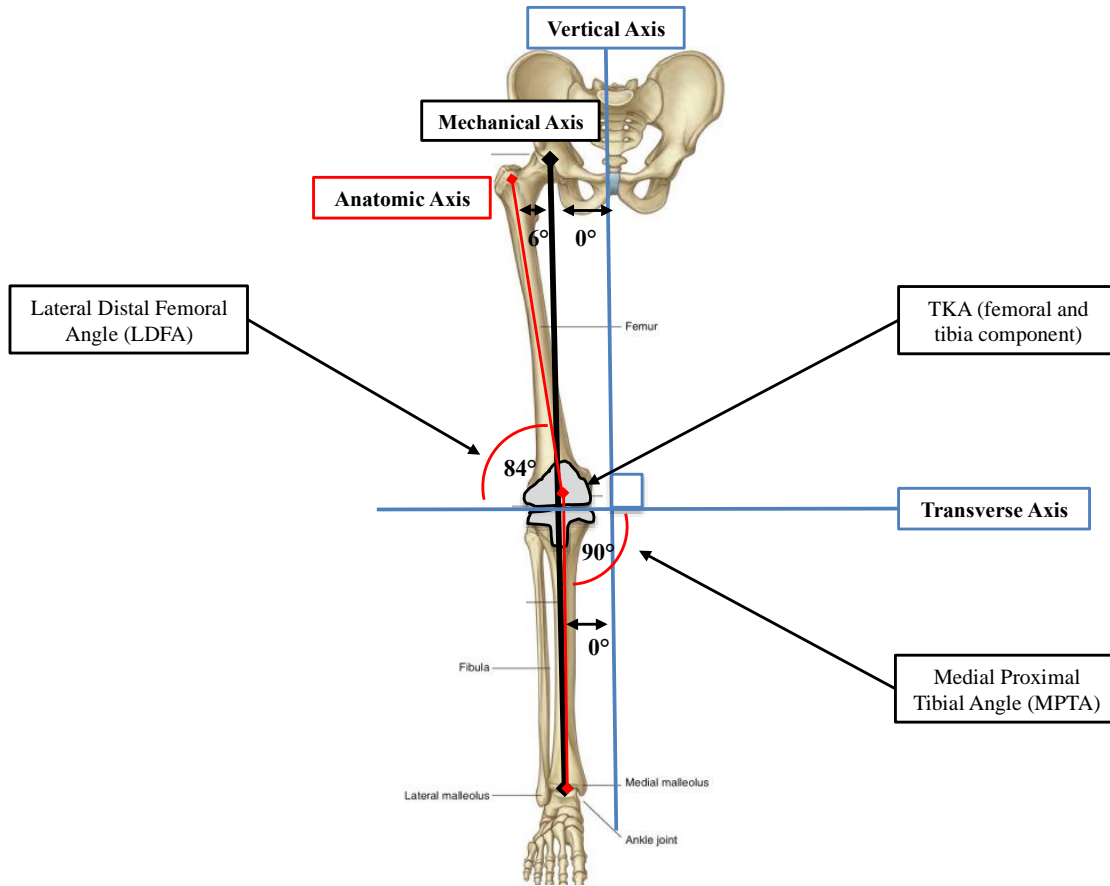


Figure 1.8. Mechanical, anatomic and joint surface angle after total knee replacement. Image modified from original obtained from: Drake, R., Vogle, A., Mitchell, A. (2015). Gray's Anatomy for Students, 3rd Edition. (Copyright approval license number: 4396780051808)

As for the AaM as well as the kinematic alignment method, the principle is to replicate the joint line while keeping a neutral mechanical axis. The joint line is naturally 2-3 degrees in varus relative to the mechanical axis and therefore parallel to the ground since the mechanical axis is normally 3 degrees from the vertical axis. The tibial cut is made at 2-3 degrees varus to the mechanical axis (or replicating the exact proximal tibial joint alignment in the kinematic method) and the femoral cut is made closer to 8-9 degrees valgus to the AAF or 2-3 degrees valgus to the MAF. In summary, the joint line is parallel to the transverse axis and to the ground. Nevertheless, both techniques are clinically equivalent and for the purpose of this study, the mechanical alignment method was used during primary and revision total knee

replacements since it is more common and is considered the gold standard. Intraoperatively, the goal is to get a neutral mechanical axis +/- 3 degrees since the literature has shown that the restoration of a neutral mechanical axis in TKA has superior long-term results, better mechanical wear patterns, and lower failure rates (Helmy et al., 2014)(Ritter et al., 2011).

Furthermore, the orthopaedic surgeon also needs to be conscious of sagittal alignment when making the bony cuts and inserting the implants. The femoral component should be placed in 0 to 3 degrees of flexion relative to the sagittal mechanical axis (Hood et al., 2017). During the proximal tibia cut, the tibial slope is usually set at 0 degrees or 3 degrees as per the manufacturer's suggested proximal tibial cut. However, there is no consensus in the literature, on the optimal posterior tibial slope in patients undergoing TKA. Ahmad et al. suggest trying to reproduce the native tibial slope in every patient and avoiding placing the implant in more than 8 degrees of posterior tibial slope as there is evidence to suggest that this may lead to anterior tibial subluxation and increased polyethylene wear (Ahmad, Patel, Mandalia, & Toms, 2016).

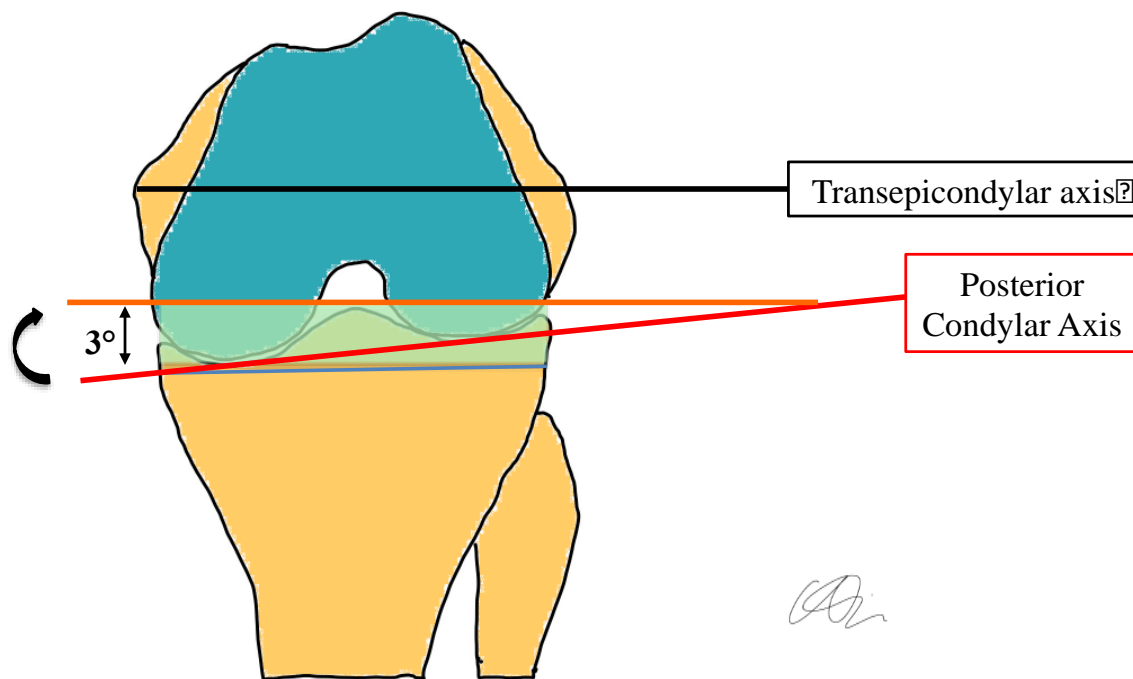


Figure 1.9. Posterior condylar axis (red), posterior femoral cut (orange) and proximal tibial cut (blue). This creates a box cut during total knee arthroplasty resulting in 3 degrees of external rotation prior to the insertion of the femoral implant. Original drawing by author.

Lastly, the MaM also describes making a posterior femur bone cut parallel to the tibial cut (refer to figure 1.9). The cut will be in 3 degrees of external rotation to the posterior condylar axis (refer to figure 1.9). Another way of describing it would be to make the cut parallel to the transepicondylar axis (TEA) (Mihalko, 2013). This creates a boxed gap and simplifies the mechanics of the implant's flexion and extension.

1.3.2 Implantation Techniques

There are two methods to achieve implant fixation at the bone-implant interface. Implant fixation can be achieved through cementless fixation or cement fixation. The choice of fixation method is dependent of implant design, patient factors and surgeon preference (Bauer & Schils, 1999; Hosein, 2013; J. B. Park, 1992).

Cementless fixation, also known as biologic fixation, is the process by which metal becomes permanently incorporated into bone. It was termed "osseointegration" by Branemark in the 1950s. Osseointegration is defined as a direct structural and functional connection between ordered living bone and the surface of load-carrying implants resulting in no relative movement between the implant and the bone (Brånemark, Brånemark, Rydevik, & Myers, 2001). Initially, the implant achieves fixation stability through press-fit fixation. With time, the bone will grow into the implant allowing for a long-lasting fixation. Therefore, it is no surprise that studies have found that most of the migration or loosening of the implants arise during the initial 3 months after surgery (Nilsson, Kärrholm, Carlsson, & Dalén, 1999). In order to achieve bony ingrowth, the press fit fixation achieved by the implant must yield less than 50 μm of micromotion (Udofia, Liu, Jin, Roberts, & Grigoris, 2007). The porous surface needed to ensure biologic bony anchoring has also been explored and the optimal surface roughness and pore size was determined as 600 μm (Taniguchi et al., 2016). Furthermore, the application of bioactive coatings has been used to optimize biologic fixation. Bioactive coatings such as hydroxyapatite (HA) is used for its osteoconductive properties in order to enhance bony ingrowth (W. S. Khan, Rayan, Dhinsa, & Marsh, 2012)(Nilsson et al., 1999).

Orthopaedic bone cement or polymethylmethacrylate (PMMA) is also used to secure the implants to the bone. Dr. John Charnley introduced it during the development of total hip replacements. It is considered a grouting material. It does not adhere the implant to bone, but instead enters the space between the bone and implant and thus creates a physical connection between the implant and bone. In TKA, the cement penetrates the bone and conforms to the shape of the implant and the bone creating a custom prosthetic fit (Hosein, 2013). Bone cement creates two interfaces called the cement/bone and cement/implant interface; both of which can fail and cause the loss of implant fixation.

In the literature, the majority of revisions of primary total knee replacements, of both cemented and uncemented components, were for proximal tibial implant loosening (Gandhi, Tsvetkov, Davey, & Mahomed, 2009). Five year survival rates for cemented and cementless techniques of implant fixation are equivalent (Nilsson et al., 1999). Ghandi et al. published a meta-analysis of the survival and clinical function of cemented and uncemented TKA. The randomized control trials (RCT) comparing the odds of implant survival in cemented and cementless fixation showed no difference. The radiostereometric analysis (RSA) studies found that uncemented TKA sustained greater early migration. The overall combined data found that cemented prostheses offered better survival than the uncemented. However, this was highly skewed since uncemented implants were generally used for younger patients, a population with higher levels of activity, higher demands and known for higher TKA failures (Gandhi et al., 2009; Julin, Jämsen, Puolakka, Kontinen, & Moilanen, 2010; Tomlinson & Harrison, 2012). Whether it is cemented or cementless, the long-term success of knee implants depends heavily on how well it becomes fixed in the first few months after the TKA.

It is believed that the bony integration achieved by cementless implants leads to better long-term durability and is preferable in high demand patients such as younger or obese patients (Bagsby et al., 2016; Bauer & Schils, 1999). Cement has been shown to deform and degrade over the years, and has a weak resistance to tension and shear forces (Gandhi et al., 2009). Nevertheless, the “gold standard” in primary and revision TKA is still cemented fixation (Bauer & Schils, 1999).

1.3.3 Implant Loading

As with the native knee, the TKA implants need to resist a multitude of forces that act on the knee during activities of daily living. The resultant forces acting on the replaced knee are a collection of functional loads (gravity, inertia, ground-reaction forces and other external forces) and forces exerted by muscles and ligaments (Eskandari, 1993). The resultant forces generate torsion, axial loads (tensile/compressive forces) and transverse shear forces. Additionally, some total knee replacement designs such as constrained implants pose increased stresses on the system. Constrained implants such as hinged knees stop the rotational movement that would occur at the knee joint with torsional forces and transfer them to the bone-implant interface (Samiezadeh, Bougherara, Abolghasemian, D'Lima, & Backstein, 2018). It is crucial for the implants to withstand these loads and maintain adequate fixation-stability in order to have a successful total knee replacement that is functional and durable.

1.4 Revision Total Knee Arthroplasty and 3D Printing

In revision TKA surgery, the failed primary TKA is removed and replaced with a revision TKA implant. Proximal tibial bone loss is encountered during rTKA because of a combination of factors. First, it occurs as a result of the mechanism of failure of the pTKA such as particle-induced osteolysis or proximal tibia stress shielding. Second, iatrogenic bone loss is also encountered when the primary TKA implant is removed. Managing bone loss is one of the most challenging aspects of revision TKA surgery (Whittaker, Dharmarajan, & Toms, 2008). In order to acquire adequate fixation-stability of the revision implant and increase the likelihood of long-term survivorship, surgeons have tried to maximize implant fixation in three regions of the proximal tibia: the epiphysis, the metaphysis, and the diaphysis (Morgan-Jones, Oussedik, Graichen, & Haddad, 2015). Revision implants often have a long stem that engages the tibial diaphysis and thus create a combination of diaphyseal and epiphyseal fixation. Unfortunately, the stiff fixation achieved in the diaphysis not only causes end-of-stem pain but also causes stress shielding and bone loss at the tibial epiphysis and metaphysis (J. J. Cherian et al., 2014; Dennis et al., 2008). Therefore, recent research has focused on acquiring better metaphyseal fixation, which has resulted in the development of metaphyseal augments. Nevertheless, the long-term survivorship of newer metaphyseal augments is unknown. The best option for the

management of bone loss that can achieve metaphyseal fixation remains unknown. Current tibial revision metaphyseal augments have non-anatomic shapes that do not conform to the proximal tibia; thus, limiting their overall fixation and creating point contact forces at the bone-implant interface, which can result in stress shielding (De Martino et al., 2015; Quilez, Seral, & Pérez, 2017). The management of proximal tibial bone loss during revision TKA surgery will be discussed in further detail in chapter 5.

There are numerous revision implants available to achieve both metaphyseal fixation and tibial bone loss substitution. However, none are tapered to the complex irregular shape of the proximal tibia. With recent advances in technology, additive manufacturing or 3D printing has become available to surgeons and offers the opportunity to produce anatomic implants. By having implants that conform to the unique shape of the proximal tibia, a better fit is achieved. This anatomic fit maximizes the bone-implant contact area, which increases fixation and decreases stress shielding by evenly distributing the forces to the surrounding bone. Additive manufacturing and 3D printed titanium implant will be reviewed in chapter 2.

1.5 Study Rationale

Total knee arthroplasty is an effective means of treating end stage knee arthritis (Meftah et al., 2016). The need for TKA is increasing every year as the population, the incidence of obesity and the life expectancy continue to rise (Cherian et al., 2016). It is expected that over the next two decades, the number of TKAs performed annually will exceed 3 million in the United States alone, a 600% increase from 2005 (J. Cherian et al., 2016). Joint replacements alone account for more than 25% of all orthopaedic surgeries in Ontario (Bauer & Schils, 1999). Furthermore, given the substantial rise in the number of TKAs, there will be a concurrent increase in revision surgery (Sheth et al., 2017).

Not to mention, younger patients undergoing primary total joint replacements are becoming more prevalent due to increasing rates of obesity and the expanded clinical criteria for eligibility. Younger patients are unfortunately known to be at higher risk of early prosthesis failure requiring revision TKA (Gandhi et al., 2009; Hosein, 2013; Julin et al., 2010). In

Sweden, patients aged less than 65 years have twice the risk of revision compared with those aged more than 75 years (M. Khan, Osman, Green, & Haddad, 2016). The problem is that revision TKAs have much poorer results than primary TKAs, with survivorship as low as 60% over shorter periods (J. Cherian et al., 2016). This is a grave issue for younger patients that need longer lasting revision TKAs in order to stay active, maintain their quality of life and avoid further surgery.

The most common indication for revision or re-revision surgery after TKA is aseptic loosening (29.8%) and more specifically proximal tibia loosening (M. Khan et al., 2016; Tomlinson & Harrison, 2012). Furthermore, during revision TKA (rTKA), proximal tibial bone loss is frequently encountered. This can complicate revision surgery, and possibly result in a less-stable bone-implant fixation.

With this in mind, it is vital that improvements in revision TKA be made in order to increase their longevity and better serve the population in order to prevent multiple revision surgery that will lead to loss of function and quality of life. This may be realized, in part, through the use of additive manufacturing or 3D printing. A 3D printed titanium alloy (Ti6Al4V) revision augment that conforms to the irregular shape of the proximal tibia was recently developed.

Thus, the overall goal of this thesis was to determine the fixation-stability that this newly developed 3D printed revision augment could achieve in comparison to the standard of care fully cemented revision stem.

1.6 Specific Objectives and Hypotheses

The specific objectives of this study were as follows:

1. Review the current literature on 3D printed musculoskeletal metal implants and identify the advantages and disadvantages associated with the human implantation of these 3D printed implants.

2. Describe and compare two micromotion measurement modalities for joint replacement systems: FARO arm vs. optical system.
3. Determine the magnitude and vector of the micromotion experienced by primary total knee replacements.
4. Determine the fixation stability of a revision total knee arthroplasty (TKA) using a novel 3D printed titanium augment compared to a conventional cemented revision.

The corresponding hypothesis were as follows:

1. The quality of the studies related to the implantation of 3D printed musculoskeletal metal implants will be poor secondary to the novelty of these implants; however, 3D printed implants will have better surgical outcomes, which reflects their inherent advantages over conventional subtractive manufacturing.
2. The FARO arm micromotion measurements will be strongly correlated to the optical system.
3. The micromotion experienced by primary total knee replacements will be greater on the medial aspect of the bone-implant interface.
4. The novel 3D printed augment will have equivalent or better fixation-stability in comparison to the conventional fully cemented revision TKA. Sufficient press-fit fixation of the 3D printed augment shown in the cadaveric model will demonstrate that bony ingrowth in-vivo would likely occur.

1.7 Thesis Overview

This thesis is written in an integrated article format. Each chapter corresponds to each objective listed above. Each chapter explains concepts that are necessary to fully understand the main study in chapter 5 comparing the micromotion of the bone-implant interface of proximal tibial revision implants using cement filling or the novel 3D printed augment. Chapter 1 went over the principles of degenerative joint disease and osteoarthritis as well as knee joint anatomy and kinematics, and the basic concepts related to total knee arthroplasty.

- Chapter 2 systematically reviews the use of 3D printed musculoskeletal implants. This chapter outlines the process of 3D printing, the surgical outcomes, the advantages and

the disadvantages of 3D printed metal implant in human musculoskeletal surgery. The reader will appreciate how and why the 3D printed augment was created.

- Chapter 3 compares the FARO arm and the optical tracking system used for measuring bone-implant interface micromotion. The chapter outlines the accuracy and reliability of the FARO arm to reproduce the measurements acquired by the optical tracking system during proximal tibial implant loading. The reader will understand how these measurement techniques work and how accurate they are at measuring the micromotion.
- Chapter 4 describes the micromotion experienced by newly implanted total knee replacements. The chapter outlines the magnitude and vector of the micromotion experienced by the primary TKAs. The reader will be aware of the principles behind primary TKA, the different TKA designs and the epidemiology of failure in primary TKA.
- Chapter 5 is the main study of this thesis. The chapter investigates the proximal tibial component fixation-stability of a revision TKA with a conventional fully cemented stem in comparison to a novel 3D printed titanium cementless augment. The reader will also be informed about the different options available for revision TKA when proximal tibia bone defects are encountered and how they relate to this new 3D printed tibial augment.
- Chapter 6 is the concluding chapter of this thesis. It outlines the main findings of the thesis along with the strengths and limitations of the study. The chapter offers suggestions for future studies in the area of revision total knee arthroplasty and additive manufacturing.

1.8 References

- Abramson, S. B., & Attur, M. (2009). Developments in the scientific understanding of osteoarthritis. *Arthritis Research and Therapy*, 11(3). <http://doi.org/10.1186/ar2655>
- Ahmad, R., Patel, A., Mandalia, V., & Toms, A. (2016). Posterior Tibial Slope: Effect on, and Interaction with, Knee Kinematics. *JBJS Reviews*, 4(4), e3–e3. <http://doi.org/10.2106/JBJS.RVW.O.00057>
- Arden, N., & Nevitt, M. C. (2006). Osteoarthritis: Epidemiology. *Best Practice and Research: Clinical Rheumatology*, 20(1), 3–25. <http://doi.org/10.1016/j.berh.2005.09.007>
- Bagsby, D. T., Issa, K., Smith, L. S., Elmallah, R. K., Mast, L. E., Harwin, S. F., ... Malkani, A. L. (2016). Cemented vs Cementless Total Knee Arthroplasty in Morbidly Obese Patients. *Journal of Arthroplasty*, 31(8), 1727–1731. <http://doi.org/10.1016/j.arth.2016.01.025>
- Bauer, T. W., & Schils, J. (1999). The pathology of total joint arthroplasty. *Skeletal Radiology*, 28, 483–497. <http://doi.org/10.1007/s002560050552>
- Bedson, J., & Croft, P. R. (2008). The discordance between clinical and radiographic knee osteoarthritis: A systematic search and summary of the literature. *BMC Musculoskeletal Disorders*, 9, 1–11. <http://doi.org/10.1186/1471-2474-9-116>
- Belleman, J., Colyn, W., Vandenneucker, H., & Victor, J. (2012). Is Neutral Mechanical Alignment Normal for All Patients? The Concept of Constitutional Varus. *Clinical Orthopaedics and Related Research*, 470(1), 45–53. <http://doi.org/10.1007/s11999-011-1936-5>
- Bierma-Zeinstra, S. M. A., & Koes, B. W. (2007). Risk factors and prognostic factors of hip and knee osteoarthritis. *Nature Clinical Practice Rheumatology*, 3(2), 78–85. <http://doi.org/10.1038/ncprheum0423>
- Blasioli, D. J., & Kaplan, D. L. (2014). The Roles of Catabolic Factors in the Development of

Osteoarthritis. *Tissue Engineering Part B: Reviews*, 20(4), 355–363.
<http://doi.org/10.1089/ten.teb.2013.0377>

Brånemark, R., Brånemark, P.-I., Rydevik, B., & Myers, R. R. (2001). Osseointegration in skeletal reconstruction and rehabilitation. *J Rehabil Res Dev*, 38(2), 1–4.

Brouwer, R., Huizinga, M., Duivenvoorden, T., van Raaij, T., Verhagen, A., Bierma-Zeinstra, S., & Verhaar, J. (2005). Osteotomy for treating knee osteoarthritis. *Cochrane Database of Systematic Reviews*, (1), CD004019.
<http://doi.org/10.1002/14651858.CD004019.pub3>

Cherian, J., Bhavé, A., Harwin, S., & Mont, M. (2016). Outcomes and Aseptic Survivorship of Revision Total Knee Arthroplasty. *The American Journal of Orthopedics*, 45((2)), 79–85.

Cherian, J. J., Kapadia, B. H., Banerjee, S., Jauregui, J. J., Issa, K., & Mont, M. A. (2014). Mechanical, anatomical, and kinematic axis in TKA: Concepts and practical applications. *Current Reviews in Musculoskeletal Medicine*, 7(2), 89–95.
<http://doi.org/10.1007/s12178-014-9218-y>

De Martino, I., De Santis, V., Sculco, P. K., D’Apolito, R., Assini, J. B., & Gasparini, G. (2015). Tantalum Cones Provide Durable Mid-term Fixation in Revision TKA. *Clinical Orthopaedics and Related Research*, 473(10), 3176–3182. <http://doi.org/10.1007/s11999-015-4338-2>

Dennis, D. A., Berry, D. J., Engh, G., Fehring, T., Macdonald, S. J., Rosenberg, A. G., & Scuderi, G. (2008). Revision Total Knee Arthroplasty. *Journal of the American Academy of Orthopaedic Surgeons*, 16(8), 442–454.

Drake, R., Vogl, A., & Mitchell, A. (Eds.). (2015). *Gray’s Anatomy for Students* (3rd Editio). Philadelphia: Churchill Livingstone, Elsevier.

Egloff, C., Hügle, T., & Valderrabano, V. (2012). Biomechanics and pathomechanisms of osteoarthritis. *Swiss Medical Weekly*, 142(JULY), 1–14.
<http://doi.org/10.4414/smw.2012.13583>

- Eskandari, H. (1993). Bone-Prosthesis interface relative displacement of the knee tibial component: Finite element analysis and measurement.
- Gandhi, R., Tsvetkov, D., Davey, J. R., & Mahomed, N. N. (2009). Survival and clinical function of cemented and uncemented prostheses in total knee replacement: A META-ANALYSIS. *Journal of Bone and Joint Surgery - British Volume*, 91-B(7), 889–895. <http://doi.org/10.1302/0301-620X.91B7.21702>
- Goldring, M. B., & Marcu, K. B. (2009). Cartilage homeostasis in health and rheumatic diseases. *Arthritis Research and Therapy*, 11(3). <http://doi.org/10.1186/ar2592>
- Guccione, A., Felson, D., Anderson, J. J., Anthony, J. M., Zhang, Y., Wilson, P. W. F., ... Kannel, W. B. (1994). The Effects of Specific Medical Conditions on the Functional Limitations of Elders in the Framingham Study. *American Journal of Public Health*, 85, 351–358.
- Helmy, N., Dao Trong, M. L., & Kühnel, S. P. (2014). Accuracy of Patient Specific Cutting Blocks in Total Knee Arthroplasty. *BioMed Research International*, 2014(October 2009). <http://doi.org/10.1155/2014/562919>
- Hirschmann, M. T., & Müller, W. (2015). Complex function of the knee joint: the current understanding of the knee. *Knee Surgery, Sports Traumatology, Arthroscopy*, 23(10), 2780–2788. <http://doi.org/10.1007/s00167-015-3619-3>
- Hood, B., Blum, L., Holcombe, S. A., Wang, S. C., Urquhart, A. G., Goulet, J. A., & Maratt, J. D. (2017). Variation in Optimal Sagittal Alignment of the Femoral Component in Total Knee Arthroplasty. *Orthopedics*, 40(2), 102–106. <http://doi.org/10.3928/01477447-20161108-04>
- Hosein, Y. K. (2013). The Effect of Stem Surface Treatment and Substrate Material on Joint Replacement Stability: An In-Vitro Investigation into the Stem-Cement Interface Mechanics under Various Loading Modes. Retrieved from <http://ir.lib.uwo.ca/etd/1479>
- Hungerford, D. S., & Krackow, K. A. (1985). Total Joint Arthroplasty of the Knee. *Clinical Orthopaedics and Related Research*, 192, 23–33. <http://doi.org/10.1097/00003086->

198501000-00004

- Insall, J., Hood, R., Flawn, L., & Sullivan, D. (1983). The total condylar knee prosthesis in gonarthrosis. A five to nine-year follow-up of the first one hundred consecutive replacements. *J Bone Joint Surg*, 65–A, 619–628. <http://doi.org/10.1302/0301-620X.96B7.33946>
- Iseki, Y., Takahashi, T., Takeda, H., Tsuboi, I., Imai, H., Mashima, N., ... Yamamoto, H. (2009). Defining the load bearing axis of the lower extremity obtained from anterior-posterior digital radiographs of the whole limb in stance. *Osteoarthritis and Cartilage*, 17(5), 586–591. <http://doi.org/10.1016/j.joca.2008.10.001>
- Jevsevar, D. (2013). AAOS Clinical Guideline Summary: Treatment of Osteoarthritis of the Knee: Evidence-Based Guideline, 2nd Edition. *J Am Acad Orthop Surg*, 21(9), 571–576.
- Julin, J., Jämsen, E., Puolakka, T., Konttinen, Y. T., & Moilanen, T. (2010). Younger age increases the risk of early prosthesis failure following primary total knee replacement for osteoarthritis: A follow-up study of 32,019 total knee replacements in the Finnish Arthroplasty Register. *Acta Orthopaedica*, 81(4), 413–419. <http://doi.org/10.3109/17453674.2010.501747>
- Khan, M., Osman, K., Green, G., & Haddad, F. S. (2016). The epidemiology of failure in total knee arthroplasty. *Bone & Joint Journal*, 98–B(1 Supple A), 105–112. <http://doi.org/10.1302/0301-620X.98B1.36293>
- Khan, W. S., Rayan, F., Dhinsa, B. S., & Marsh, D. (2012). An osteoconductive, osteoinductive, and osteogenic tissue-engineered product for trauma and orthopaedic surgery: How far are we? *Stem Cells International*, 2012. <http://doi.org/10.1155/2012/236231>
- Kharb, A., Saini, V., Jain, Y., & Dhiman, S. (2011). A review of gait cycle and its parameters. *IJCEM Int J Comput Eng Manag*, 13(July), 78–83. http://doi.org/10.1007/3-540-49384-0_1
- Kirkley, A., Birmingham, T., Litchfield, R., Giffin, R., Willits, K., Wong, C., ... Fowler, P.

- (2017). A Randomized Trial of Arthroscopic Surgery for. *New England Journal of Medicine*, 359(11), 1097–1107. <http://doi.org/10.1056/NEJMoa1602615>
- Laupattarakasem, W., Laopaiboon, M., Laupattarakasem, P., & Sumananont, C. (2008). Arthroscopic debridement for knee osteoarthritis. *Cochrane Database of Systematic Reviews*, (1). <http://doi.org/10.1002/14651858.CD005118.pub2>
- Leighton, R., Fitzpatrick, J., Smith, H., Crandall, D., Flannery, C. R., & Conrozier, T. (2018). Systematic clinical evidence review of NASHA (Durolane hyaluronic acid) for the treatment of knee osteoarthritis. *Open Access Rheumatology: Research and Reviews*, Volume 10, 43–54. <http://doi.org/10.2147/OARRR.S162127>
- Leopold, S. S. (2009). Minimally Invasive Total Knee Arthroplasty for Osteoarthritis. *New England Journal of Medicine*, 360(17), 1749–1758. <http://doi.org/10.1056/NEJMct0806027>
- Loughlin, J. (2005). The genetic epidemiology of human primary osteoarthritis: Current status. *Expert Reviews in Molecular Medicine*, 7(9), 1–12. <http://doi.org/10.1017/S1462399405009257>
- Macdonald, K. V., Sanmartin, C., Langlois, K., & Marshall, D. A. (2014). Symptom onset , diagnosis and management of osteoarthritis, 25(9), 10–17.
- Man, G. S., & Mologhianu, G. (2014). Osteoarthritis pathogenesis - a complex process that involves the entire joint. *Journal of Medicine and Life*, 7(1), 37–41. Retrieved from </pmc/articles/PMC3956093/?report=abstract>
- Masouros, S. D., Bull, A. M. J., & Amis, A. A. (2010). (i) Biomechanics of the knee joint. *Orthopaedics and Trauma*, 24(2), 84–91. <http://doi.org/10.1016/j.morth.2010.03.005>
- Meftah, M., White, P. B., Ranawat, A. S., & Ranawat, C. S. (2016). Long-term results of total knee arthroplasty in young and active patients with posterior stabilized design. *Knee*, 23(2), 318–321. <http://doi.org/10.1016/j.knee.2015.10.008>
- Mihalko, W. M. (2013). *Campbell's Operative Orthopaedics*. (S. Canale & J. Beaty, Eds.) (12th

ed.). Philadelphia: Elsevier. <http://doi.org/10.1177/003591573102400728>

Morgan-Jones, R., Oussedik, S. I. S., Graichen, H., & Haddad, F. S. (2015). Zonal fixation in revision total knee arthroplasty. *The Bone & Joint Journal*, 97–B(2), 147–149.

<http://doi.org/10.1302/0301-620X.97B2.34144>

Murphy, L., Schwartz, T. A., Helmick, C. G., Renner, J. B., Tudor, G., Koch, G., ... Jordan, J. M. (2015). Lifetime Risk of Symptomatic Knee Osteoarthritis. *Arthritis Rheum.*, 59(9), 1207–1213. <http://doi.org/10.1002/art.24021.Lifetime>

Nilsson, K. G., Kärrholm, J., Carlsson, L., & Dalén, T. (1999). Hydroxyapatite coating versus cemented fixation of the tibial component in total knee arthroplasty: prospective randomized comparison of hydroxyapatite-coated and cemented tibial components with 5-year follow-up using radiostereometry. *The Journal of Arthroplasty*, 14(1), 9–20.

[http://doi.org/10.1016/S0883-5403\(99\)90196-1](http://doi.org/10.1016/S0883-5403(99)90196-1)

Park, J. B. (1992). Orthopedic prosthesis fixation. *Annals of Biomedical Engineering*, 20(6), 583–594. <http://doi.org/10.1007/BF02368607>

Pereira, D., Ramos, E., & Branco, J. (2015). Osteoarthritis. *Acta Médica Portuguesa*, 28(1), 99–106.

Quilez, M. P., Seral, B., & Pérez, M. A. (2017). Biomechanical evaluation of tibial bone adaptation after revision total knee arthroplasty: A comparison of different implant systems. *PLoS ONE*, 12(9), 1–14. <http://doi.org/10.1371/journal.pone.0184361>

Ritter, M. A., Davis, K. E., Meding, J. B., Pierson, J. L., Berend, M. E., & Malinzak, R. A. (2011). The Effect of Alignment and EMI on Failure of Total Knee Replacement, 1588–1596.

Samiezadeh, S., Bougherara, H., Abolghasemian, M., D’Lima, D., & Backstein, D. (2018). Rotating hinge knee causes lower bone–implant interface stress compared to constrained condylar knee replacement. *Knee Surgery, Sports Traumatology, Arthroscopy*, 0(0), 0. <http://doi.org/10.1007/s00167-018-5054-8>

- Sheth, N. P., Bonadio, M. B., & Demange, M. K. (2017). Bone Loss in Revision Total Knee Arthroplasty. *Journal of the American Academy of Orthopaedic Surgeons*, 25(5), 348–357. <http://doi.org/10.5435/JAAOS-D-15-00660>
- Taniguchi, N., Fujibayashi, S., Takemoto, M., Sasaki, K., Otsuki, B., Nakamura, T., ... Matsuda, S. (2016). Effect of pore size on bone ingrowth into porous titanium implants fabricated by additive manufacturing: An in vivo experiment. *Materials Science and Engineering C*, 59, 690–701. <http://doi.org/10.1016/j.msec.2015.10.069>
- Tomlinson, M., & Harrison, M. (2012). The New Zealand Joint Registry. *Foot and Ankle Clinics*, 17(January 1999), 719–723. <http://doi.org/10.1016/j.fcl.2012.08.011>
- Udofia, I., Liu, F., Jin, Z., Roberts, P., & Grigoris, P. (2007). The initial stability and contact mechanics of a press-fit resurfacing arthroplasty of the hip. *Journal of Bone and Joint Surgery - British Volume*, 89-B(4), 549–556. <http://doi.org/10.1302/0301-620X.89B4.18055>
- Vandekerckhove, P. J. T. K., Matlovich, N., Teeter, M. G., MacDonald, S. J., Howard, J. L., & Lanting, B. A. (2017). The relationship between constitutional alignment and varus osteoarthritis of the knee. *Knee Surgery, Sports Traumatology, Arthroscopy*, 25(9), 2873–2879. <http://doi.org/10.1007/s00167-016-3994-4>
- Whittaker, J. P., Dharmarajan, R., & Toms, A. D. (2008). The management of bone loss in revision total knee replacement. *The Journal of Bone and Joint Surgery*, 90(8), 981–987. <http://doi.org/10.1302/0301-620X.90B8.19948>
- Wong, I., Hiemstra, L., Ayeni, O. R., Getgood, A., Beavis, C., Volesky, M., ... MacDonald, P. B. (2018). Position Statement of the Arthroscopy Association of Canada (AAC) Concerning Arthroscopy of the Knee Joint—September 2017. *Orthopaedic Journal of Sports Medicine*, 6(2), 1–4. <http://doi.org/10.1177/2325967118756597>
- Xie, F., Thumboo, J., & Li, S. C. (2007). True Difference or Something Else? Problems in Cost of Osteoarthritis Studies. *Seminars in Arthritis and Rheumatism*, 37(2), 127–132. <http://doi.org/10.1016/j.semarthrit.2007.01.001>

Zhang, W., Nuki, G., Moskowitz, R. W., Abramson, S., Altman, R. D., Arden, N. K., ...
Tugwell, P. (2010). OARSI recommendations for the management of hip and knee
osteoarthritis. Part III: Changes in evidence following systematic cumulative update of
research published through January 2009. *Osteoarthritis and Cartilage*, 18(4), 476–499.
<http://doi.org/10.1016/j.joca.2010.01.013>

Zingde, S. M., & Slamin, J. (2017). Biomechanics of the knee joint, as they relate to
arthroplasty. *Orthopaedics and Trauma*, 31(1), 1–7.
<http://doi.org/10.1016/j.mporth.2016.10.001>

CHAPTER 2

2 Surgical outcomes of 3D printed musculoskeletal metal implants: A systematic review

Overview: This chapter reviews additive manufacturing or 3D printing of metal implants that are destined for human musculoskeletal implantation. It goes over the surgical outcomes and the advantages and disadvantages of 3D printed metal implants. The reader can appreciate the process needed to create a 3D printed implant as well as the inherent benefits of 3D printed implants.

2.1 Introduction

Additive manufacturing, also known as three-dimensional printing (3DP), was invented in the 1980's (Bauermeister, Zuriarrain, & Newman, 2016). It is a type of manufacturing that converts 3D images of structures into physical structures from a variety of materials such as plastic, glass, ceramic and metal. It can produce complex free-form structures that would be impossible to produce using conventional subtractive manufacturing. In the last decade, advances in technology have resulted in radical improvements in additive manufacturing. This has created opportunities for novel applications of this technology in fields such as surgery.

3D printing has been used in manufacturing to produce prototypes and low volume entities quickly, accurately and cheaply (Cavanaugh, Mounts, & Vaccaro, 2015). In surgery, 3D models have been created for pre-operative planning and teaching. More recently, 3D printing has allowed the production of implants suitable for human implantation (Ackland et al., 2017;

Aranda, Jiménez, Rodríguez, & Varela, 2017; Chen, Xu, Wang, Hao, & Wang, 2015; Fan et al., 2015; Hamid, Parekh, & Adams, 2016; Hatamleh, Bhamrah, Ryba, Mack, & Huppa, 2016; Imanishi & Choong, 2015; D. Kim et al., 2017; U. L. Lee, Kwon, Woo, & Choi, 2016; Leiser, Shilo, & Wolff, 2016; X. Li et al., 2017; Liang, Ji, Zhang, Wang, & Guo, 2017; Mao et al., 2015). It is important to understand the basic principles of additive manufacturing before truly comprehending its potential impact on surgical research and practice.

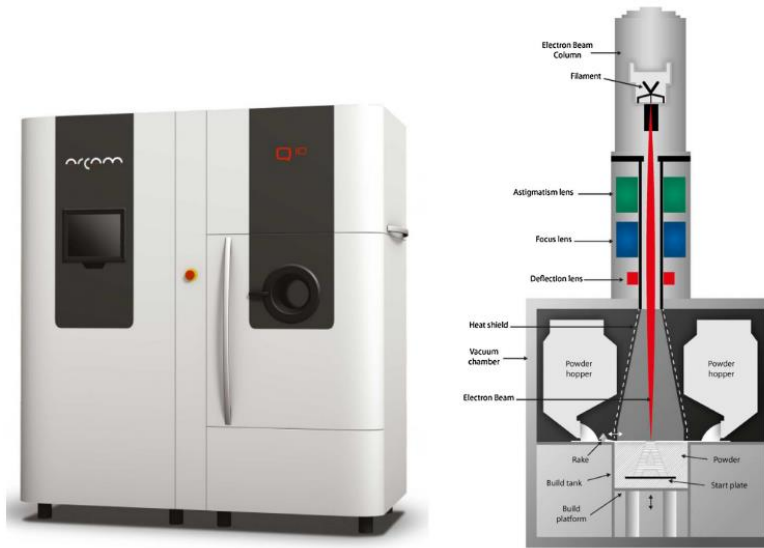


Figure 2.1. Schematic representation of electron beam melting, a type of Metal-based additive manufacturing (Prabhakar, Sames, Dehoff, & Babu, 2015).

Basic Principles of 3D Printing

3D printing is accomplished in three steps: Acquisition, manipulation and manufacturing. These three steps are termed the “digital workflow” of 3D printing (Barazanchi et al., 2017). First, medical imaging modalities such as computed tomography (CT) and magnetic resonance imaging (MRI) are used to acquire 2D data in the form of Digital Imaging and Communications in Medicine (DICOM). Second, computer-aided design (CAD) software is used to manipulate the data and produce 3D digital models. The 3D digital model’s mechanical characteristics can be determined prior to printing using methods such as computer modelling and finite element analysis. Finally, the 3D models are manufactured in the desired

material layer by layer through computer-aided manufacturing (CAM) using one of the numerous methods of 3D printing.

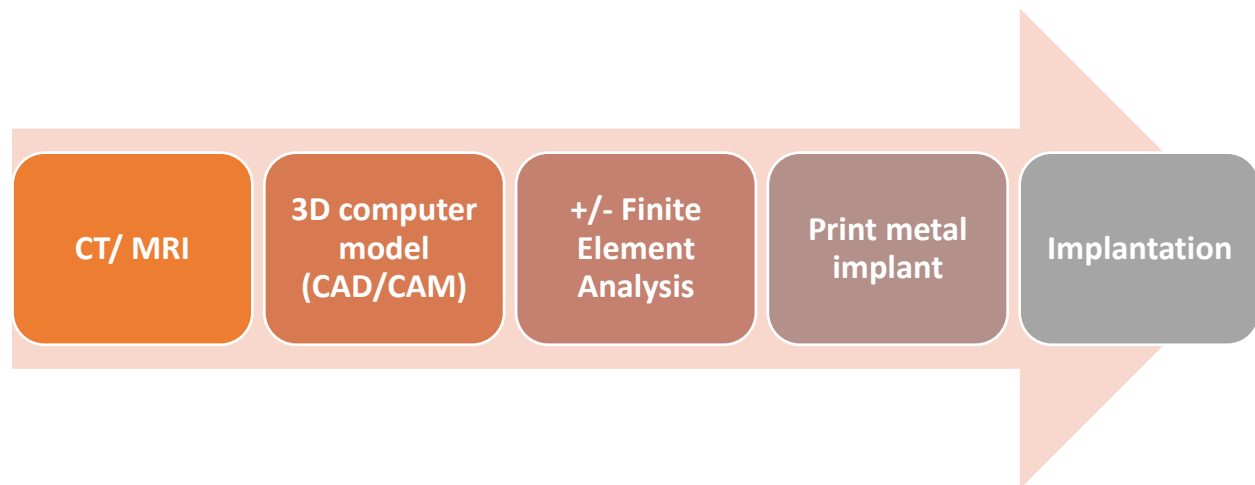


Figure 2.2. Workflow of 3D printing

3D Printing Techniques

Stereolithography (SLA) was the first 3D printing technique available and was first used in the biomedical field in 1994 to bridge a skull defect (G. B. Kim et al., 2016)(Almeida e Silva et al., 2014). SLA is the process by which a computer controlled ultraviolet laser beam hardens a liquid polymer resin creating a structure layer by layer (Barazanchi et al., 2017). Other types of liquid printing have been described such as multi-jet printing (MJP), PolyJet printing (PJP), Color-jet printing (CJP) and Fused deposition modeling (FDM).

More recently, metal-based additive manufacturing (MAM) has evolved to produce long-lasting implants (X. Wang et al., 2016). MAM techniques include: Electron Beam Melting (EBM), Selective Laser Melting (SLM), Selective Laser Sintering (SLS) and Laser Metal Deposition (LMD). These techniques all use heat treatment in the form of lasers (Fiber or CO2 laser) to melt or sinter metal powder, layer by layer to produce a desired construct (Figure 1).

3D Printing in Musculoskeletal Surgery

3D printing of metal structures has revolutionized musculoskeletal surgery, such as orthopaedic surgery, neurosurgery, maxillofacial surgery, plastic surgery and thoracic surgery

(Tack, Victor, Gemmel, & Annemans, 2016). Titanium is the most common material used in MAM due to its material properties and biocompatibility. The titanium alloy, Ti6Al4V, has an elastic modulus around 110 GPa, which is low in comparison to other metals such as cobalt chrome molybdenum (CoCrMo) that has a modulus of 210. Nevertheless, implants made of these materials are usually much stiffer than natural bone. Cortical bone has an elastic modulus ranging from 3 to 30 GPa (X. Wang et al., 2016). Therefore, due to this modulus mismatch, there is insufficient load transfer from the implant to the surrounding bone resulting in bone reabsorption and eventually loosening of the prosthetic implant (Moiduddin et al., 2016). With 3D printing, stress shielding can be avoided by adjusting the implants shape and porosity to match the bone's stiffness; therefore, creating an improved load transfer interface. Simoneau et al. (Simoneau, Terriault, Jetté, Dumas, & Brailovski, 2017) described a reduction in proximal femur stress shielding with porous 3D printed femoral stems. There has been a rapid increase in interest regarding potential applications and benefits of MAM in musculoskeletal surgery.

Purpose

The purpose of the present study is to evaluate the post-operative outcomes of 3D printed metal implants in musculoskeletal surgery. This review will identify the advantages and disadvantages of 3D printing and discuss its potential role in the future of surgical practice.

2.2 Materials and Methods

Search Strategy

We conducted a systematic search of the online bibliographic databases Medline (1946 to December 2017), Embase (1946 to December 2017), Scopus (1960 to December 2017), CINAHL (1982 to December 2017) and Cochrane databases to identify eligible studies that related to the surgical implantation of 3D printed metal implants in musculoskeletal surgery. Database appropriate search terms including “3D printing”, “implant” and “musculoskeletal” were used. A summary of the specific search strategy used is included in appendix 1.0. References from review articles and potentially relevant studies were reviewed for additional relevant articles.

Table 2.1. Inclusion and Exclusion Criteria

Inclusion	Exclusion
English/ French	Review articles
3D printed/ custom/ additive manufacturing	Animal trials
Metal implants	Not implanted
Musculoskeletal application of implants	
Implantation of 3D printed structure	

Screening for Eligible Studies

Two independent reviewers (C-A.D. & M.P.) assessed the titles and abstracts of articles found in the initial search strategy. Eligible studies were included based on the inclusion and exclusion criteria listed in Table 2.1. All titles and abstracts that met the eligibility criteria and any marked uncertain were obtained in full text and independently reviewed by the same two reviewers using the same eligibility criteria. Any disagreements between the two reviewers were noted and resolved with discussion. A flow diagram summarizing the systematic review process is illustrated in Figure 3. Twenty-five articles remained after final screening.

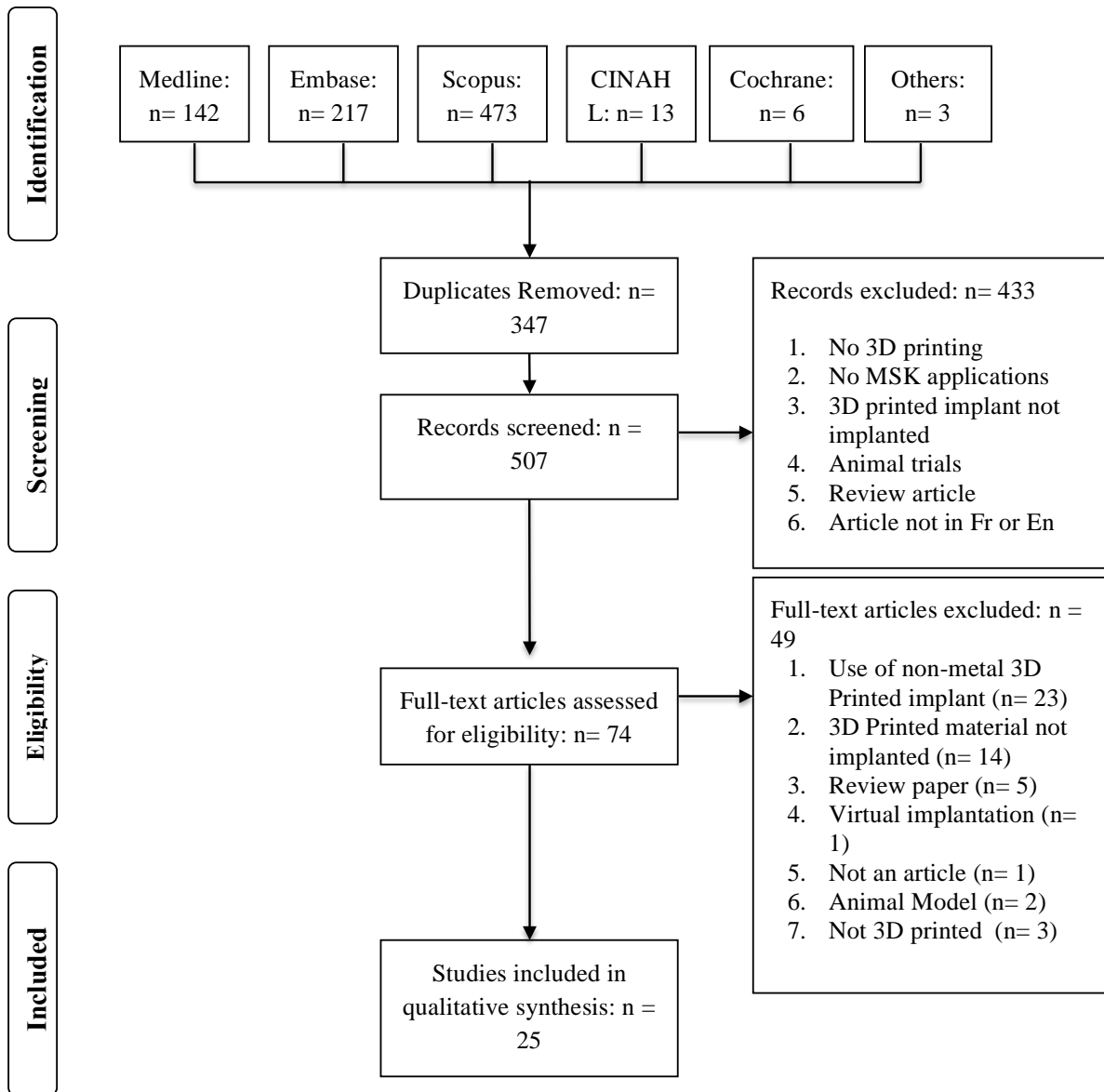


Figure 2.3. Flow diagram summarizing the identification, screening and data collection of relevant articles.

Quality Assessment and Data Abstraction

Methodological quality assessment was performed by the reviewers using the Single Subject Research Design Quality Assessment Tool (Logan, Hickman, Harris, & Heriza, 2008). Two reviewers (C.A.D. & M.P.) independently extracted data from eligible studies. The data included in Table 2 were abstracted from each study.

Table 2.2. Data extraction

Authors/ Title/ Journal	Type of Study
Year	Country
Age	Gender
Number of participants	Surgical specialty
Joint/Bone	Indication for surgical procedure
Type of 3D printing (method/material)	Time of follow-up
Surgical Outcomes	Complications
Conclusions	Any conflicts of interest

Statistical Analysis

The majority of the data collected was qualitative data. However, any quantitative radiographic or clinical mean scores and standard deviations were also collected. A single reviewer performed the qualitative data analysis. Inter-observer agreement was assessed using the Kappa statistic (Viera & Garrett, 2005).

2.3 Results and Discussion

A total of 507 articles were found after the initial electronic search. Twenty-five articles fit the eligibility criteria when the papers were screened independently. The articles were of weak to moderate quality with a mean score of 7.44 +/- 2.04 based on the Single Subject Research Design Quality Assessment Tool (Logan et al., 2008). This is expected in the study of rare or novel treatment methods such as 3D printed custom metal implants. The earliest articles

found in the literature dated back to 2015. The strength of the inter-observer agreement during the screening process was good with a kappa of 0.71 +/- 0.04. The study characteristics of each article are summarized in Table 3. Out of the 25 articles included in the review, 17 were cases reports, four were cases series, two were prospective cohorts and two were retrospective cohorts. Most articles originated from China (n=9) and Australia (n=4). Orthopaedic Surgery (n=13) and Oromaxillofacial Surgery (n=6) were amongst the most popular fields of study involving 3D printed metal implants. The most common type of 3D printer utilized in the studies was Electron Beam Melting (12/25). The studies were categorized based on their anatomic location.

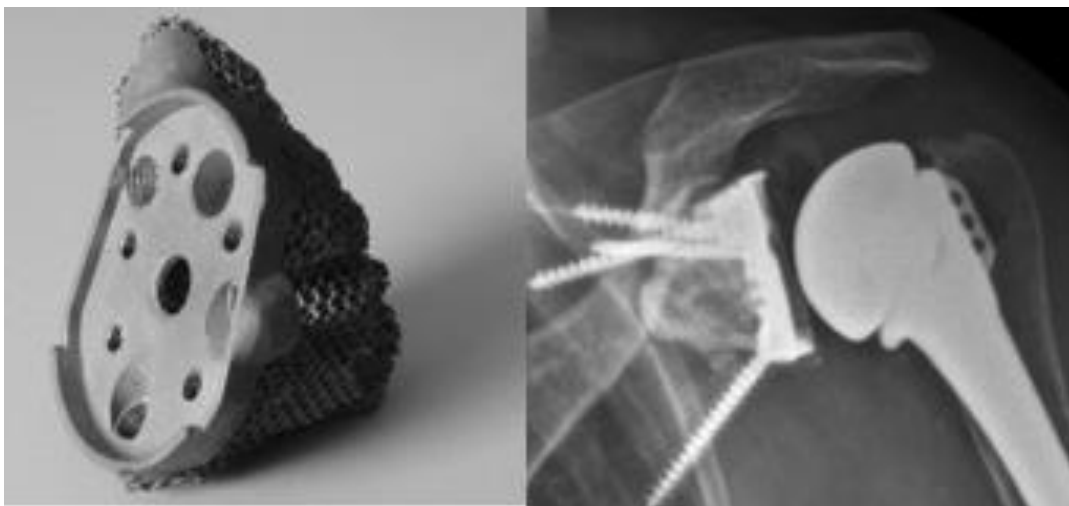


Figure 2.4. Picture and x-ray of 3D printed glenoid metal augment implanted during revision total shoulder arthroplasty with severe glenoid bone defect (Stoffelen, Eraly, & Debeer, 2015)

Spine

Spine-related articles found that the use of 3D printed implants yielded excellent clinical results. There was minimal post-operative pain (D. Kim et al., 2017), excellent bony fusion (X. Li et al., 2017; Mobbs, Coughlan, Thompson, Sutterlin, & Phan, 2017; Phan, Sgro, Maharaj, D’Urso, & Mobbs, 2016), no implant subsidence at 12 months (X. Li et al., 2017) and a reduction in operative time (Mobbs et al., 2017; Phan et al., 2016).

Pelvis

Pelvis-related articles showed a similar trend. The mean Harris Hip Score improved from 36 +/- 8 to 82 +/- 18 ($p < 0.001$) after the reconstruction of a massive acetabular bone defect during revision total hip arthroplasty using a 3D printed implant (Liang et al., 2017). The use of 3DP implants resulted in an adequate reduction in stress shielding (K. C. Wong, Kumta, Geel, & Demol, 2015), precise bone substitution after tumour excision and a Mean Musculoskeletal Tumour Society 93 (MSTS-93) score of 22.7 for patients with iliac prosthesis (Liang et al., 2017).

Hand and upper limbs

Fan et al. quoted an MSTS-93 score of 93, 73 and 90 in patients undergoing tumour resection and bone defect substitution using 3DP implants for clavicle, scapular and pelvic tumours. During total shoulder replacements with severe glenoid bone loss, the use of 3DP glenoid implants yielded a 28% increase in Shoulder Pain and Disability Index as well as a 40.9% improvement of the Disabilities of the Arm, Shoulder, and Hand score.

Foot and ankle

Hsu et al. (Hsu & Ellington, 2015) used a 3DP titanium truss cage for tibiototalcalcaneal arthrodesis and found that it resulted in a stable alignment and ankle fusion at the 5 months post-operative follow up. The patients had minimal pain at the 1 year follow up and they returned to their activities of daily living. The replacement of a calcaneus with a 3DP calcaneus after its resection due to calcaneal chondrosarcoma resulted in an American Orthopaedic Foot and Ankle Society (AOFAS) Ankle-Hindfoot Scale score of 82. The patient was pain free and walking unsupported five months after surgery (Imanishi & Choong, 2015).

Skull

Articles related to the reconstructions of skull defects with 3DP implants showed that there was a satisfactory skull-shape symmetry on CT and physical exam (E.-K. Park et al., 2016). Temporomandibular joint reconstruction resulted in a normal jaw opening distance of more than 40.0 mm (Ackland et al., 2017; Leiser et al., 2016)

Thorax

A parasternal reconstruction with a 3DP implant gave excellent cosmetic results and a preservation of thoracic morphology on CT (L. Wang, Cao, Li, & Huang, 2016).

A detailed summary of the surgical outcomes and complications of every study is available in the appendix. The most common surgical indication for the insertion of the 3D printed implant was for the reconstruction of bone defects. Twenty articles were related to the reconstruction of bone defects secondary to tumour excision or bone loss encountered during revision surgery. Other studies were associated with osteosynthesis surgery (n=2), spine decompression/ fusion surgery (n=1), foot realignment surgery (n=1) and primary joint replacement surgery (n=1). All 25 studies reported promising post-surgical outcomes and numerous advantages to using 3D printed metal implants compared to the current standard of care.

Advantages of 3D printing

Xu et al. described spine reconstruction after a C2 spondylectomy using conventional implants compared to 3D printed implants. They found favourable post-surgical outcomes due to specific features associated to 3D printing. The microstructure of the 3D printed implant is highly organized and has uniform pores and a continuous strut that makes it resistant to compressive stress. Its customized stiffness or flexibility matches the host bone. These advantages are associated with less stress shielding and the prevention of implant subsidence (Xu et al., 2016; Fan et al., 2015; Hsu & Ellington, 2015).

3D printing offers the possibility for optimized pore density resulting in increased area of rough bone-metal interface conducive to osseointegration (Stoffelen et al., 2015). This can offer an overall better fixation-stability. The customized implant can also minimize the need for bone graft as well as reduce the risks associated with bone graft harvest such as post-operative pain and infection (Xu et al., 2016; Phan et al., 2016).

Another key feature of 3D printing is the capacity for customized topology. 3D printed implants are based on custom computer-aided design models that match the actual size and

unique shape of the site. This increases the contact area and improves the bone-implant interface giving the implant additional stability and therefore may help reduce stress risers that lead to implant fracture, periprosthetic fractures and/or implant collapse (Xu et al., 2016). A more even stress distribution on the bone-implant interface may reduce uneven bone remodelling and proximal bone resorption. Wei et al. (Wei, Guo, Ji, Zhang, & Liang, 2017) reported a more reliable reconstruction and a better fixation-stability when a custom-made sacral prosthesis was used after total bloc sacrectomy. The prosthesis matched the osteotomy planes of L5 and bilateral ilia. Kim et al. (D. Kim et al., 2017) described how conventional pelvic reconstructions typically use more than two grafts and geometrically different cages, which takes a considerable amount of operating time. With their 3DP implant, they not only eliminated the need for multiple grafts and cages but also minimized dead space. The geometrical fit of the implant maintained better stability and diminished postoperative pain. Stoffelen et al. also described a better geometrical fit when an irregular glenoid bone defect was reconstructed with a 3DP augment during revision total shoulder arthroplasty (Stoffelen et al., 2015).

3D printed personalized implants can simplify complex reconstructive surgery that would otherwise need multiple conventional implants. 3DP could reduce operating time (Phan et al., 2016) by reducing the need for bone graft harvest (U. L. Lee et al., 2016), improving surgical planning and using patient specific tools. The preoperative design process associated with 3DP increases the surgeons' stereotypic understanding of the patient's anatomy and accelerates surgical decision-making (D. Kim et al., 2017). Furthermore, the reduction in operative time could reduce operative complications and the overall cost of the operation (Phan et al., 2016).

The 3DP technology and development of customized titanium prosthesis has increased the limb salvage surgery in recent years (Fan et al., 2015) mainly because traditional subtractive manufacturing cannot replicate complex anatomy or internal features. Fan et al. (Fan et al., 2015) explained that the custom 3DP titanium scapula implanted in the study eliminated the risk of scapular allograft resorption during conventional attempts at limb salvage and was therefore the preferred surgical option for scapular reconstruction involving limb salvage.

Imanishi et al. also illustrated that with the use of a custom 3DP calcaneus after a total calcanectomy had excellent post-operative results and was a valid limb-salvage surgical option (Imanishi & Choong, 2015).

3D printed implants offers the surgeon a lower profile or less prominent insert that is more anatomic and therefore yielding better post-surgical outcomes (Smith et al., 2016). The anatomic alignment achieved with 3DP yields near-perfect functional and cosmetic results such as in skull defect reconstruction (E.-K. Park et al., 2016), sternocostal reconstruction (Aranda et al., 2017) and mandibular reconstruction (Ackland et al., 2017; Leiser et al., 2016; Hatamleh et al., 2016; Shan, Chen, Liang, Huang, & Cai, 2015; Stoor, Suomalainen, Mesimaki, & Kontio, 2017).

Disadvantages of 3D printing

Li et al. (Li, Qu, Mao, Dai, & Zhu, 2016) described an increased risk of superior gluteal nerve injury and hip dislocation with the use of a custom 3D printed acetabular cage in hip reconstruction surgery. This was mainly due to the substantial exposure of the ilium required to accurately place the custom cage. The authors retrospectively described that they could have used a trochanteric osteotomy to relieve some tension of the superior gluteal nerve. They could have inserted the screws percutaneously to reduce the overall dissection and risk of dislocation secondary to lack of soft tissue tension.

The introduction of 3D printing in musculoskeletal surgery is only recent and lacks the long term follow up to adequately compare it to traditional techniques (Phan et al., 2016). Thus, it has a complicated approval process (Fan et al., 2015). Without proper standardization within the manufacturing process, there is a potential for low quality implants. However, implementation of international standards of 3DP would improve the quality of 3DP implants. Furthermore, intraoperative modification is limited and operative fit is based on the accuracy of the bony resection in tumor removal surgery. Implant insertion using intra-operative navigation has been shown to improve the accuracy of implantation (Chen et al., 2015). If intra-operative

modifications are needed to accommodate the implant, conventional techniques of bone defect substitution can be used.

Potential drawbacks to 3D printing technology currently have high costs due to its customized single use profile, the inter-disciplinary pre-operative planning and the approval required by health authorities, hospitals and insurers (Phan et al., 2016; Hatamleh et al., 2016). Hsu et al. quoted an \$8400 cost involved with the trials and implants themselves, as well as over 12 hours spent outside of surgery editing the computer generated surgical plan and getting ethics approval for a tibiototalcaneal arthrodesis implant. Hamid et al. said that the implant and patient-specific instrumentation in a limb-salvage 3DP distal tibial mesh was approximately \$20,000; however, they demonstrated that amputation costs over a lifetime care cycle are more cost-prohibitive than previously thought owing to prosthetic cost. Wang et al. quoted that during thoracic rib reconstruction, the 3DP process cost about \$300 for thoracic model and \$13,800 for the titanium ribs. To better understand the economic impact, the increased surgical costs of 3DP needs to be compared to the costs of traditional treatments in a holistic manner; including societal costs of managing patients.

Table 2.3. Study characteristics

Authors	Type of study	Specialty/ location	Location	Year	N	Age (years)	Method of 3D printing	Follow-up time
Wei et al.	Case Report	Orthopaedic Oncology	Sacrum	2017	1	62	EBM	3, 8, 12 months
Ackland et al.	Case Report	Oral and Maxillofacial Surgery	TMJ	2017	1	58	SLM	6 months
Phan et al.	Case Report	Neurosurgery Spine Surgery	C-spine	2016	1	65	U/S	2 months
Leiser et al.	Case Report	Oral and Maxillofacial Surgery	Mandible	2016	1	25	SLS	6 months
Hatamleh et al.	Case Report	Oral and Maxillofacial Surgery	Mandible	2016	1	26	SLS	Not reported
Park et al.	Prospective Cohort	Neurosurgery	Skull	2016	21	28.6 +/- 19.4	EBM	6-22 months

Mobbs et al.	Case Series	Neurosurgery Spine Surgery	C/L-Spine	2017	2	63 and 52	U/S	9 and 12 months
Kim et al.	Case Report	Neurosurgery Spine Surgery	Sacrum	2017	1	16	EBM	1 year
Liang et al.	Retrospective Cohort	Orthopaedic Oncology	Pelvis	2017	35	36.9 +/- 17.1	EBM	20.5 months (6 to 30)
Wang et al.	Case Report	Thoracic Surgery	Ribs	2016	1	60	SLS	15 days
Li et al.	Retrospective Cohort	Orthopaedic Surgery	Hip	2015	24	7.3	DMLS	67 months (24–120)
Xu et al.	Case Report	Orthopaedic Spine Surgery	C-spine	2016	1	12	EBM	3m, 6m, 1 year
Wong et al.	Case Report	Orthopaedic oncology	Pelvis/ Hip	2015	1	65	SLM	10 months
Shan et al.	Case Series	Oral and Maxillofacial surgery	Maxilla/ Mandible	2015	4	35 +/- 11.3	U/S	6 month, 2 years, 5 years
Smith et al.	Case Series	Orthopaedic Surgery	MTP	2016	2	16 and 64	U/S	12 weeks
Imanishi et al.	Case Report	Orthopaedic Surgery Oncology	Calcaneus	2015	1	71	EBM	5 months
Stoffelen et al.	Case Report	Orthopaedic Surgery	Shoulder	2015	1	56	U/S	2.5 years
Stoor et al.	Prospective Cohort	Oral and Maxillofacial Surgery	Mandible	2017	14	62.4 +/- 10.4	EBM	33 months (6-49)
Hsu et al.	Case Report	Orthopaedic trauma	Ankle	2015	1	63	SLM	1 year
Aranda et al.	Case Report	Thoracic Surgery	Sternocostal Joint	2015	1	54	EBM	12 days
Li et al.	Case Report	Orthopaedic Spine Surgery	C-Spine	2017	1	53	EBM	12 months
Lee et al.	Case Report	Oral and Maxillofacial Surgery	TMJ/ Mandible	2016	1	25	EBM	2 weeks
Hamid et al.	Case Report	Orthopaedic Surgery	Ankle	2016	1	46	U/S	15 months
Fan et al.	Case Series	Orthopaedic Surgery Oncology	Shoulder/ Pelvis	2015	3	37.3 (21-56)	EBM	18, 21, 24 months
Chen et al.	Case Report	Orthopaedic surgery oncology	Pelvis	2015	1	62	EBM	Unknown

* Electron Beam Melting (EBM), Selective Laser Melting (SLM), Selective Laser Sintering (SLS), Unspecified (U/S), Direct Metal Laser Sintering (DMLS), Temporomandibular Joint (TMJ), Metatarsophalangeal Joint (MTP)

This systematic review is the first of its kind to specifically examine the surgical implantation of 3D printed metal inserts in musculoskeletal surgery. Due to the novelty of this technology and the recent advances that make it suitable for human implantation, poor quality studies such as case reports were expected and are inherently part of the limitations of this study. The surgical outcomes found in the reported studies are reported mostly as patient reported outcomes and have numerous sources of bias. Nevertheless, this review shows the feasibility and reproducibility of incorporating 3DP in surgical practice.

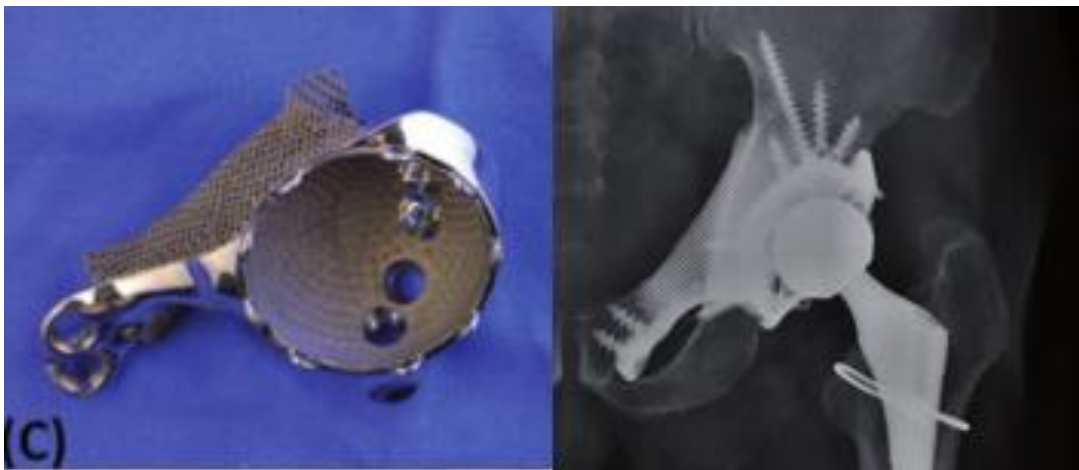


Figure 2.5. Picture and x-ray of 3D printed acetabular metal augment implanted during revision total hip (K. C. Wong et al., 2015)

2.4 Conclusion

The rapid increase in the popularity of 3D printing is a testament to its potential utility in surgery. Studies have shown promising results and have unveiled numerous potential advantages of using additive manufacturing. Nevertheless, in the medical field, 3D printing still requires a multidisciplinary team. Most surgeons are not familiar with the techniques involved in 3D printing and surgical planning may require interfacing with engineering colleagues

(Hoang, Perrault, Stevanovic, & Ghiassi, 2016). Further quality research is needed to fully grasp the role of 3D printed implants in musculoskeletal surgery. With further advances in technology, an increase in accessibility of 3D printing through cheaper production and easy-to-use software is expected. Real-time creation of specialized implants is becoming an option to musculoskeletal surgeons. With further research, 3D printing technology may enable substantial advances in surgical innovation.

2.5 References

- Ackland, D. C., Robinson, D., Redhead, M., Lee, P. V. S., Moskaljuk, A., & Dimitroulis, G. (2017). A personalized 3D-printed prosthetic joint replacement for the human temporomandibular joint: From implant design to implantation. *Journal of the Mechanical Behavior of Biomedical Materials*, 69(September 2016), 404–411. <http://doi.org/10.1016/j.jmbbm.2017.01.048>
- Almeida e Silva, J. S., Erdelt, K., Edelhoff, D., Araújo, É., Stimmelmayer, M., Vieira, L. C. C., & Güth, J. F. (2014). Marginal and internal fit of four-unit zirconia fixed dental prostheses based on digital and conventional impression techniques. *Clinical Oral Investigations*, 18(2), 515–523. <http://doi.org/10.1007/s00784-013-0987-2>
- Aranda, J. L., Jiménez, M. F., Rodríguez, M., & Varela, G. (2017). Tridimensional titanium-printed custom-made prosthesis for sternocostal reconstruction. *European Journal of Cardio-Thoracic Surgery*, 48(August 2015), e92-294. <http://doi.org/10.1093/ejcts/ezv265>
- Barazanchi, A., Li, K. C., Hons, B., Al-amleh, B., Lyons, K., Waddell, J. N., & Denttech, M. (2017). Additive Technology : Update on Current Materials and Applications in Dentistry, 26, 156–163. <http://doi.org/10.1111/jopr.12510>
- Bauermeister, A. J., Zuriarrain, A., & Newman, M. I. (2016). Three-dimensional printing in plastic and reconstructive surgery a systematic review. *Annals of Plastic Surgery*, 77(5), 569–576. <http://doi.org/10.1097/SAP.0000000000000671>

- Cavanaugh, P. K., Mounts, T., & Vaccaro, A. R. (2015). Use of 3-Dimensional Printing in Spine Care. *Contemporary Spine Surgery*, 16(1), 1–6.
- Chen, X., Xu, L., Wang, Y., Hao, Y., & Wang, L. (2015). Image-guided installation of 3D-printed patient-specific implant and its application in pelvic tumor resection and reconstruction surgery, 5, 66–78.
- Fan, H., Fu, J., Li, X., Pei, Y., Li, X., Pei, G., & Guo, Z. (2015). Implantation of customized 3-D printed titanium prosthesis in limb salvage surgery : a case series and review of the literature. *World Journal of Surgical Oncology*, 13(308), 1–10.
<http://doi.org/10.1186/s12957-015-0723-2>
- Hamid, K. S., Parekh, S. G., & Adams, S. B. (2016). Salvage of Severe Foot and Ankle Trauma With a 3D Printed Scaffold. *Foot & Ankle International*, 37(4), 433–439.
<http://doi.org/10.1177/1071100715620895>
- Hatamleh, M. M., Bhamrah, G., Ryba, F., Mack, G., & Huppa, C. (2016). Simultaneous Computer-Aided Design/Computer-Aided Manufacture Bimaxillary Orthognathic Surgery and Mandibular Reconstruction Using Selective-Laser Sintered Titanium Implant. *Journal of Craniofacial Surgery*, 27(7), 1810–1814.
<http://doi.org/10.1097/SCS.00000000000003039>
- Hoang, D., Perrault, D., Stevanovic, M., & Ghiassi, A. (2016). Surgical applications of three-dimensional printing : a review of the current literature & how to get started, 4(23).
<http://doi.org/10.21037/atm.2016.12.18>
- Hsu, A., & Ellington, J. K. (2015). Evolving Techniques } 3-Dimensional Printed Titanium Truss Cage With Tibiototalcalcaneal Arthrodesis for Salvage of Persistent Distal Tibia Nonunion. *Foot & Ankle SPecialist*, 8(6), 483–489.
<http://doi.org/10.1177/1938640015593079>.
- Imanishi, J., & Choong, P. F. M. (2015). CASE REPORT – OPEN ACCESS *International Journal of Surgery Case Reports* Three-dimensional printed calcaneal prosthesis

following total CASE REPORT – OPEN ACCESS. *International Journal of Surgery Case Reports*, 10, 83–87. <http://doi.org/10.1016/j.ijscr.2015.02.037>

Kim, D., Lim, J. Y., Shim, K. W., Han, J. W., Yi, S., Yoon, D. H., ... Shin, D. A. (2017). Sacral reconstruction with a 3D-printed implant after hemisacrectomy in a patient with sacral osteosarcoma: 1-year follow-up result. *Yonsei Medical Journal*, 58(2), 453–457. <http://doi.org/10.3349/ymj.2017.58.2.453>

Kim, G. B., Lee, S., Kim, H., Yang, D. H., Kim, Y., Kyung, Y. S., & Kim, C. (2016). Three-Dimensional Printing : Basic Principles and Applications in Medicine and Radiology, 17(2), 182–197.

Lee, U. L., Kwon, J. S., Woo, S. H., & Choi, Y. J. (2016). Simultaneous Bimaxillary Surgery and Mandibular Reconstruction With a 3-Dimensional Printed Titanium Implant Fabricated by Electron Beam Melting: A Preliminary Mechanical Testing of the Printed Mandible. *Journal of Oral and Maxillofacial Surgery*, 74(7), 1501.e1-1501.e15. <http://doi.org/10.1016/j.joms.2016.02.031>

Leiser, Y., Shilo, ã. D., & Wolff, ã. A. (2016). Functional Reconstruction in Mandibular Avulsion Injuries, 27(8), 2113–2116. <http://doi.org/10.1097/SCS.00000000000003104>

Li, H., Qu, X., Mao, Y., Dai, K., & Zhu, Z. (2016). Custom Acetabular Cages Offer Stable Fixation and Improved Hip Scores for Revision THA With Severe Bone Defects. *Clinical Orthopaedics and Related Research*, 474(3), 731–740. <http://doi.org/10.1007/s11999-015-4587-0>

Li, X., Wang, Y., Zhao, Y., Liu, J., Xiao, S., & Mao, K. (2017). Multi-level 3D printing implant for reconstructing cervical spine with metastatic papillary thyroid carcinoma. *SPINE*.

Liang, H., Ji, T., Zhang, Y., Wang, Y., & Guo, W. (2017). Reconstruction with 3D-printed pelvic endoprostheses after resection of a pelvic tumour. *Bone and Joint Journal*, 99–B(2), 267–275. <http://doi.org/10.1302/0301620X.99B2.BJJ20160654.R1>

- Logan, L., Hickman, R., Harris, S., & Heriza, C. (2008). Review research design : recommendations for levels of evidence and quality rating. *Developmental Medicine & Child Neurology* 2008, 50, 99–103. <http://doi.org/10.1111/j.1469-8749.2007.02005.x>
- Mao, Y., Xu, C., Xu, J., Li, H., Liu, F., Yu, D., & Zhu, Z. (2015). The use of customized cages in revision total hip arthroplasty for Paprosky type III acetabular bone defects. *International Orthopaedics*, 39(10), 2023–2030. <http://doi.org/10.1007/s00264-015-2965-6>
- Mobbs, R. J., Coughlan, M., Thompson, R., Sutterlin, C. E., & Phan, K. (2017). The utility of 3D printing for surgical planning and patient-specific implant design for complex spinal pathologies: case report. *Journal of Neurosurgery: Spine*, 26(4), 513–518. <http://doi.org/10.3171/2016.9.SPINE16371>
- Moiduddin, K., Al-Ahmari, A., Kindi, M. Al, Nasr, E. S. A., Mohammad, A., & Ramalingam, S. (2016). Customized porous implants by additive manufacturing for zygomatic reconstruction. *Biocybernetics and Biomedical Engineering*, 36(4), 719–730. <http://doi.org/10.1016/j.bbe.2016.07.005>
- Park, E.-K., Lim, J.-Y., Yun, I.-S., Kim, J.-S., Woo, S.-H., Kim, D.-S., & Shim, K.-W. (2016). Cranioplasty Enhanced by Three-Dimensional Printing. *Journal of Craniofacial Surgery*, 27(4), 943–949. <http://doi.org/10.1097/SCS.0000000000002656>
- Phan, K., Sgro, A., Maharaj, M. M., D’Urso, P., & Mobbs, R. J. (2016). Application of a 3D custom printed patient specific spinal implant for C1/2 arthrodesis. *Journal of Spine Surgery (Hong Kong)*, 2(4), 314–318. <http://doi.org/10.21037/jss.2016.12.06>
- Shan, X. F., Chen, H. M., Liang, J., Huang, J. W., & Cai, Z. G. (2015). Surgical Reconstruction of Maxillary and Mandibular Defects Using a Printed Titanium Mesh. *Journal of Oral and Maxillofacial Surgery*, 73(7), 1437.e1-1437.e9. <http://doi.org/10.1016/j.joms.2015.02.025>
- Simoneau, C., Terriault, P., Jetté, B., Dumas, M., & Brailovski, V. (2017). Development of a porous metallic femoral stem: Design, manufacturing, simulation and mechanical testing. *Materials and Design*, 114, 546–556. <http://doi.org/10.1016/j.matdes.2016.10.064>

- Smith, K. E., Dupont, K. M., Safranski, D. L., Blair, J. W., Buratti, D. R., Zeetser, V., ... Gall, K. (2016). Use of 3D printed bone plate in novel technique to surgically correct hallux valgus deformities. *Techniques in Orthopaedics*, 31(3), 181–189.
<http://doi.org/10.1097/BTO.0000000000000189>
- Stoffelen, D. V. C., Eraly, K., & Debeer, P. (2015). The use of 3D printing technology in reconstruction of a severe glenoid defect : a case report with 2 . 5 years of follow-up. *Journal of Shoulder and Elbow Surgery*, 24(8), e218–e222.
<http://doi.org/10.1016/j.jse.2015.04.006>
- Stoor, P., Suomalainen, A., Mesimaki, K., & Kontio, R. (2017). Rapid prototyped patient specific guiding implants in critical mandibular reconstruction. *Journal of Cranio-Maxillo-Facial Surgery*, 45, 63–70. <http://doi.org/10.1016/j.jcms.2016.10.021>
- Tack, P., Victor, J., Gemmel, P., & Annemans, L. (2016). 3D - printing techniques in a medical setting : a systematic literature review, 1–21. <http://doi.org/10.1186/s12938-016-0236-4>
- Viera, A. J., & Garrett, J. M. (2005). Understanding Interobserver Agreement : The Kappa Statistic. *Family Medicine*, 37(5), 360–363.
- Wang, L., Cao, T., Li, X., & Huang, L. (2016). Three-dimensional printing titanium ribs for complex reconstruction after extensive posterolateral chest wall resection in lung cancer. *Journal of Thoracic and Cardiovascular Surgery*, 152(1), e5–e7.
<http://doi.org/10.1016/j.jtcvs.2016.02.064>
- Wang, X., Xu, S., Zhou, S., Xu, W., Leary, M., Choong, P., ... Min, Y. (2016). Biomaterials Topological design and additive manufacturing of porous metals for bone scaffolds and orthopaedic implants : A review. *Biomaterials*, 83, 127–141.
<http://doi.org/10.1016/j.biomaterials.2016.01.012>
- Wei, R., Guo, W., Ji, T., Zhang, Y., & Liang, H. (2017). One-step reconstruction with a 3D-printed, custom-made prosthesis after total en bloc sacrectomy: a technical note. *European Spine Journal*, 26(7), 1902–1909. <http://doi.org/10.1007/s00586-016-4871-z>

Wong, K. C., Kumta, S. M., Geel, N. V., & Demol, J. (2015). One-step reconstruction with a 3D-printed, biomechanically evaluated custom implant after complex pelvic tumor resection. *Computer Aided Surgery*, 20(1), 14–23.

<http://doi.org/10.3109/10929088.2015.1076039>

Xu, N., Wei, F., Liu, X., Jiang, L., Cai, H., Li, Z., ... Liu, Z. (2016). Reconstruction of the Upper Cervical Spine Using a Personalized 3D-Printed Vertebral Body in an Adolescent With Ewing Sarcoma. *SPINE*, 41(1), E50–E54.

<http://doi.org/10.1097/BRS.0000000000001179>

CHAPTER 3

3 Measuring micromotion: A comparative study between the FARO arm and the digital image correlation system

Overview: This chapter familiarizes the reader with different methods of measuring bone-implant micromotion. It goes over the FARO Gage arm as well as the digital image correlation (DIC) system. The FARO arm is compared to the gold standard, DIC, and a linear regression is used to determine if the FARO arm correlates well with the DIC and whether it could be a convenient and accurate way of measuring bone-implant micromotion.

3.1 Introduction

In total knee arthroplasty (TKA), the motion between the components and the bone has been studied in great detail. Bone-implant micromotion is a measurement of implant fixation-stability and is used to predict implant loosening and failure (Jensen, Petersen, Schröder, Flivik, & Lund, 2012; Ryd et al., 1995). Clinically, implant migration is observed through radiographic analysis. Gross migration causing implant subsidence or radiolucency can be identified as signs of implant failure (Chambers, Fender, McCaskie, Reeves, & Gregg, 2001; Ro et al., 2016). In vivo, more accurate three-dimensional musculoskeletal implant motion techniques such as radiostereometric analysis (RSA) have been employed (Yuan et al., 2018). During the RSA technique, tantalum markers are inserted into the bone and prosthetic implant. Biplanar radiographs are taken of the limb and the position of the tantalum beads relative to each other is recorded in micrometers. Newer RSA methods use model-based radiostereometric analysis (MBRSA). A 3D model of the prosthetic implant captured by the radiographs is compared to the tantalum beads in the bone to measure the micromotion experienced by the

prosthetic implant. Yet, RSA can only accurately track changes that are more than 100 μ m and still lacks the precision of in-vitro measurement techniques that can predict small repetitive bone-implant micromotions that cause implant failure (Conlisk, Howie, & Pankaj, 2018). Digital image correlation (DIC) is one of numerous ways of measuring micromotion in vitro. With the improvement of high-resolution cameras, DIC has become the gold standard for bone-implant micromotion (Favre et al., 2016; Hosein, 2013; H. Xie & Kang, 2014). It can accurately measure bone-implant movement on the order of 3 μ m and has been described as more accurate than linear variable differential transducers (LVDT's). DIC measures true micromotion at the bone-implant interface and is not affected by confounders such as bones elastic deformation, which can affect LVDT measurements (Eitner, Köntges, & Brendel, 2010; Favre et al., 2011; Hosein, 2013). DIC is basically an optical system linked to a computer for storage of optical data. The optical system is composed of a high-resolution camera, a telecentric lens and a diffuse illuminator, which captures images of two points of interest in the same frame. The pixels of the acquired images are used as units of measurement between the two points of interest. The distance measured in pixels is then converted into micrometers. DIC has been used more recently in orthopaedic implant research to quantify bone-implant micromotion and predict implant loosening.

Moreover, tibial component aseptic loosening is a leading cause of primary and revision TKA failure requiring revision or re-revision surgery (Australian Orthopaedic Association, 2017; Canadian Institute for Health Information, 2015; Tomlinson & Harrison, 2012). Thus, improvements are constantly being made in order to increase tibial component fixation and decrease the burden of revision surgery. A cadaveric study was created to test a novel 3D printed titanium revision augment that fits into the proximal tibia during revision surgery. The goal of the 3D printed implant was to increase tibial component fixation-stability and prevent aseptic loosening. During the study both the primary and revision bone-implant micromotion was measured using both digital image correlation and the FARO Gage arm. The current study focuses on comparing the motion measurements acquired by the FARO Gage arm and the DIC system during this aforementioned study.

The FARO Gage arm is a coordinate measuring machine (CMM). It is a high-precision, portable 3D coordinate measurement system with measurement accuracy of 18 μ m. It has 6

degrees of freedom. Each joint has rotary optical encoders. The signals from the encoders are processed with advanced error coding and temperature compensation technology and the resultant positional data is sent to the host computer. Thus, it captures 3D data from objects and gives the position (XYZ) of the objects. The FARO Gage is mainly used in the industrial workplace or processing centers for part inspection, machine alignment, tool building and certification, and prototype scanning in fields such as aerospace engineering, reverse engineering and the automotive industry (FARO Technologies, 2014). To our knowledge, the FARO Gage arm has never been used for measurement of bone-implant micromotion. The purpose of this study was to compare the bone-implant micromotion measurement taken with the FARO Gage Arm (FARO Technologies, Lake Mary, FL, USA) and compare it to the measurements taken by the digital image correlation system (DIC). We hypothesized that the FARO Gage Arm would be a convenient way of measuring micromotion and would be comparable to DIC.

3.2 Materials and Methods

After institutional Research Ethics Board approval, eleven paired fresh-frozen cadavers (22 tibias) were tested at the University Hospital Orthopaedic Biomechanics Laboratory (UHOB-L). All specimens were thawed at room temperature overnight, skeletonized and potted into custom fixtures with screws and dental cement prior to testing. Primary total knee arthroplasty (pTKA) surgery was performed on all tibias. Fixation stability testing was conducted using a three-stage eccentric loading protocol. Static eccentric (70% medial/ 30% lateral) loading of 2100 N was applied to the implants before and after subjecting them to 5×10^3 loading cycles of 700 N at 2 Hz using an AMTI VIVO joint motion simulator. Bone-implant micromotion was measured using a digital image correlation system and a FARO Gage arm before, during and after each static load. The pTKAs were removed and revision surgery was performed on each tibia. One tibia from each pair was allocated to the experimental group using a systemic sampling model with random start, and rTKA was performed with a titanium 3D printed augment using selective laser melting. The contralateral side was assigned to the control

group (revision with cement filling). The three-stage eccentric loading protocol was used to test the revision TKAs and micromotion was assessed using both the DIC and FARO Gage arm.

Statistical analysis was performed to compare the FARO Gage arm measurement technique in relation to the DIC system. Linear regression of the pTKA and rTKA FARO and DIC data was done to assess the coefficient of correlation (R) and the coefficient of determination (R^2). The Pearson correlation was also calculated to determine the strength of the relationship between the FARO and DIC as an estimate of how the FARO measurements reflect the control (DIC).

3.2.1 FARO Gage Arm Measurements

Prior to data collection, the FARO Gage arm was calibrated using known immobile structures such as the VIVO base plate. A computer-aided design (CAD) model of the tibial tray was constructed using continuous data point collection with the FARO spherical probe (refer to figure 3.1). This CAD model was used to display the location (X,Y,Z) of the point relative to the CAD model on the CAM2® SmartInspect Basic v1.2 data acquisition software (FARO Technologies, Lake Mary, FL, USA, 2014). In order to capture specific points in space using the FARO Gage arm, spherical holes were placed in the tibial tray and in the bone in order to dock the FARO spherical probe (refer to figure 3.1). These docking holes were placed at five locations around the bone-implant interface. They were placed anteriorly, laterally, posterior-laterally, posterior-medially, and medially. During micromotion measurement, the FARO spherical probe was docked in the holes and the location of the point was recorded three times using the FARO “point mode”. The three measurements were taken in three different FARO arm positions while the probe was properly seated, in order to help triangulate the point of interest in space. The measurements of all bone and implant holes were done three times during every micromotion assessment, for a total of 9 recorded values per hole/point.

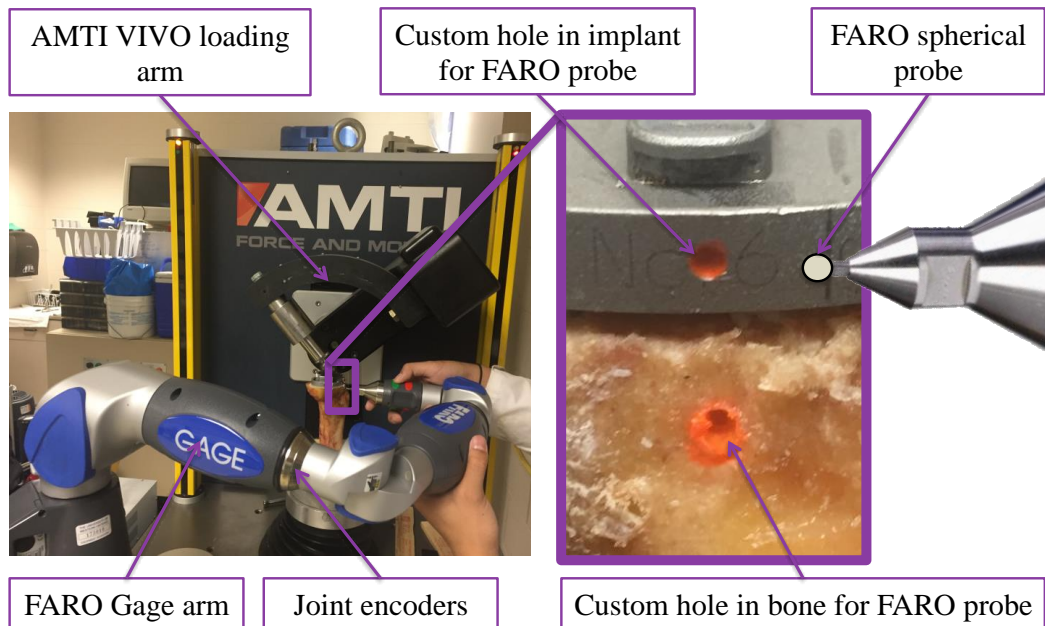


Figure 3.1. FARO Gage arm tibial bone-implant micromotion measurement technique

3.2.2 DIC System Measurements

Before micromotion measurement, the DIC camera was calibrated by taking a picture of a calibration grid with known division lengths of 0.05mm. The calibration yielded a pixel to μm conversion factor of $3.43\mu\text{m}/\text{pixel}$. The optical system used during this study consisted of: the pilot GigE Series piA 2400-12gm/gc camera (Basler AG, Ahrensburg, Germany); the telecentric lens (Opto Engineering, Matua, Italy); and the axial diffuse illuminator (Advanced Illumination, Rochester, VT, USA) (refer to figure 3.2). The resolution of the camera was 2452 by 2056 pixels and the field of view was 8 mm by 8 mm. This optical system was validated during a previous study by Hosein et al (Hosein, 2013). In order to create a large contrast between the markers and the background, liquid paper was placed on the implant and bone as a background for the fluorescent orange paint markers that were placed on top of the liquid paper. These markers were placed adjacent to the FARO Gage arm holes anteriorly, medially and posterior-laterally. The ImageJ (National Institutes of Health, Bethesda, USA) image software was then used to color threshold the markers and calculate the centroids of the markers (refer to

figure 3.2). The distance between these centroid (implant/bone) was calculated in an unloaded and loaded state in order to calculate the micromotion of the implant relative to the bone.

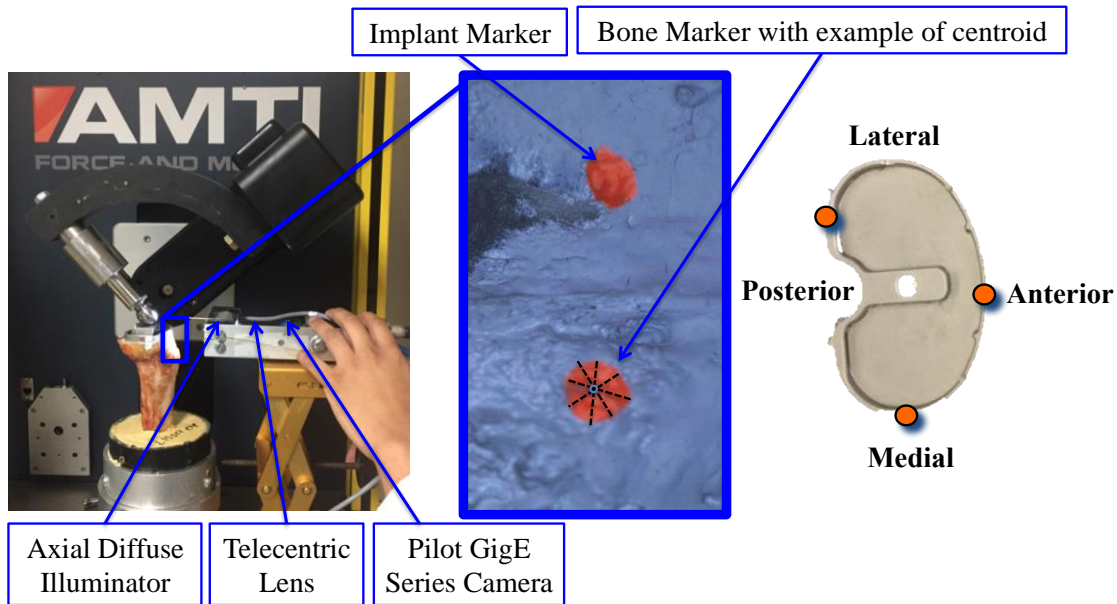


Figure 3.2. Digital image correlation system tibial bone-implant micromotion measurement technique.

3.3 Results

The bone-implant micromotion experienced by the pTKAs and the rTKAs during the 3 stage eccentric loading protocols was measured by both the FARO Gage arm and the DIC system. The mean axial micromotion is illustrated in Table 3.1.

Table 3.1. Mean axial micromotion measurements of the tibial component bone-implant interface in primary TKA (rTKA) and revision TKA (rTKA) using the FARO Gage Arm and the digital image correlation system (DIC).

Location	FARO pTKA		DIC pTKA		FARO rTKA		DIC rTKA	
	Mean	SD	Mean	SD	Mean	SD	Mean	SD
Medial	52.0	± 41.3	43.5	± 35.3	43.9	± 55.2	32.4	± 43.9
Anterior	49.1	± 40.3	51.1	± 35.9	37.0	± 48.3	29.4	± 24.6
PostLat	17.4	± 152.8	17.5	± 12.1	14.4	± 60.3	13.5	± 11.7

When the mean micromotion measurements taken by the FARO Gage arm and the DIC system are compared, they seem quite similar. The lowest implant subsidence in the primary TKA was posterior-laterally in both the FARO and DIC measurements. The medial and anterior aspects of the bone-implant interface experienced the greatest mean micromotion in both the FARO and the DIC system. The Shapiro-Wilk test determined that both the FARO and DIC data were non-parametric; therefore the Mann-Whitney U test was used to assess the significance of mean differences between the two types of revision implants. The DIC data found a statistically significant difference in vertical micromotion with higher micromotion in the revision TKA using conventional fully cemented stems in comparison to a revision TKA using the novel 3D printed titanium augment. These were significant before ($p=0.04$) and after ($p=0.009$) cyclic loading. Conversely, the FARO Gage data also found a significantly higher vertical micromotion in the conventional fully cement stem in comparison to the 3D printed implant. Again, these were also significant before ($p=0.04$) and after ($p=0.004$) cyclic loading.

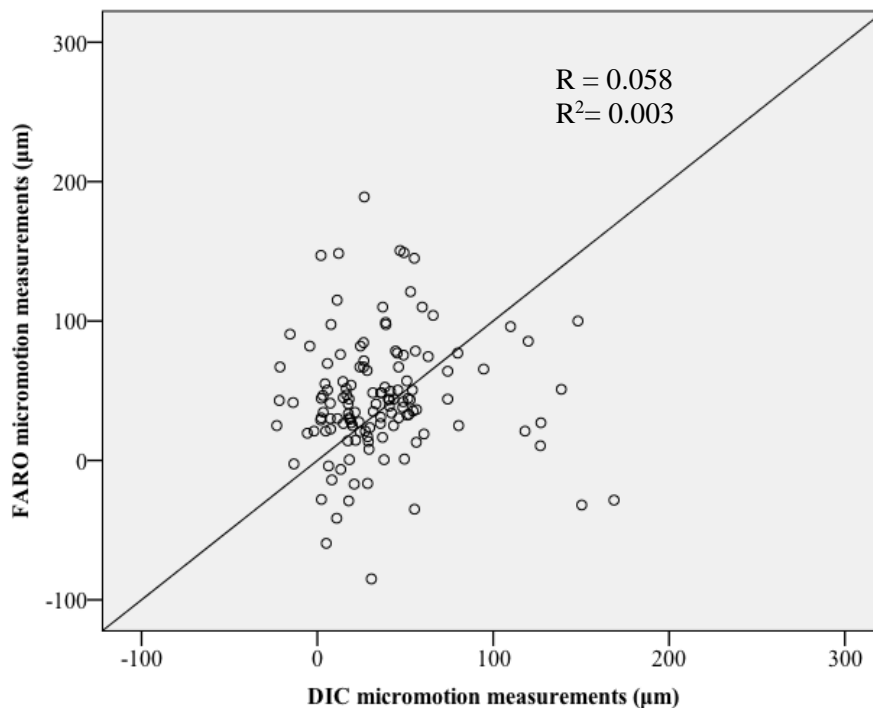


Figure 3.3. Linear regression of the FARO micromotion measurements and the DIC micromotion measurements of the tibial bone-implant motion in primary TKAs.

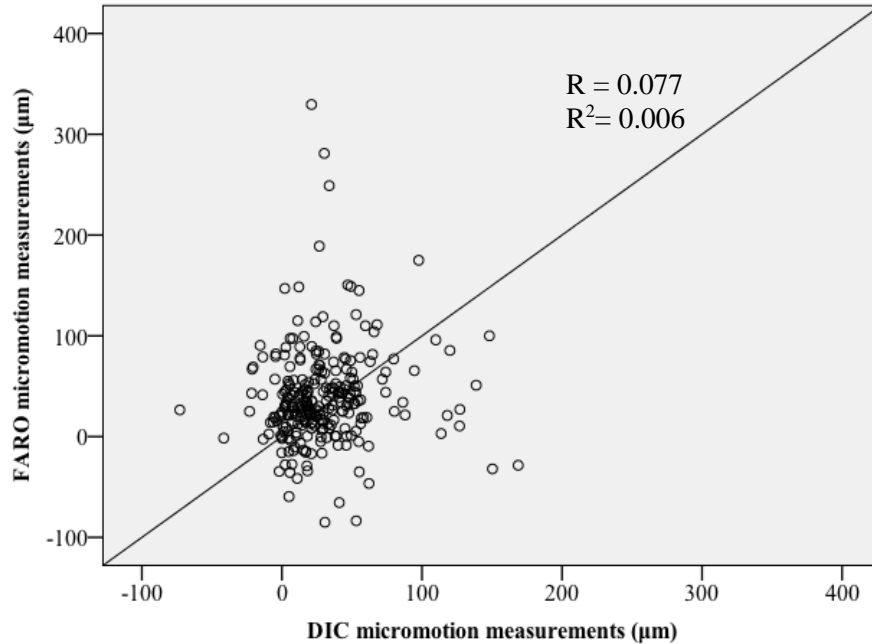


Figure 3.4. Linear regression of the FARO micromotion measurements and the DIC micromotion measurements of the tibial bone-implant motion in primary and revision TKAs.

Nevertheless, when the correlation between the FARO data and the DIC data was examined, it resulted in a low degree of relationship between the two measurement techniques. The FARO data is not correlated with the data from the DIC system, a highly precise measurement technique that has been proven to be effective at measuring bone-implant micromotion (Hosein, 2013). In primary TKA micromotion, the Pearson correlation between the FARO and DIC data was 0.058. The total motion data obtained from the revision and primary TKAs, from the FARO and DIC, resulted in a Pearson correlation of 0.077. These correlations are quite poor since they are far from 1.0 or -1.0. Furthermore, the linear regression models (refer to figure 3.3 and 3.4) also prove that the FARO and DIC measurements are not correlated with a R^2 of 0.003 for pTKA measurements and a R^2 of 0.006 for all measurements (pTKA and rTKA).

3.4 Discussion

With the advancement of technology, newer precision instruments are available for industrial and research based measurement. The FARO Gage arm is an example of a remarkably powerful tool that has been used for high-precision measurements in the fields of aerospace and automotive engineering (FARO Technologies, 2014). In medicine, the FARO arm has been studied for its use in computer-assisted-image-guided neurosurgery, knee surgery and kinematic studies of joints (Martelli, 2003; Rohling, Munger, Hollerbach, & Peters, 1995). It has also been used for anthropometric measurement in sport (Zampagni et al., 2006). In the current study, the FARO Gage arm was tested in order to determine if it could be used in orthopaedic bone-implant micromotion studies. The application of the FARO Gage arm was evaluated by comparing how close it mimics the measurements taken by a digital image correlation system, the gold standard in precise bone-implant micromotion measurement.

This study revealed that the FARO Gage Arm is unfortunately not a valid substitute to measure bone implant micromotion. Its correlation to the DIC system measurements was poor with a low coefficient of correlation (R) of 0.058 and 0.077. Crause et al. studied the use of the FARO Arm (Platinum) for the re-alignment and testing of the Southern African Large Telescope's Spherical Aberration Corrector. They found that single measurements of the same position were considerably less reliable when the arm is operated in widely different orientations. They determined that there was an overall uncertainty of approximately 90 μ m with measurements of fixed points. This was 50 μ m higher than the manufacturer specifications of the FARO arm that they used. They concluded that the most reliable results were obtained by taking 1000 measurements per point with the operator exercising the arm as much as possible. They also determined that a continuous stream of readings is more accurate than having the operator press the green button on the wrist of the arm for every data point (Crause, O'Donoghue, O'Connor, & Strümpfer, 2010). While 1000 measurements seems time consuming, the FARO arm can acquire data continuously at more than 50 Hz, which means that it would take 20 seconds to complete 1000 measurements (Martelli, 2003).

Mathematically, since the uncertainty of the FARO Gage Arm is known as 0.018mm, we can calculate the error propagation using a simple equation (2) (Martelli, 2003). The q

represents the quantity and the x and y the measurement values. We determined the distance between 2 measured points by subtracting their coordinates. Therefore, the uncertainty of each subtracted value needs to be added; thus, increasing the uncertainty from 18 μ m to 36 μ m. Furthermore, since we subtract the distance between the markers of the load (x) and pre-load (y) conditions to measure micromotion (q), the uncertainty of x and y are, again, added to obtain the error propagation of 72 μ m. The summary of the error propagation is presented in equation (4) and (5).

Values added or subtracted to calculate the quantity of micromotion:

$$q = x(+ \text{ or } -) y \quad (1)$$

Error propagation with known uncertainty:

$$\Delta q = \Delta x + \Delta y \quad (2)$$

Error propagation with random uncertainty:

$$\Delta q = \sqrt{(\Delta x^2 + \Delta y^2)} \quad (3)$$

Step 1 - Calculating distances between two recorded points:

$$Uncertainty = 0.018mm + 0.018mm = 0.036mm \quad (4)$$

Step 2 - Calculating Micromotion (difference between two distances):

$$Uncertainty = 0.036mm + 0.036mm = 0.072mm \quad (5)$$

In summary, the error propagation calculated indicates that the FARO Gage Arm would have an accuracy of 72 μ m for micromotion measurements, which, is not ideal when assessing bone-implant motion that often is less than 72 μ m. The authors accept that this study has limitations that may affect the validity of the results. To start, the holes made in the bone for the

docking of the FARO spherical probe were subject to deformation from probe insertion and from the loading of the bone by the VIVO joint simulator. The DIC and FARO data was acquired from different points that were adjacent to each other on the implant and bone, which might have yielded slightly different motion values. The acquisition of more points could have helped increase the precision and accuracy of the FARO Gage arm; however, the error margin would still be too high in comparison to the DIC system with an accuracy of 3 μ m (Hosein, 2013).

3.5 Conclusions

This study suggests that the FARO Gage arm is not a substitute for the digital image correlation system for the measurement of bone-implant micromotion. While it is not accurate enough for bone-implant micromotion measurements in orthopaedic research, other parts of medicine will surely benefit from its use and its convenience.

3.6 References

- Australian Orthopaedic Association. (2017). Australian Orthopaedic Association National Joint Replacement Registry; Hip, Knee & Shoulder Arthroplasty: Annual Report 2017. National Joint Replacement Registry, 1–380. Retrieved from [https://aoanjrr.sahmri.com/documents/10180/397736/Hip%2C Knee %26 Shoulder Arthroplasty](https://aoanjrr.sahmri.com/documents/10180/397736/Hip%2C%20Knee%26%20Shoulder%20Arthroplasty)
- Canadian Institute for Health Information. (2015). Hip and Knee Replacements in Canada: Canadian Joint Replacement Registry 2015 Annual Report, (September), 1–63. Retrieved from https://se-cure.cihi.ca/free_products/CJRR_2015_Annual_Report_EN.pdf
- Chambers, I. R., Fender, D., McCaskie, A. W., Reeves, B. C., & Gregg, P. J. (2001). Radiological features predictive of aseptic loosening in cemented Charnley femoral stems. *The Journal of Bone and Joint Surgery. British Volume*, 83(6), 838–42.

<http://doi.org/10.1302/0301-620x.83b6.11659>

- Conlisk, N., Howie, C. R., & Pankaj, P. (2018). Quantification of interfacial motions following primary and revision total knee arthroplasty: A verification study versus experimental data. *Journal of Orthopaedic Research*, 36(1), 387–396. <http://doi.org/10.1002/jor.23653>
- Crause, L. a., O'Donoghue, D. E., O'Connor, J. E., & Strümpfer, F. (2010). Use of a Faro Arm for optical alignment, 7739(July 2010), 77392S. <http://doi.org/10.1117/12.856810>
- Eitner, U., Köntges, M., & Brendel, R. (2010). Use of digital image correlation technique to determine thermomechanical deformations in photovoltaic laminates: Measurements and accuracy. *Solar Energy Materials and Solar Cells*, 94(8), 1346–1351. <http://doi.org/10.1016/j.solmat.2010.03.028>
- Favre, P., Perala, S., Vogel, P., Fucntese, S. F., Goff, J. R., Gerber, C., & Snedeker, J. G. (2011). In vitro assessments of reverse glenoid stability using displacement gages are misleading - Recommendations for accurate measurements of interface micromotion. *Clinical Biomechanics*, 26(9), 917–922. <http://doi.org/10.1016/j.clinbiomech.2011.05.002>
- Favre, P., Seebeck, J., Thistlethwaite, P. A. E., Obrist, M., Steffens, J. G., Hopkins, A. R., & Hulme, P. A. (2016). In vitro initial stability of a stemless humeral implant. *Clinical Biomechanics*, 32, 113–117. <http://doi.org/10.1016/j.clinbiomech.2015.12.004>
- Hosein, Y. K. (2013). The Effect of Stem Surface Treatment and Substrate Material on Joint Replacement Stability: An In-Vitro Investigation into the Stem-Cement Interface Mechanics under Various Loading Modes. Retrieved from <http://ir.lib.uwo.ca/etd/1479>
- Martelli, S. (2003). New method for simultaneous anatomical and functional studies of articular joints and its application to the human knee. *Computer Methods and Programs in Biomedicine*, 70(3), 223–240. [http://doi.org/10.1016/S0169-2607\(02\)00028-7](http://doi.org/10.1016/S0169-2607(02)00028-7)
- Ro, D. H., Cho, Y., Lee, S., Chung, K. Y., Kim, S. H., Lee, Y. M., ... Lee, M. C. (2016). Extent of vertical cementing as a predictive factor for radiolucency in revision total knee arthroplasty. *Knee Surgery, Sports Traumatology, Arthroscopy*, 24(8), 2710–2717. <http://doi.org/10.1007/s00167-016-4011-7>

- Rohling, R., Munger, P., Hollerbach, J. M., & Peters, T. (1995). Comparison of relative accuracy between a mechanical and an optical position tracker for image-guided neurosurgery. *Computer Aided Surgery*, 1(1), 30–34.
<http://doi.org/10.3109/10929089509106823>
- Technologies, F. (2014). CAM2 ® SmartInspect Basic v1.2 FaroArm/FARO Gage Training Workbook.
- Tomlinson, M., & Harrison, M. (2012). The New Zealand Joint Registry. *Foot and Ankle Clinics*, 17(January 1999), 719–723. <http://doi.org/10.1016/j.fcl.2012.08.011>
- Xie, H., & Kang, Y. (2014). Digital image correlation technique. *Optics and Lasers in Engineering*, 65, 1–2. <http://doi.org/10.1016/j.optlaseng.2014.07.010>
- Yuan, X., Broberg, J. S., Naudie, D. D., Holdsworth, D. W., & Teeter, M. G. (2018). Radiostereometric analysis using clinical radiographic views: Validation with model-based radiostereometric analysis for the knee. *Journal of Engineering in Medicine*, 232(8), 759–767. <http://doi.org/10.1177/0954411918785662>
- Zampagni, M. L., Dona, G., Motta, M., Martelli, S., Benelli, P., & Marcacci, M. (2006). a New Method for Anthropometric Acquisition of the Upper Extremity Parameters in Elite Master Swimmers. *Journal of Mechanics in Medicine and Biology*, 06(01), 1–11.
<http://doi.org/10.1142/S0219519406001741>

CHAPTER 4

4 Quantifying the magnitude and direction of micromotion in primary total knee arthroplasty

Overview: This chapter reviews primary total knee arthroplasty. A cadaveric study was completed looking at the magnitude and direction of micromotion experienced by primary total knee arthroplasty. These results were compared to the literature and can serve as a basis to improve pTKA in the goal of reducing micromotion and thus decreasing implant loosening.

4.1 Introduction

Cemented total knee arthroplasty (TKA) is the international standard of care for treating patients suffering from debilitating knee pain caused by end-stage knee arthritis (Australian Orthopaedic Association, 2017; Canadian Institute for Health Information, 2015; M. Khan et al., 2016; S. M. Kurtz et al., 2011; S. M. Lee, Seong, Lee, Choi, & Lee, 2012; Meftah et al., 2016; Tomlinson & Harrison, 2012). By replacing the damaged cartilage, TKA is highly successful at restoring function and relieving pain. In a survey of 18 countries, an estimated 1,324,000 TKAs are performed annually (S. M. Kurtz et al., 2011). The annual demand for primary total knee arthroplasty (pTKA) is expected to increase substantially in the years to come. In the United States alone, the demand for TKA is projected to rise by 673% by 2030 (M. Khan et al., 2016). Furthermore, a recent trend has demonstrated an increase in younger patients undergoing pTKA likely due to higher rates of obesity and the expanded clinical criteria for TKA eligibility (M. Khan et al., 2016; McCalden et al., 2013). Primary TKA has a survival rate of 90-95% at 10-15 years (Skwara et al., 2009). However, this might change with the introduction of younger patients getting knee replacement surgery. Patients under 55 years

old have a 5% risk of revision at only 3 years after surgery (Canadian Institute for Health Information, 2015). Aseptic loosening of the tibial component remains a major reason for failure of primary TKAs especially in the younger demographic (Canadian Institute for Health Information, 2015; Tomlinson & Harrison, 2012). Younger patients are at higher risk of early prosthesis failure requiring revision TKA because of their higher functional demands, which creates additional stress on the bone-implant interface (Gandhi et al., 2009; Hosein, 2013; Julin et al., 2010). Micromotion of the bone-implant interface leads to implant loosening (Ryd et al., 1995). There have been numerous studies evaluating tibial component micromotion using radiostereometric analysis (RSA). Yet, while RSA is an improvement in accuracy over standard X-rays, it can only track changes that are more than 100 μ m and is unable to track smaller repetitive micromotions that play a key role in implant loosening and failure (Conlisk et al., 2018). In order to track micromotion with accuracy, in vitro studies are needed with high precision tools such as digital image correlation (DIC) or linear variable differential transducers (LVDT's) in order to accurately measure bone-implant micromotion. Moreover, there are few studies in the literature that both quantify the magnitude and direction of the bone-implant micromotion experienced when pTKAs are subject to loading conditions. The purpose of this biomechanical cadaveric study was to determine the magnitude and direction of the tibial component bone-implant micromotion in primary fully cemented total knee arthroplasty and determine if there was a difference in micromotion between different regions of the TKA tibial implant.

4.2 Materials and Methods

After institutional Research Ethic Board approval, 22 tibias from 11 fresh frozen cadavers were tested at the University Hospital Orthopaedic Biomechanics Laboratory (UHOB-L) from November 2017 to January 2018. The cadaver specimens were completely de-identified. The implant retrieval lab at the University Hospital supplied the total knee replacement implants used during the study. These implants were cleaned prior to testing. All specimens were frozen (-20 degrees Celsius) and then thawed at room temperature overnight for 12 hours prior to testing. The specimens were cut to keep 18 cm of proximal tibia. The tibias

were skeletonized and the tibial shafts were potted into custom fixtures using dental cement and screws.

Primary total knee arthroplasty was completed on each tibia using a fully cemented technique, cementing both the baseplate and the stem. The Stryker Triathlon universal tibial baseplate (Stryker, Kalamazoo, MI, USA) and a 1.5 cm stem were used as the implant of choice for all TKAs.

4.2.1 Primary TKA technique

After the specimen was thawed overnight and skeletonized, the tibia was placed on a vertical intramedullary rod that was secured to the table. The rod was placed inside the intramedullary canal of the tibia (5cm). The vertical axis now represented the anatomic axis of the tibia. An extramedullary tibial guide (Stryker Triathlon knee system) was placed on the tibia. The tibial slope was set at 0 degrees. The proximal tibia cutting jig was adjusted with a lobster claw or angel wing caliper to ensure that the least amount of bone was removed during the proximal tibial bone cut. Three pins were placed in the proximal tibia cutting jig once it was aligned with the anatomic axis of the tibia. The proximal tibia was cut by an oscillating saw. The cut was perpendicular to the anatomic axis. A circular bubble level was placed on top of the tibial plateau to make sure the cut was neutral anterior-posteriorly and medial-laterally. The distal tibial cut was then made 18 cm from the proximal tibial cut using a ruler and oscillating saw. The tibia was removed from the intramedullary stand. The tibia was then placed in custom fixture ensuring that the proximal tibial cut remains neutral in the fixture. Once the dental cement (Denstone) from the custom fixtures was fully hardened the primary TKA was continued.

The tibia was then sized by placing a tibial component sizing jig (Universal tibial template) on the tibia. The sizing jig was aligned relative to the tibial tubercle and secured in place by two pins. The appropriate keel punch guide was then placed on the sizing jig. A keel punch was hammered into the proximal tibia using a mallet. The boss reamer was used to ream the intramedullary canal at the depth of the keel of the primary implant. The headless 3” pins, keel punch guide and tibial component sizing jib were removed. The polymethylmethacrylate (PMMA) bone cement (Surgical Simplex P, Stryker Howmedica Osteonics Corp, Rutherford,

NJ) was mixed without the use of a vacuum mixing device. Four minutes was given for the cement to acquire a workable state. The cement was applied to the undersurface of the tibial component and the proximal tibia. A constant pressure was applied on the implant after it as impacted into the proximal tibia until the cement was hard.

4.2.2 Testing protocol

Once the pTKAs were completed the markers were placed on the anterior, medial and posterior-lateral face of the bone-implant interface. These markers were used for the digital image correlation micromotion measurements. The specimen was transferred to the AMTI VIVO joint motion simulator. Fixation stability testing was conducted using a three-stage eccentric loading protocol. The loading was conducted using a straight vertical physiologic load. Static eccentric (70% medial/ 30% lateral) loading of 2100 N was applied to the implants before and after subjecting them to 5×10^3 loading cycles of 700 N at 2 Hz (Egloff et al., 2012; Mann, Miller, Goodheart, Izant, & Cleary, 2014; Peters, Mohr, Craig, & Bachus, 2001). Bone-implant micromotion was measured using digital image correlation. DIC provides micromotion analysis with greater precision than alternative methods such as linear variable displacement transducers (Small et al., 2016). Micromotion was measured in 3 locations: the anterior, medial and posterior-lateral face of the bone-implant interface. Liquid paper was placed on the implant and bone as a background and small drops of fluorescent orange paint were used as markers. The centroids of the markers were acquired after colour thresholding. The distance between the centroids (implant/bone) was calculated and was used to calculate the micromotion of the implant relative to the bone. The camera was calibrated in order to convert pixel data into micrometers. Statistical analysis was completed using SPSS Statistics version 23 (Armok, NY). The Shapiro-Wilk test was done to determine if data was normally distributed. The Mann-Whitney U test was used to compare the non-parametric data. A literature review was done to identify studies that could be compared to the results.

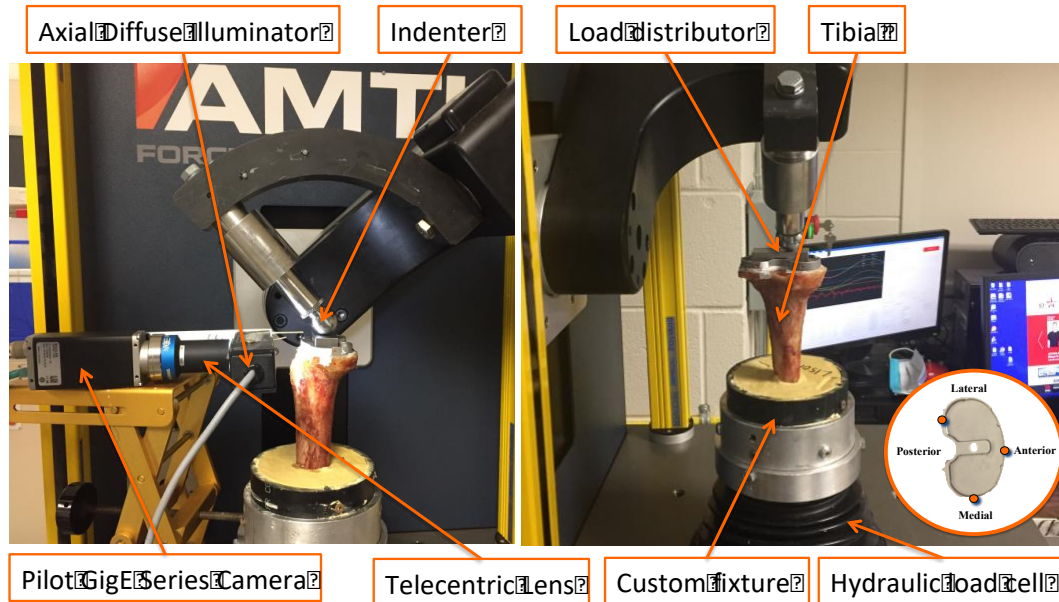


Figure 4.1. Setup for primary TKA load testing and micromotion measurement with the AMTI VIVO joint simulator and the Pilot GigE optical system. The location of the micromotion measurement is displayed in the bottom right corner.

4.3 Results

4.3.1 Vertical (Axial) micromotion

Primary total knee arthroplasty was successfully completed on 22 tibias using a fully cemented tibial component. No complications, such as intra-operative fractures, were seen that could compromise the integrity of the fixation-stability of the implants. The mean total vertical micromotion was $37.7\mu\text{m} \pm 36.5\mu\text{m}$ pre-cyclic loading and $33.4\mu\text{m} \pm 33.5\mu\text{m}$ post-cyclic loading. There were no significant differences in total mean vertical micromotion before or after cyclic loading ($p=0.37$).

The bone-implant micromotion was then subdivided into the location of measurement. The micromotion measured anteriorly, medially and posterior-laterally is summarized in table 4.1 and figure 4.2. A Kruskal-Wallis Test (one-way ANOVA on ranks) determined that there was a significant difference between the medial, anterior and posterior-lateral vertical micromotion (implant subsidence) ($p<0.001$). A post hoc test using the Bonferroni correction

and the Mann-Whitney U test proved that the anterior and medial vertical micromotion was significantly greater than posterior-lateral micromotion ($P < 0.001$) (refer to table 4.1).

Table 4.1. Significance of differences in vertical micromotion between anterior, medial and posterior-lateral micromotion. *Post hoc* Mann-Whitney U test with Bonferroni correction.

Comparison	Significance	Adjusted Significance
Posterolateral-Medial	<0.001	<0.001
Posterolateral-Anterior	<0.001	<0.001
Medial-Anterior	0.079	0.237

* the significance level is $p=0.05$

4.3.2 Horizontal or transverse micromotion

The variability of the transverse micromotion was high with a calculated variance of 8075. While the post-cycle data showed a trend for anterior-medial translation and some external rotation, the pre-cycle data showed posterior and more external rotation. The null hypothesis of the Kruskal-Wallis Test was retained; therefore, there was no significant difference in transverse micromotion between the medial, anterior and posterior-lateral regions of measurement. The mean micromotion after cyclic loading was $41.3\mu\text{m} \pm 119.5\mu\text{m}$ anteriorly for the medial marker, $1.5\mu\text{m} \pm 21.8\mu\text{m}$ medially for the anterior marker, and $21.8\mu\text{m} \pm 104.5\mu\text{m}$ medially for the posterior-lateral marker (refer to table 4.2 and figure 4.2).

Table 4.2. Vertical and horizontal micromotion (μm) pre and post-cycle

Location	Vertical Pre-cycle		Vertical Post-cycle		Horizontal Pre-cycle		Horizontal Post-cycle	
	Mean (μm)	SD (μm)	Mean (μm)	SD (μm)	Mean (μm)	SD (μm)	Mean (μm)	SD (μm)
Medial	46.6	± 37.6	38.6	± 35.7	-49.4	± 65.3	41.3	± 119.5
Anterior	51.9	± 38.9	50.3	± 33.5	-13.1	± 74.0	1.5	± 57.1
PostLat	14.5	± 18.6	11.3	± 15.4	12.3	± 81.3	6.9	± 7.2

- Note: Standard Deviation (SD)
 - Vertical: Positive values represent compression or inferior translation
 - Horizontal: Positive values represent medial translation for the anterior marker/location and anterior translation for the medial and posterior-lateral marker/location. SD: Standard deviation



Figure 4.2. Schematic representation of primary TKA post-cycle micromotion.

4.4 Discussion

Aseptic loosening is the leading cause of failure in primary total knee arthroplasty. Tibial component loosening is a major reason for revision TKA surgery (Australian Orthopaedic Association, 2017; Canadian Institute for Health Information, 2015; M. Khan et al., 2016; S. M. Kurtz et al., 2011; Morgan, Battista, & Leopold, 2005). The fixation-stability of the tibial component is therefore an important factor for achieving long term TKA survivorship. Numerous factors contribute to the success of the tibial component fixation such as prosthetic

design, degree of constraint, cementing technique and penetration, and type of fixation (Baker, Khaw, Kirk, Esler, & Gregg, 2007; Bert & Mcshane, 1998; Small et al., 2016).

This study compared the vertical micromotion experienced at the medial, anterior and posterior-lateral aspect of the bone-implant interface. There was a significantly greater implant subsidence at the anterior-medial aspect of proximal tibia ($p < 0.001$) with an axial micromotion of $38.6\mu\text{m} \pm 35.7\mu\text{m}$ medially and $50.6\mu\text{m} \pm 33.5\mu\text{m}$ anteriorly.

Lift-off is defined as the implant lifting off the bone when the contralateral side subsides. There was no lift-off seen during testing. Moreover, Bert et al. described maximal lift-off at the lateral bone-implant interface of the tibial component of TKA as $50\mu\text{m}$. They had a 2446 N load set posteromedially. The loading conditions were ambiguous and they used a LVDT to measure micromotion. The only measurable lift-off was in an implant that had an uncemented stem and a 1 mm cemented mantle under the tibial tray. Therefore, our study supports their conclusion that fully cemented tibial components have little to no lift-off in comparison to components with a thin surface cement mantle (Bert & Mcshane, 1998).

A study by Luring et al. compared cemented tibial stems versus hybrid fixation in a sawbone model with four loading condition. The implant was loaded anteriorly, laterally, medially and posteriorly. These loading conditions were not physiologic; nevertheless, anterior loading resulted in the highest micromotion and fully cemented tibial components had significantly lower bone-implant micromotion. This supports our findings that there was significantly higher amounts of anterior micromotion (Luring et al., 2006).

Small et al.'s 2016 study looked at micromotion at the tibial plateau of composite tibias in primary TKA. They compared fixed versus rotating platform designs. The tibial component was tested with posteromedial compressive loading followed by 10 degrees of external tibiofemoral malalignment. They used DIC for micromotion analysis. They found that fixed bearing primary tibial trays exhibited significantly higher micromotion in the medial and posteromedial measurement regions. They measured higher micromotion values posteromedially ($271\mu\text{m}$), posterolaterally ($235\mu\text{m}$) and laterally ($260\mu\text{m}$). These findings go against what was found in the current study. Yet, it was unclear whether the micromotion in Small et al.'s study represented total or axial micromotion. The micromotion values are also

substantially higher than any other study found in the literature as well as the current study, which might suggest that proper implant fixation was not achieved prior to testing.

Peters et al. reported bone-implant micromotion in the proximal tibia of primary TKA in a study comparing full versus surface cementation techniques. He found no difference in micromotion of the implant with either surface or full cementation. They used eccentric loading of 50N to 1500N for 6000 cycles at one Hz and measured higher micromotions medially and anteriorly in both surface and full cementation. These findings agree with what was demonstrated in this study.

The horizontal translation of the tibial component created from an axial load can be explained by implant subsidence. As the medial and anterior aspect of the tibial tray collapsed, the vertical load that was once perpendicular to the implant has now a component of its force that is applied parallel to the implant, thus creating shear forces and horizontal translation. Moreover, the subsidence of the implant and the change in the direction of the load relative to the implant also creates a moment and thus torque that can create rotational movement. There was a very high variability in the transverse micromotion measured during testing. The true direction of the horizontal motion measured during loading can be disputed due to its high variability; however, the fact remains that transverse and rotatory micromotion was seen and indicates that the pTKA might not be as rotationally and translationally stable as previously thought. Our cadaveric specimens were very heterogenous and differed in age, size and bone quality, which might have contributed to this high variability.

4.4.1 Limitations

The authors acknowledge limitation in the methods of this study. This study used a simplified version of human physiologic loading. A vertical eccentric load was applied to the tibial component of a primary TKA. Studies have demonstrated that the native knee and TKA joint contact force is 60-70% medial and 30-40% lateral (Egloff et al., 2012; Mann et al., 2014; Peters et al., 2001) during the stance phase of gait. Therefore, implant loading was performed 60-70% medial. Nevertheless, these conditions do not fully replicate the in vivo loading

conditions during gait. The tibial rotation, abduction/adduction and anterior-posterior/medial-lateral translation experienced relative to the femur were not accounted for in the loading protocol. Furthermore, the muscle and ligament forces were also excluded in this study.

Also, the results apply only to the implant tested, and may not be generalizable to other knee replacement systems (Small et al., 2016).

The markers used for the optical system were placed by hand and were not perfectly circular. Therefore, this can affect the accuracy of the location of the centroid calculated by ImageJ. Future improvements in DIC can develop a technique to place perfect circle as markers in order to have maximum accuracy during the calculation of the centroids and thus maximum accuracy during micromotion measurements.

4.5 Conclusions

This study examined, in detail, the micromotion experienced by the tibial component of primary fully cemented TKAs. It demonstrated that there was significantly higher implant subsidence at the anterior and medial bone-implant interface. This study revealed key issues in primary TKA implant migration. These findings can be used to improve current primary TKA implants and further reduce micromotion that would lead to reductions in implant loosening and failure.

4.6 References

Australian Orthopaedic Association. (2017). Australian Orthopaedic Association National Joint Replacement Registry; Hip, Knee & Shoulder Arthroplasty: Annual Report 2017. National Joint Replacement Registry, 1–380. Retrieved from [https://aoanjrr.sahmri.com/documents/10180/397736/Hip%2C Knee %26 Shoulder Arthroplasty](https://aoanjrr.sahmri.com/documents/10180/397736/Hip%2C%20Knee%26%20Shoulder%20Arthroplasty)

- Baker, P. N., Khaw, F. M., Kirk, L. M. G., Esler, C. N. A., & Gregg, P. J. (2007). A randomised controlled trial of cemented versus cementless press-fit condylar total knee replacement: 15-YEAR SURVIVAL ANALYSIS. *Journal of Bone and Joint Surgery - British Volume*, 89–B(12), 1608–1614. <http://doi.org/10.1302/0301-620X.89B12.19363>
- Bert, J. M., & Mcshane, M. (1998). Is It Necessary to Cement the Tibial Stem in Cemented Total Knee Arthroplasty ?, (356), 73–78.
- Canadian Institute for Health Information. (2015). Hip and Knee Replacements in Canada: Canadian Joint Replacement Registry 2015 Annual Report, (September), 1–63. Retrieved from https://se-cure.cihi.ca/free_products/CJRR_2015_Annual_Report_EN.pdf
- Conlisk, N., Howie, C. R., & Pankaj, P. (2018). Quantification of interfacial motions following primary and revision total knee arthroplasty: A verification study versus experimental data. *Journal of Orthopaedic Research*, 36(1), 387–396. <http://doi.org/10.1002/jor.23653>
- Egloff, C., Hügle, T., & Valderrabano, V. (2012). Biomechanics and pathomechanisms of osteoarthritis. *Swiss Medical Weekly*, 142(JULY), 1–14. <http://doi.org/10.4414/smw.2012.13583>
- Gandhi, R., Tsvetkov, D., Davey, J. R., & Mahomed, N. N. (2009). Survival and clinical function of cemented and uncemented prostheses in total knee replacement: A META-ANALYSIS. *Journal of Bone and Joint Surgery - British Volume*, 91–B(7), 889–895. <http://doi.org/10.1302/0301-620X.91B7.21702>
- Hosein, Y. K. (2013). The Effect of Stem Surface Treatment and Substrate Material on Joint Replacement Stability: An In-Vitro Investigation into the Stem-Cement Interface Mechanics under Various Loading Modes. Retrieved from <http://ir.lib.uwo.ca/etd/1479>
- Julin, J., Jämsen, E., Puolakka, T., Konttinen, Y. T., & Moilanen, T. (2010). Younger age increases the risk of early prosthesis failure following primary total knee replacement for osteoarthritis: A follow-up study of 32,019 total knee replacements in the Finnish Arthroplasty Register. *Acta Orthopaedica*, 81(4), 413–419. <http://doi.org/10.3109/17453674.2010.501747>

- Khan, M., Osman, K., Green, G., & Haddad, F. S. (2016). The epidemiology of failure in total knee arthroplasty. *Bone & Joint Journal*, 98–B(1 Supple A), 105–112.
<http://doi.org/10.1302/0301-620X.98B1.36293>
- Kurtz, S. M., Ong, K. L., Lau, E., Widmer, M., Maravic, M., Gómez-Barrena, E., ... Röder, C. (2011). International survey of primary and revision total knee replacement. *International Orthopaedics*, 35(12), 1783–1789. <http://doi.org/10.1007/s00264-011-1235-5>
- Lee, S. M., Seong, S. C., Lee, S., Choi, W. C., & Lee, M. C. (2012). Outcomes of the different types of total knee arthroplasty with the identical femoral geometry. *Knee Surgery & Related Research*, 24(4), 214–20. <http://doi.org/10.5792/ksrr.2012.24.4.214>
- Luring, C., Perlick, L., Trepte, C., Linhardt, O., Perlick, C., Plitz, W., & Grifka, J. (2006). Micromotion in cemented rotating platform total knee arthroplasty: Cemented tibial stem versus hybrid fixation. *Archives of Orthopaedic and Trauma Surgery*, 126(1), 45–48.
<http://doi.org/10.1007/s00402-005-0082-5>
- Mann, K. A., Miller, M. A., Goodheart, J. R., Izant, T. H., & Cleary, R. J. (2014). Peri-implant bone strains and micro-motion following in vivo service: A postmortem retrieval study of 22 tibial components from total knee replacements. *Journal of Orthopaedic Research*, 32(3), 355–361. <http://doi.org/10.1002/jor.22534>
- McCalden, R. W., Robert, C. E., Howard, J. L., Naudie, D. D., McAuley, J. P., & MacDonald, S. J. (2013). Comparison of outcomes and survivorship between patients of different age groups following TKA. *Journal of Arthroplasty*, 28(8 SUPPL), 83–86.
<http://doi.org/10.1016/j.arth.2013.03.034>
- Meftah, M., White, P. B., Ranawat, A. S., & Ranawat, C. S. (2016). Long-term results of total knee arthroplasty in young and active patients with posterior stabilized design. *Knee*, 23(2), 318–321. <http://doi.org/10.1016/j.knee.2015.10.008>
- Morgan, H., Battista, V., & Leopold, S. S. (2005). Constraint in Primary Total Knee Arthroplasty. *J Am Acad Orthop Surg*, 13(8), 515–524.
- Peters, C. L., Mohr, R. A., Craig, M. A., & Bachus, K. N. (2001). Tibial component fixation

with cement: full versus surface cementation techniques, 84132.

Ryd, L., Albrektsson, B. E., Carlsson, L., Dansgard, F., Herberts, P., Lindstrand, A., ...

Toksvig-Larsen, S. (1995). Roentgen stereophotogrammetric analysis as a predictor of mechanical loosening of knee prostheses. *J Bone Joint Surg Br*, 77(3), 377–383.

<http://doi.org/0301-620X/95/3974>

Skwara, A., Figiel, J., Knott, T., Paletta, J. R. J., Fuchs-Winkelmann, S., & Tibesku, C. O.

(2009). Primary stability of tibial components in TKA: In vitro comparison of two cementing techniques. *Knee Surgery, Sports Traumatology, Arthroscopy*, 17(10), 1199–1205. <http://doi.org/10.1007/s00167-009-0849-2>

Small, S. R., Rogge, R. D., Malinzak, R. A., Reyes, E. M., Cook, P. L., Farley, K. A., & Ritter, M. A. (2016). Micromotion at the tibial plateau in primary and revision total knee

arthroplasty: fixed versus rotating platform designs. *Bone and Joint Research*, 5(4), 122–129. <http://doi.org/10.1302/2046-3758.54.2000481>

Tomlinson, M., & Harrison, M. (2012). The New Zealand Joint Registry. *Foot and Ankle*

Clinics, 17(January 1999), 719–723. <http://doi.org/10.1016/j.fcl.2012.08.011>

CHAPTER 5

5 Revision total knee arthroplasty using a novel 3D printed titanium augment: A biomechanical cadaveric study.

Overview: This chapter is the main study of the thesis. It goes over revision arthroplasty, and the current options available to treat the tibial bone defect encountered during revision TKA. The chapter compares the fixation-stability of the proximal tibial component after revision TKA using the conventional fully cemented stem versus a novel 3D printed titanium augment.

5.1 Introduction

Total knee arthroplasty (TKA) is an effective means of treating end stage arthritis (Arima et al., 1998; Jacobs, Clement, & Wymenga, 2005; S. M. Kurtz et al., 2011; Maradit Kremers et al., 2015). With the aging population, the rising prevalence of risk factors such as obesity and the necessity to maintain active lifestyles, the demand for primary total knee arthroplasty (pTKA) is expected to increase considerably. In the United States alone, the demand for TKA is projected to rise by 673% to 3.48 million procedures by 2030 (M. Khan et al., 2016).

With the increasing number of total knee arthroplasty procedures performed annually, the burden of revision surgery (rTKA) is also expected to increase. Total knee arthroplasty revisions are projected to grow from 38,300 in 2005 to over 268,200 in 2030 (S. Kurtz, Ong, Lau, Mowat, & Halpern, 2007) if the revision burden (the ratio of primary to revision arthroplasties) stays constant at around 8%. This might be an underestimation of the shear growth in numbers of rTKAs since the revision burden may also increase with time. The

number of younger patients undergoing primary total joint replacements is rising due to increasing rates of obesity and the expanded clinical criteria for TKA eligibility. Due to this demographic shift, the demand for TKA amongst patients aged less than 65 years is predicted to account for more than 50% of the primary TKAs in the next 2 decades (M. Khan et al., 2016). Younger patients are known for having a higher risk of early prosthesis failure requiring revision TKA because of their higher functional demands (Gandhi et al., 2009; Hosein, 2013; Julin et al., 2010). In Sweden, patients aged less than 65 years have twice the risk of revision compared with those aged more than 75 years (M. Khan et al., 2016). The underlying issue with this inevitable rise in revision knee surgery is that compared to primary TKA, revision TKAs have poorer results in terms of patient satisfaction and longevity (Bole, Teeter, Lanting, & Howard, 2018). Their survivorship have been quoted as low as 60% over shorter periods (J. Cherian et al., 2016). Therefore, improvement of revision knee surgery is mandated.

There are multiple reasons for failure of primary TKAs such as infection, pain, instability, periprosthetic fracture, osteolysis, dislocation and bearing surface wear. Nevertheless, the most common indication for revision surgery after primary TKA is aseptic loosening (29.8%) and more specifically loosening of the proximal tibial component (M. Khan et al., 2016; Tomlinson & Harrison, 2012; J. Cherian et al., 2016; Goodheart, Miller, & Mann, 2014). Additionally, during revision TKA, proximal tibial bone loss is frequently encountered. This can complicate revision surgery, and possibly result in a less-stable bone-implant fixation.

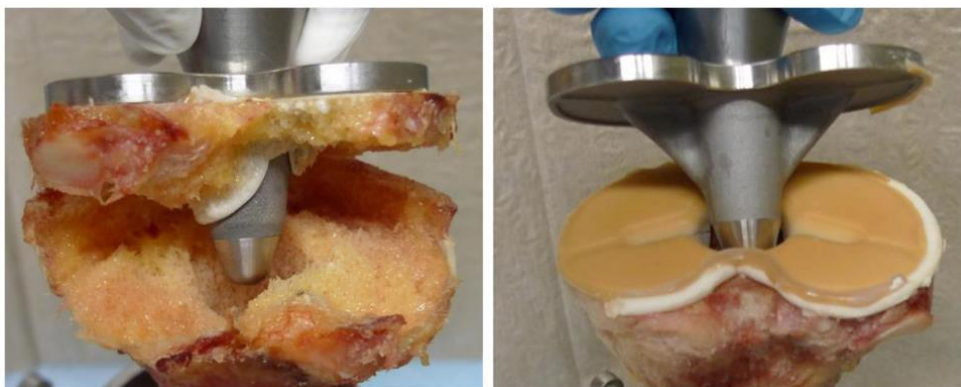


Figure 5.1. Example of TKA removal with failure of the cement-bone interface (left) vs. the cement-implant interface (right). Image taken from (Schlegel, Bishop, Püschel, Morlock, & Nagel, 2014): copyright SICOT-J under the Creative Commons license.

In more detail, the bone loss during rTKA can result from the underlying etiology that caused implant failure as well as the iatrogenic bone lost during implant removal. During removal of primary TKA, bone loss can occur when the implant/cement is removed along with some bone or when the cement separates from the implant and careful removal of this residual cement from the proximal tibia is required. The old cement needs to be removed in order to have virgin bone that will allow for the interdigitation of the newly applied cement securing the revision implant (refer to figure 5.1). Proximal tibial bone defects have been classified in numerous different ways (Bole et al., 2018)(Saleh et al., 2001). The Anderson Orthopaedic Research Institute (AORI) classification of bone defects is the most widely used classification of bone defect and is useful for guiding revision TKA (Panegrossi et al., 2014). (refer to figure 5.2).

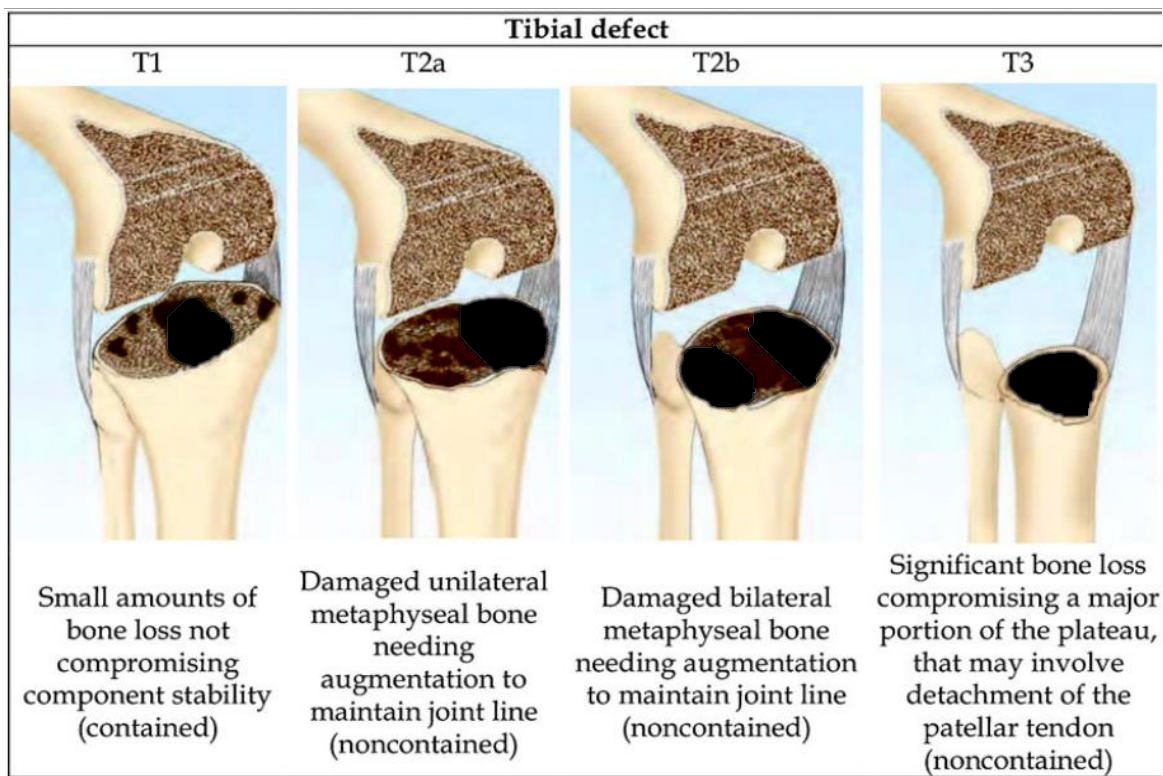


Figure 5.2. Anderson Orthopaedic Research Institute (AORI) tibia bone defect classification. Image taken from (Panegrossi et al., 2014): copyright SICOT-J under the Creative Commons license.

Regardless of the size of the bone defect, the aim of revision surgery is to relieve pain and improve function while reconstructing a stable platform to transfer load to the host bone (Whittaker, Dharmarajan, & Toms, 2008b). Consequently, the bony defects can be treated with the use of longer stems in combination with cement filling, modular metal augments or bone grafts (Efe et al., 2011). Long fully cemented tibial stems have been used for over two decades in revision knee surgery and have been considered the standard of care in the case of poor bone stock (Bole et al., 2018; Dennis et al., 2008; Whaley, Trousdale, Rand, & Hanssen, 2003; Whittaker et al., 2008b). Nevertheless, there is a clear need for improvement. Cement has been shown to deform and degrade over years and has weak resistance to tension and shear forces (Gandhi et al., 2009). Creep, or plastic deformation of cement over time, is a problem that steadily compromises the long-term fixation of implants (Jeffers, Browne, & Taylor, 2005).

5.1.1 Revision total knee arthroplasty and tibial bone loss

The proximal tibia can be divided into three anatomic zones of fixation during revision total knee arthroplasty: zone 1, the epiphysis or joint surface; zone 2, the metaphysis; and zone 3, the diaphysis (Morgan-Jones et al., 2015) (refer to figure 5.3). Proper rTKA fixation-stability can be achieved with a combination of any one of these zones.

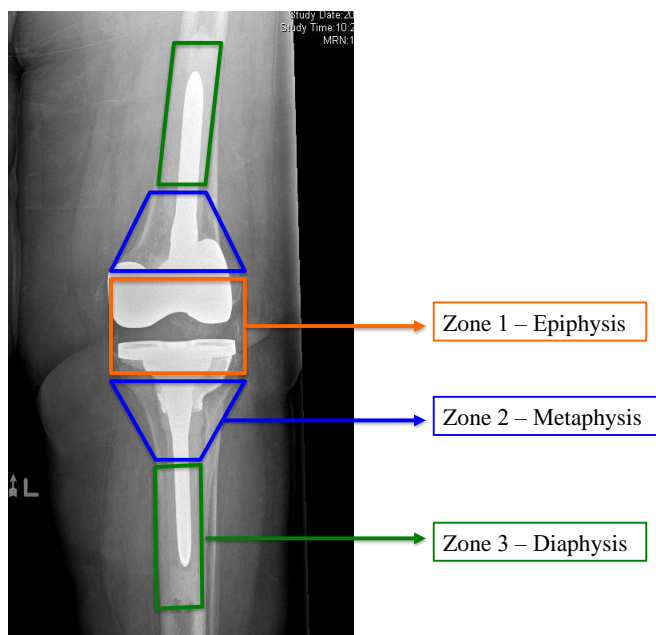


Figure 5.3. Zones of fixation during revision TKA.

5.1.1.1 **Epiphyseal fixation**

During revision surgery, it is necessary to establish a stable surface free of cement debris and avascular bone in order to ensure proper zone 1, epiphyseal fixation. Biologic or cement fixation can be used during implantation. Yet, Morgan-Jones states that zone 1 fixation can only be reliably achieved with polymethylmethacrylate cement (Morgan-Jones et al., 2015).

5.1.1.2 **Diaphyseal fixation**

In order to improve the quality of the alignment and stability, rTKA systems have increasingly used long intramedullary stems. These can be cemented or press-fit in a cementless fashion. While the use of a stems gives the rTKA additional fixation, it is also a source of intractable end-of-stem pain requiring re-revision surgery (Alexander, Bernasek, Crank, & Haidukewych, 2013; Barnett et al., 2014). Some have quoted that up to 23% of patients undergoing rTKA with stems complained of end-of-stem pain (Alexander et al., 2013). End-of-stem pain exists because of a stiffness mismatch between the tip of the prosthetic stem and the host bone. This mismatch results in proximal stress shielding as well as increased peak contact pressures at the tip of the stem (Glenn, Sokoloski, Damer, & Tabit, 2010). Furthermore, the stiff fixation achieved in the diaphysis has been demonstrated to off-load the metaphysis and initially protect the epiphyseal cemented interface from failure. However, because of this, it has also shown to cause stress shielding and bone loss at the epiphysis-metaphysis compromising long term fixation (Whittaker et al., 2008b). Consequently, recent studies have been focused on achieving better metaphyseal fixation.

5.1.1.3 **Metaphyseal fixation**

Metaphyseal rTKA fixation and bone reconstruction is guided by the AORI classification (Daines & Dennis, 2012). For AORI type 1 bone defects, where the lower metaphyseal bone is intact, cement filling is used to fill the bone loss and achieve proper implant fixation. This can be reinforced with screws if the defect approaches a AORI type II (Panegrossi et al., 2014).

For AORI type II bone defects, where the metaphyseal bone is damaged and is uncontained, different methods have been described to reconstruct the bone defect. Bone grafts such as impacted morsellized bone grafts have been used historically to restore the bone loss. However, the defect needed to be contained, and the bone chips need to be a specific size to ensure bony integration. The chips less than 0.5 mm are reabsorbed by the inflammatory process and the chips bigger than 10 mm have a slow inconvenient integration (Whiteside, 1998). Modular metal augments are used for AORI type II and III bone defects and are connected to the undersurface of the tibial tray. These give a surgeon the ability to rapidly fill a bone defect. Still, in the long run, the difference in stiffness or elasticity between the metal and bone caused stress shielding and bone loss. Newer modular implants have a higher volumetric porosity and the potential for bony ingrowth (Panegrossi et al., 2014).

AORI type III bone defects are uncontained defects compromising the majority of the tibial plateau. Historically, for younger patients, the bone defect was reconstructed with structural bone allograft. This had the potential to re-establish bone stock. Conversely, its disadvantages include late resorption secondary to immune reaction, fracture and non-union. Moreover, other options for type III bone defects are metaphyseal trabecular metal cones. These titanium or tantalum cones have a high coefficient of friction and are highly porous allowing for bony integration (Haidukewych, Hanssen, & Jones, 2011). They are inserted by press-fit technique into the proximal tibia. The tibial tray is then cemented to the cone. While they are found to have predictable radiographic bony ingrowth and have good short term clinical outcomes, they are costly and tend to irritate the surrounding soft tissues (De Martino et al., 2015; Long & Scuderi, 2009; Meneghini, Lewallen, & Hanssen, 2008; Haidukewych et al., 2011; Panegrossi et al., 2014). Another option for type III bone defect reconstruction is metaphyseal sleeves. With the use of broach technique to prepare the bone for press-fit implantation, the sleeves are inserted and have the capacity for osseointegration. Sleeves enhance rotational stability. They have yielded encouraging short-term results; however, they can cause tibial fractures when broaching the sleeves. Most of the studies on tantalum cones and sleeves have the cones or sleeves coupled with the use of long diaphyseal cemented or press-fit stems; therefore, it is difficult to truly appreciate whether the fixation-stability was achieved secondary to metaphyseal fixation with the sleeve or cone, or whether it was achieved more by the diaphyseal fixation of the stem (Haidukewych et al., 2011). Not to mention the re-

revision surgery required to treat the intractable end-of-stem pain (Barrack, Stanley, Burt, & Hopkins, 2004; Beckmann et al., 2011; Glenn et al., 2010; Kimpton, Crocombe, Bradley, & Gavin Huw Owen, 2013; Ranawat, Atkinson, & Paterson, 2012). Trabecular cones and sleeves have shown some promise for tibial bone defect reconstruction but few long-term outcome studies are available on these new techniques.

In summary, even with the current available options for revision surgery, revision total knee arthroplasty is less successful in longevity and patient satisfaction than primary TKA (Bole et al., 2018). The New Zealand Joint Registry has analyzed the cause of re-revision surgery after rTKA. The top three reasons for re-revision surgery were deep infection, pain and loosening of the tibial component. Therefore, the need for stronger longer-lasting proximal tibial rTKA fixation is evident. The need for better implant fixation is particularly important at zone 2 or at the metaphysis to reduce our dependency on diaphyseal fixation, which is known to cause end-of-stem pain, a leading cause of re-revision surgery. The increasing number of patients undergoing TKA and at a younger age foreshadows the exponential need for revision TKA (Haidukewych et al., 2011). In order to avoid the personal and economic burden associated with the poor outcomes of revision TKA surgery, innovative fixation techniques are mandated.

Recent advances in technology have made 3D printing or additive manufacturing suitable for human implantation. 3D printing can create complex free-form structures that would be impossible using conventional subtractive manufacturing (Chen et al., 2015). Therefore, a 3D printed titanium alloy (Ti6Al4V) revision augment that conforms to the irregular shape of the proximal tibia was recently developed. The first step in testing this newly developed implant was to test its fixation stability in a cadaveric model with the iatrogenic bone defect (AORI type 1) encountered after removal of the primary total knee replacement. The revision TKA with the novel 3D printed augment was compared to the current standard of care in revision surgery.

5.1.2 Purpose and hypothesis

The purpose of this cadaveric biomechanical study is to determine the fixation stability of a revision total knee arthroplasty (TKA) using a novel 3D printed titanium augment in comparison to a conventional fully cemented revision stem in AORI type 1 bone defects. We hypothesized that the press-fit fixation achieved in a cadaveric model by the novel 3D printed augment would have equivalent or better fixation-stability in comparison to the conventional fully cemented revision TKA. Sufficient press-fit fixation of the 3D printed augment shown in the cadaveric model would demonstrate that bony ingrowth in-vivo would occur and lead to potential long-term improvements in fixation stability of revision total knee replacements.

5.2 Materials and Methods

5.2.1 Novel augment design and printing

Preliminary research was done on the shape of the proximal tibia as well as the shape of the bone defect encountered after the removal of failed primary TKAs during revision surgery. The co-authors were involved in a study on tibial bone defect size and shape following total knee revision surgery (Bole et al., 2018). In this study, 118 patients who underwent revision TKA from January 2005 to February 2014 were included. Tibial defect size and shape was assessed. The anteroposterior and lateral views of the six-week post-operative radiographs were taken and measurements of the bone defects were analyzed using ImageJ. Bone defect was determined by measurements of the implants, augments and cement mantle. This study, along with the expert opinion of fellowship trained arthroplasty surgeons were the foundation for the creation of an anatomic proximal tibial augment for revision TKA. A 3D digital model of the implant was created. The novel tibial augments were then printed using this 3D digital model by selective laser melting of a titanium alloy (Ti6Al4V) by Additive Design in Surgical Solutions (ADEISS) in London, Ontario (refer to figure 5.4).



Figure 5.4. Novel 3D printed titanium revision TKA augment for the proximal tibia.

5.2.2 Experimental method

5.2.2.1 Specimen preparation

Eleven paired fresh cadavers (22 knees) were tested at the University Hospital Orthopaedic Biomechanics Laboratory (UHOB-L) from November 2017 to January 2018. The cadaver specimens were completely de-identified. The implant retrieval lab at the University Hospital supplied the total knee replacement implants used during the study. These implants were cleaned prior to testing. All specimens were frozen (-20 degrees Celsius) and then thawed at room temperature overnight for 12 hours prior to testing. The specimens were cut to keep 18

cm of proximal tibia. The tibias were skeletonized and the tibial shafts were potted into custom fixtures using dental cement and screws (refer to figure 5.5).

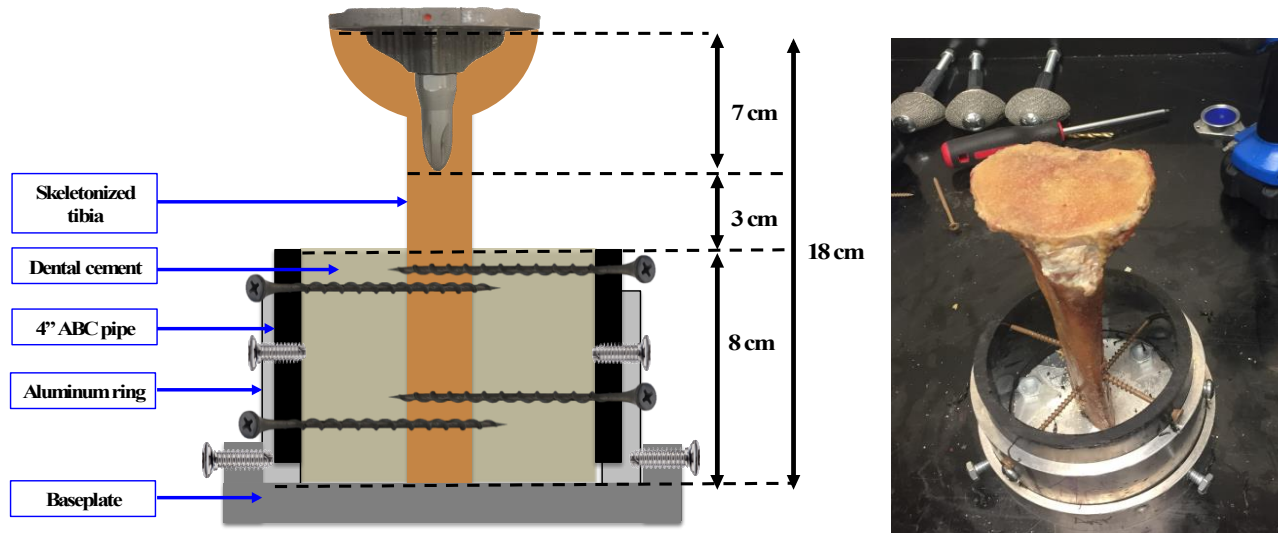


Figure 5.5. Schematic (left) and actual (right) representation of the custom fixtures used for testing. Note that the actual representation represents the screw fixation acquired prior to pouring the dental cement.

5.2.2.2 General protocol

After institutional Research Ethics Board approval was obtained, preliminary testing was done with four sawbone specimens prior to actual testing with the 22 cadaveric tibias. This was done in order to have a learning curve during preliminary testing and minimize any learning curve during cadaveric testing; thus, standardizing the cadaveric testing. Examples of the sawbones used during preliminary testing are presented in figure 5.9 (refer to figure 5.9).

Primary total knee arthroplasty (pTKA) surgery was performed on all tibias. The Stryker Triathlon universal tibial baseplate (Stryker, Kalamazoo, MI, USA) system was used with a 1.5 cm stem for primary TKA surgery. Fixation stability testing was conducted using a three-stage eccentric loading protocol and the resultant micromotion was measured using a

digital image correlation system (DIC). The primary TKAs were removed surgically by a single surgeon (CAD) and the bone defect was measured using the Anderson Orthopaedic Research Institute (AORI) classification as well as volumetric measurements using silicone mold casting. Time to complete explantation of the pTKA was recorded. The allocation of the control and experimental group was completed. One tibia from each pair was allocated to the experimental group using a systemic sampling model with random start, and revision TKA was performed with the 3D printed titanium augment. The contralateral side was assigned to the control group, and revision TKA was performed with a conventional fully cemented stem. The Stryker Triathlon universal tibial baseplate (Stryker, Kalamazoo, MI, USA) was used with a 5 cm long stem for the revision TKA for both the control and experimental group. The three-stage eccentric loading protocol was repeated and micromotion measurements were obtained for both the control and experimental groups. The rTKAs were explanted by a single surgeon (CAD) and the resultant bone defect was assessed using volumetric measurements. Time to complete explantation of the rTKA was recorded.

5.2.2.3 **Statistical analysis**

Statistical analysis was completed using SPSS Statistics version 23 (Armok, NY). The Shapiro-Wilk test was done to determine if data was normally distributed. The non-parametric data (not normally distributed) obtained for the micromotion were compared using the Mann-Whitney U test. P values less than 0.05 were considered significant. The parametric data (normally distributed) from the bone defect volumes were compared using an independent T-test. Absolute values were used to compare the magnitude of the micromotion and the true values were used to describe the vector of the micromotion. The coefficient of variation or relative standard deviation was used to express the precision and repeatability of the volumetric measurement of the proximal tibial bone defect using the silicone molding technique.

5.2.3 Description of the equipment

5.2.3.1 Loading device

The AMTI VIVO six degree of freedom joint simulator was used for the testing protocol. The VIVO joint simulator provides accurate robotic joint motion simulation for the knee. VIVO was used to apply both static and cyclic loads during testing of the primary and revision TKAs (refer to figure 5.6). The custom fixtures were securely bolted to the VIVO mounting plate on the lower stage. A custom metal load distributor was manufactured. The load distributor fit perfectly on the tibial tray. Its medial-lateral length was measured and a 1mm hole was placed medial to its center (70% medial relative to total length of load distributor). This hole accommodated the indenter and gave it additional stability during loading. Anterior-posteriorly, the center of the tibial tray was determined and the load distributor was placed at this location. During testing, the specimen was slowly raised in order to properly position the indenter on the load distributor. Once the indenter was in contact with the load distributor, the load was gradually applied over a few seconds by raising the lower stage.

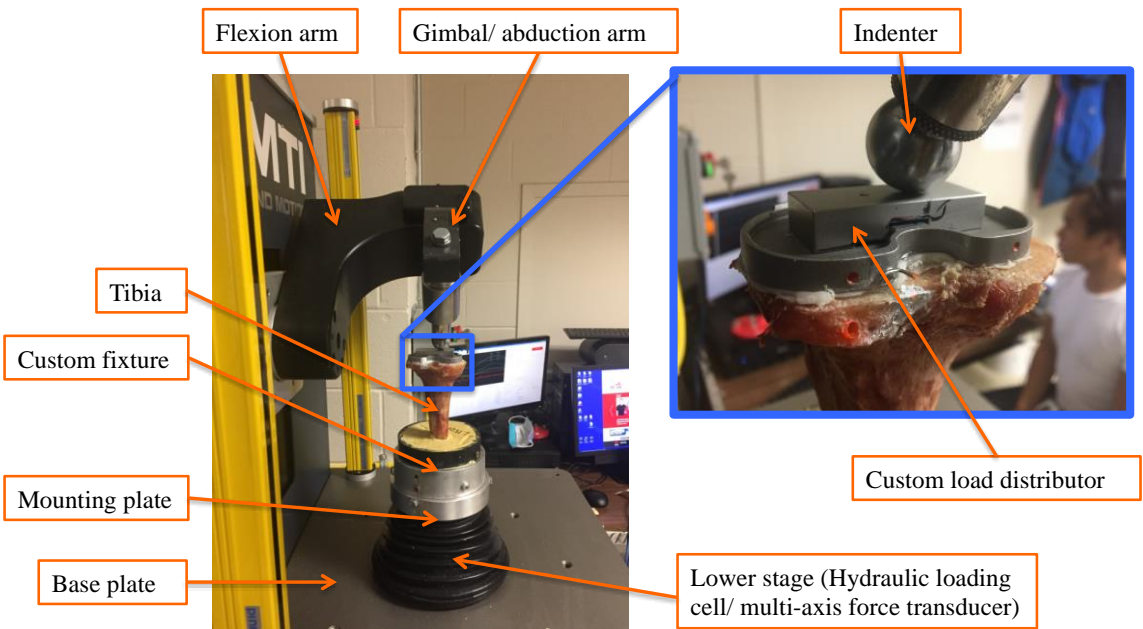


Figure 5.6. Setup for specimen loading.

5.2.3.2 Micromotion measurement– Digital Image Correlation System

Implant micromotion is a measurement of stability and is used clinically and in in-vitro studies to assess implant fixation-stability and predict implant loosening. It is also a measurement that can predict the likelihood of implant osseointegration in implants that can achieve biologic fixation. Implants that show continuous migration ($> 200\mu\text{m}$) between 1 and 2 years after surgery are considered being at a higher risk for future aseptic loosening (Jensen, Petersen, Schröder, Flivik, & Lund, 2012; Ryd et al., 1995). Furthermore, bone ingrowth was observed in-vivo for bone-prosthesis interface micromotion ranging from 20-50 μm (Chong, Hansen, & Amis, 2010; Jasty et al., 1997; Udofia et al., 2007). Anything above this micromotion threshold of 50 μm would lead to an unstable fibrous tissue layer formation between the metallic implant and host bone.

Clinically, implant migration is observed through radiographic analysis. Gross migration causing implant subsidence or radiolucency can be identified as signs of implant migration and failure (Chambers et al., 2001; Ro et al., 2016). For more precise in-vivo monitoring of three-dimensional musculoskeletal implant motion, techniques such as radiostereometric analysis (RSA) have been developed and validated RSA provides the highest measurement accuracy in vivo and is the gold standard in clinical orthopaedic radiographic studies (Yuan et al., 2018). In RSA, tantalum markers are inserted into the bone during surgery or implantation of prosthetics such as total knee replacements. Tantalum markers are also inserted into the implant itself during classic RSA or the implant is used as a model reference for bone markers during the modified model-based RSA (MBRSA). Radiographic analysis is then done visualizing the tantalum markers and making movement measurements based on the distance between the markers.

During in-vitro experiments, there are multiple ways of measuring micromotion between the bone-implant interfaces. Linear variable differential transducers (LVDT's) were the most accurate form of micromotion measurement for orthopaedic implants. Holes are drilled through the bone and implant. Pins are inserted and connected to the LVDT. Displacement of the implant relative to the bone is recorded by the LVDT as a change in voltage and converted into a measurement of micromotion. High-resolution micro differential variable reluctance transducers can make a accurate position measurement on the order of 1 μm

(DiSilvestro, Sherman, & Dietz, 2004). Yet, some may argue that by drilling holes and connecting something to the implant and bone, the integrity of the bone-implant interface is affected. Favre et al. found that gage measurements were actually less accurate than other forms of micromotion measurements such as optical systems. They argued that gage measurements quantify elastic deformation and not true interface micromotion and therefore would report values higher than the actual micromotion experienced at the bone-implant interface (Favre et al., 2011).

Digital image correlation (DIC) or optical systems have been more recently used as a method to measure micromotion at the implant-bone interface (Hosein, 2013; Race, Miller, & Mann, 2010). This method gives an accurate position measurement on the order of 3 μm (Eitner et al., 2010; Hosein, 2013). This method basically uses a high-resolution camera with a telecentric lens coupled with a diffuse illuminator in order to capture the image of two points of interest. Like all cameras, reflected light enters the camera and is focused on the camera's sensor, which itself is made up of thousands of sensors called pixels. The sensor collects the transmitted light and, with the help of a charged couple device, converts the light into an electric charge, which is then converted as a digital image (Hosein, 2013). For micromotion measurement, the software associated with the camera then takes the pixels of the image captured and converts them into micrometers. The telecentric lens is needed because it gives the camera a consistent image magnification and reduces distortion and perspective errors. The axial diffuse illuminator gives the camera uniform light intensity for a clearer image, reducing errors due to spectral reflection.

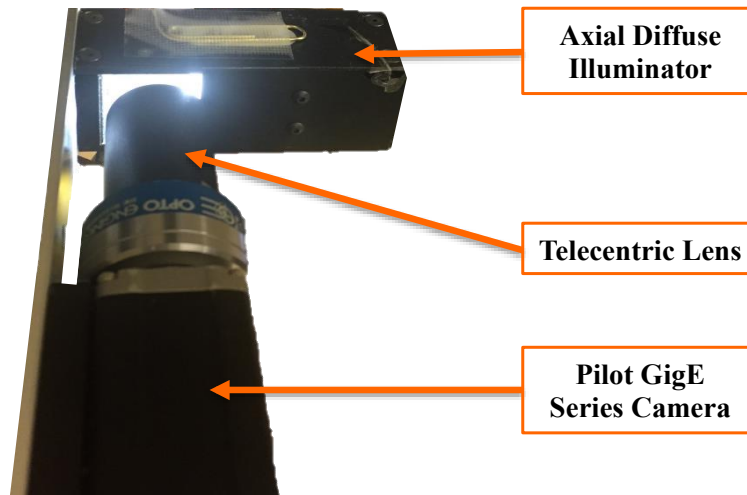


Figure 5.7. Optical tracking system hardware

In this study, the pilot GigE Series piA 2400-12gm/gc camera (Basler AG., Ahrensburg, Germany) with telecentric lens (Opto Engineering, Matua, Italy) and axial diffuse illuminator (Advanced Illumination, Rochester, VT, USA) were used as the hardware for the optical system (refer to figure 5.7). The resolution of the camera was 2452 by 2056 pixels and the field of view was 8 mm by 8 mm. This optical system was validated during a previous study by Hosein et al (Hosein, 2013). ImageJ (National Institutes of Health, Bethesda, USA) was the image software used during data acquisition. This program uses java-based functions and a color thresholding method to detect the markers. The optical system works best when there is a large contrast between the markers and the background. We used liquid paper on the implant and bone as a background and placed small drops of fluorescent orange paint as markers. Additionally, the centroids of the markers were acquired after colour thresholding. The distance between these centroid (implant/bone) was calculated in an unloaded and loaded state in order to calculate the micromotion of the implant relative to the bone. The camera was calibrated by taking a picture of a calibration grid/ line with known division lengths of 0.05mm. The calibration yielded a pixel to μm conversion factor of $3.43\mu\text{m}/\text{pixel}$.

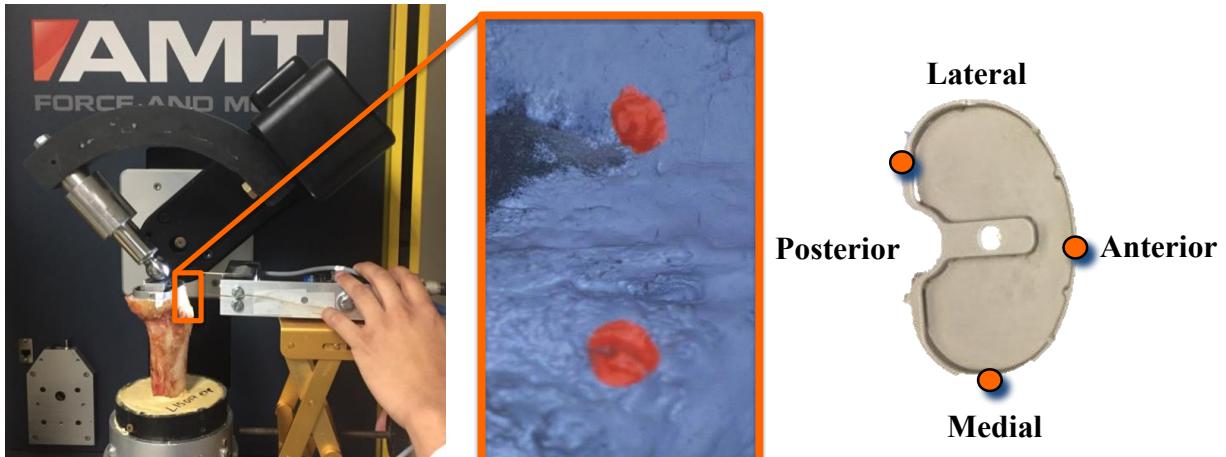


Figure 5.8. Optical system measuring micromotion of implant relative to bone. The markers are shown in the middle. The location of implant-bone micromotion measurements on the implant are illustrated on the right.

During image acquisition, the camera was placed perpendicular to the specimen 6.3 cm away since the camera’s working distance is 63.30mm. Measurements were taken at 3 different locations: Anteriorly, medially and posterolaterally.

5.2.3.3 **Bone defect measurement – Silicone mold and volumetric measurement**

All bone defects, after removal of the primary TKA, were AORI type 1 bone defects. In order to have a more precise measurement of bone loss, volumetric measurements were obtained. Silicone casting or molding was used as a volumetric measurement technique. A polyethylene wrap was used to cover the bone and prevent interdigitation of the silicone. The Amazing Remelt silicone mold by Alumilite (Alumilite, Kalamazoo, MI, USA) was used to make a mold of the bone defect. The silicone softens and becomes liquid at 57-60 degrees Celsius and has a specific gravity of 1.25 and density of 1.25 (g/ml). The Amazing melt silicone was melted in a microwave on high for 2 minutes. The contents were well stirred and poured into the bone defect cavity. The cavity was filled until the silicone reached the most proximal point of the proximal tibia. The specimen was then placed in a freezer for 10 minutes in order to cool down the silicone and accelerate the hardening process. The specimen was taken out for an additional 10 minutes at room temperature until the silicone was fully hardened. The silicone

mold was then removed from the proximal tibia and the weight of the silicone mold was precisely measured using a Mettler Toledo AG245 analytical balance precise to 0.1 mg (refer to figure 5.9).

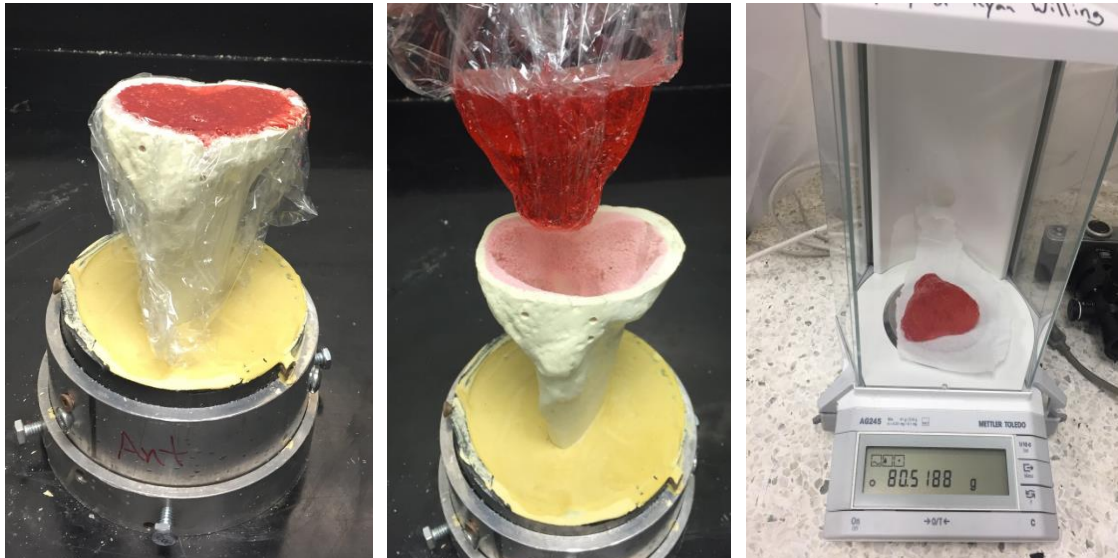


Figure 5.9. Volumetric measurement of bone defect after removal of primary TKA.
Illustration of sawbones used during preliminary testing.

The density (g/mL or g/cm^3) of the substance was used to calculate the volume of the silicone mold (bone defect) by dividing the weight measurement by the density. Additionally, the silicone mold was then fully submerged in a measuring cup full of water in order to calculate the water displacement caused by the silicone mold. This value was compared to the previous volumetric measurement.

5.2.3.4 Biomechanical testing protocol

A three-stage eccentric loading protocol was used to test the implants. Throughout the loading protocol, a physiologic or eccentric load representing in-vivo loading conditions was applied to the specimen using the AMTI VIVO joint motion simulator. On the coronal plane, this consisted of a 70% medial and 30% lateral load (Egloff et al., 2012; Mann et al., 2014; Peters et al., 2001). On the sagittal plane, the load was applied in the middle of the implant in

line with the longitudinal axis of the diaphysis of the tibia. The load was applied straight vertically with no transverse or rotational component. The three stages of loading are listed below:

1. Pre-cycle loading (static):

- a. A static eccentric (70% medial/ 30% lateral) load of 2100 N was applied to the implant. This load was applied for 15 minutes. After two minutes, micromotion was measured with the optical system. It took on average 10 minutes to complete all micromotion measurements. Marker position measurements were also taken before (pre-load) and after (post-load) loading as a reference to calculate micromotion by comparing implant position during unloaded and loaded conditions. The pre-cycle loading stage is designed to “condition” the specimen and is a reference to see the effects on cyclic loading on the fixation-stability of the implants.

2. Cyclic loading:

- a. The implants were then subjected to a cyclic eccentric (70% medial/ 30% lateral) load of 700 N, representing 1 body weight (BW), for 5×10^3 loading cycles at 2 Hz. No micromotion measurements were done during this stage. Cyclic loading lasted for 42 minutes. This stage is designed to simulate day-to-day loading (walking) by repeating a cyclic load and attempt to loosen the implants.

3. Post-cycle loading (static):

- a. The loading conditions for the third stage are the same as the first stage. A static eccentric (70% medial/ 30% lateral) load of 2100 N was applied to the implant. This load was also applied for 15 minutes. After two minutes, micromotion was measured with the optical system. Marker position measurements were also taken before (pre-load) and after (post-load) loading.

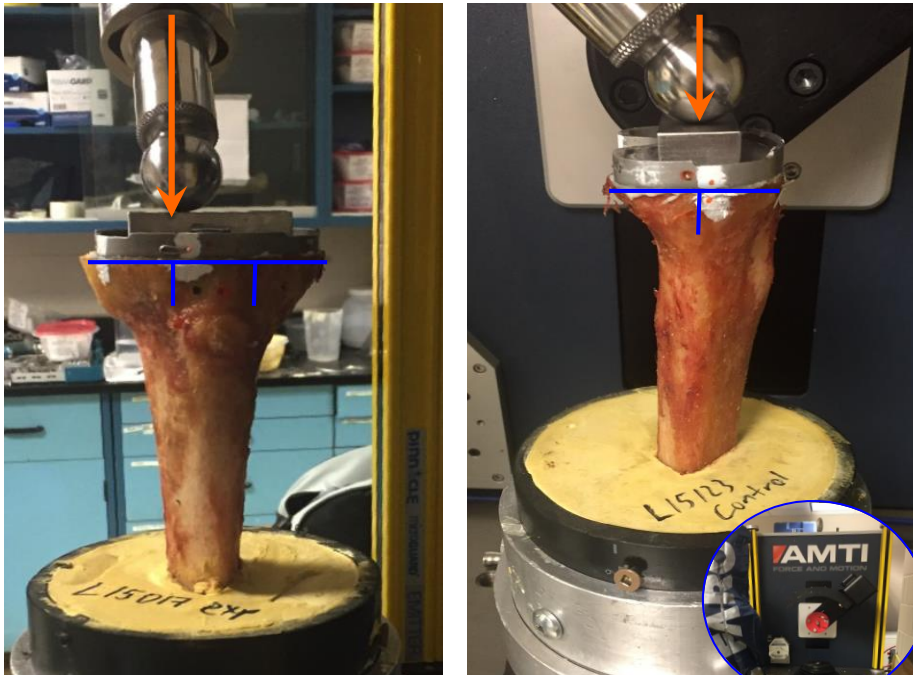


Figure 5.10. Anterior and lateral pictures of tibial component loading with the AMTI VIVO machine. Notice that the implant was loaded approximately 70% medial (medial third) (left) and in line with the tibial shaft (right).

5.2.4 Surgical techniques

5.2.4.1 Primary TKA technique

A fully cemented stem technique was used for the primary TKA. After the specimens have been thawed overnight and skeletonized, a primary total knee arthroplasty was performed on the proximal tibia. The tibia was placed on a vertical intramedullary rod that was secured to the table. The rod was placed inside the intramedullary canal of the tibia (5cm). The vertical axis now represented the anatomic axis of the tibia. An extramedullary tibial guide (Stryker Triathlon knee system) was placed on the tibia. The tibial slope was set at 0 degrees. The proximal tibia cutting jig was adjusted with a lobster claw or angel wing caliper to ensure that the proximal tibia cut took as little bone as possible. Three pins were placed in the proximal tibia cutting jig once it was aligned with the vertical axis or anatomic axis of the tibia. The proximal tibia was cut by an oscillating saw. The cut was perpendicular to the anatomic axis. A circular bubble level was placed on top of the tibial plateau to make sure the cut was neutral anterior-posteriorly and medial-laterally. The distal tibial cut was then made 18 cm from the proximal tibial cut using a ruler and oscillating saw. The tibia was removed from the

intramedullary stand. The tibia was then placed in custom fixtures ensuring that the proximal tibial cut remains neutral. Once the dental cement from the custom fixtures was fully hardened the primary TKA resumed.

The tibia was then sized by placing a tibial component sizing jig (Universal tibial template) on the tibia. The sizing jig was aligned relative to the tibial tubercle and secured in place by two pins. The appropriate keel punch guide was then placed on the sizing jig. A keel punch was hammered into the proximal tibia using a mallet. The boss reamer was used to ream the intramedullary canal at the depth of the keel of the primary implant. The headless 3” pins, keel punch guide and tibial component sizing jig were removed. The polymethylmethacrylate (PMMA) bone cement (Surgical Simplex P, Stryker Howmedica Osteonics Corp, Rutherford, NJ) was stored and prepared in a controlled environment. Simplex P cement was used for its medium viscosity, higher bone intrusion depth and lower or plastic deformation in comparison to other bone cements (Jeffers et al., 2005; Stryker, 2017). The cement was manually mixed without the use of a vacuum mixing device. Around 4 minutes was given for the cement to have a doughy, workable state. The tibial component was composed of a 1.5cm stem screwed onto a tibial tray. The cement was applied to the undersurface of the tibial component, the tibial bone surface (layered application technique) to achieve adequate penetration depths of the trabecular bone (Vanlommel et al., 2011). A constant pressure was applied, maintaining a neutral component alignment, until the cement was hard. The markers were placed for micromotion measurements and the specimen was transferred to the VIVO machine. Refer to figure 5.11 for an illustration of the TKA instrumentation.

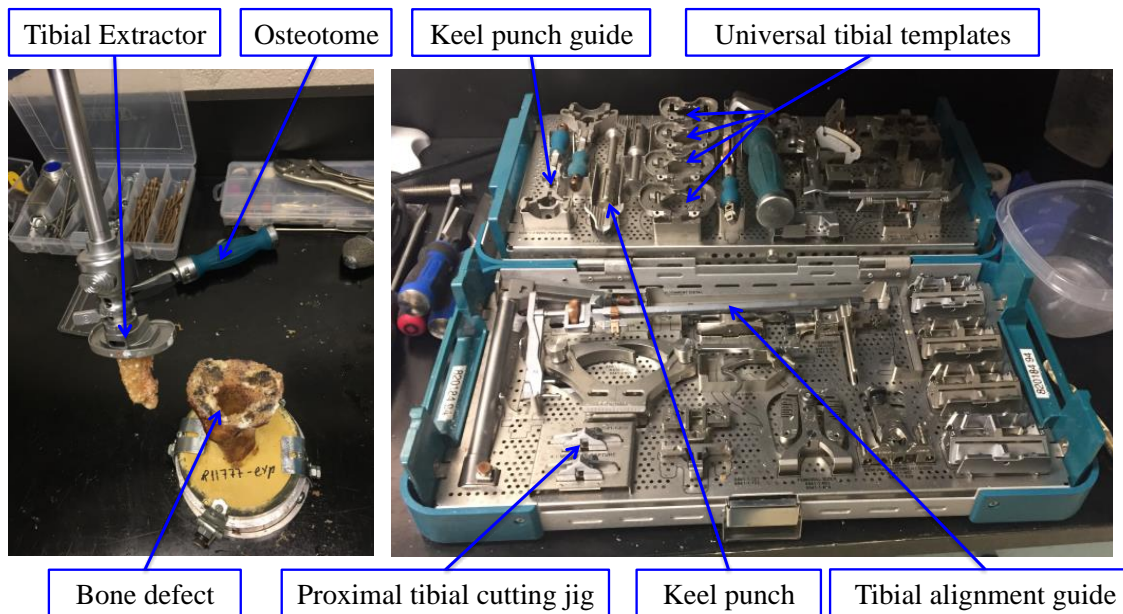


Figure 5.11. Primary and revision total knee arthroplasty instrumentation

5.2.4.2 Revision TKA technique

The primary TKA was explanted using a combination of a fine oscillating saw, osteotomes, a mallet and the Tibial Impactor/Extractor. First, the oscillating saw was used to remove the underlying cement under the tibial baseplate. Osteotomes were used to remove additional cement under the tibial baseplate. The Tibial Impactor/ Extractor was then connected to the top of the tibial baseplate and the baseplate was removed. All excess cement was removed with a fine osteotome and rongeur.

5.2.4.2.1 Fully cemented revision stem (control)

For the fully cemented revision stem technique, the tibial component sizing jig was aligned with the medial third of the tibial tubercle and secured in place to the tibia using headless pins. The keel punch guide was attached and the boss reamer was used to ream the tibia's intramedullary canal using power. The tibia was reamed to accommodate a 5 cm revision stem. The simplex P cement was then used in a similar fashion to the primary TKA. It was applied in a layered technique and the bone defect was filled with cement. The baseplate was impacted with a mallet and tibial impactor. A constant pressure was applied, maintaining a neutral component alignment, until the cement was hard. The markers were placed for micromotion measurements and the specimen was transferred to the VIVO machine. After

testing, the revision implant was removed with an oscillating saw, osteotomes and the tibial impactor/ extractor.

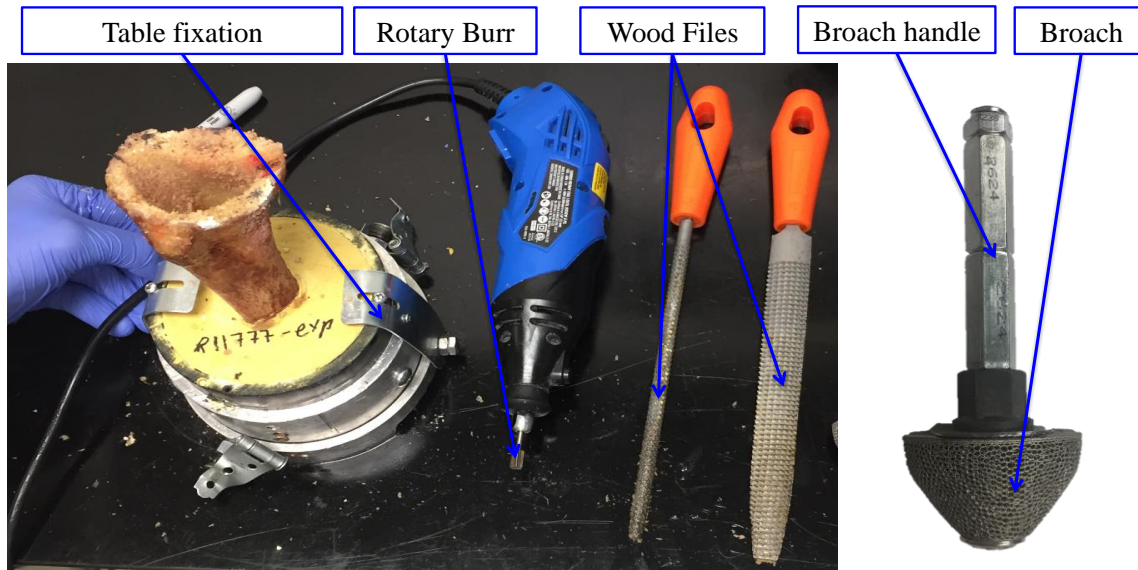


Figure 5.12. Tools used for shaping and insertion of 3D printed revision tibial augment

5.2.4.2.2 3D printed titanium augment (experimental)

For the 3D printed augment with hybrid fixation technique, the tibial component sizing jig was aligned with the medial third of the tibial tubercle and secured in place to the tibia using headless pins. The keel punch guide was attached and the boss reamer was used to ream the tibia's intramedullary canal using power. The tibia was reamed to accommodate a 5 cm revision stem. A rotary burr was used to remove the bone and make space for the 3D printed augment. Broaches were built with smaller 3D printed augments. Serial broaching of the tibia was performed until a perfect fit was achieved for the definitive implant. Wood files were used for fine-tuning of the space created for the implant. The volume of the cavity created for the 3D printed implant was measured using silicone molding. The 3D printed augment was inserted and impacted with a mallet and impactor. The Simplex P bone cement was prepared in the same fashion as previously explained for primary TKA. The cement was inserted into the reamed tibial intramedullary canal and the augment. The revision tibial baseplate with the 5 cm stem

was inserted into the 3D printed augment. The baseplate was impacted with a mallet and impactor. Constant pressure was sustained on the baseplate until the cement was fully hardened. The markers were placed for micromotion measurements and the specimen was transferred to the VIVO machine. After testing, the revision implant was removed with an oscillating saw, osteotomes and the tibial impactor/ extractor.

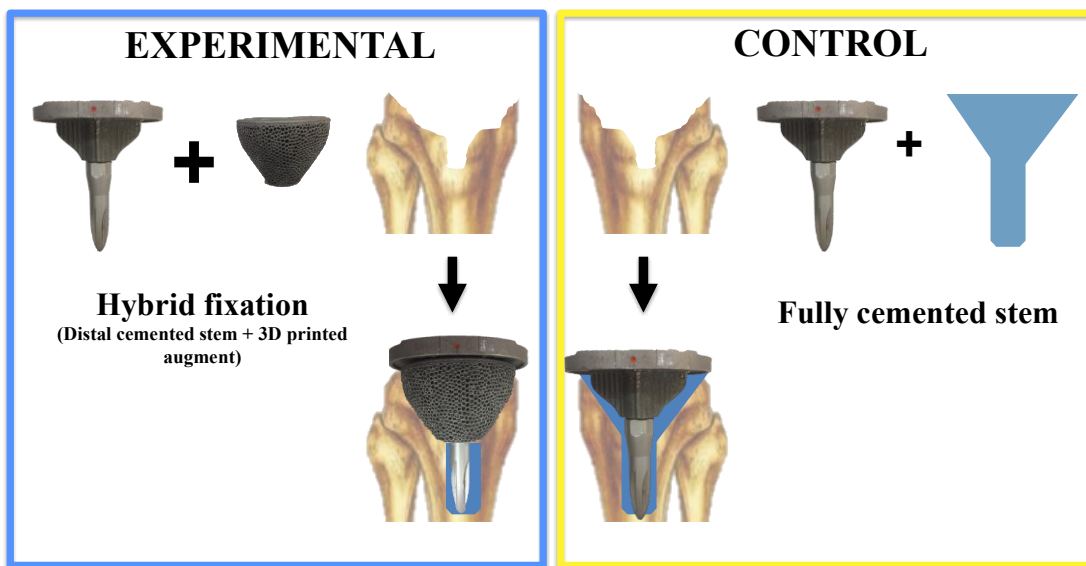


Figure 5.13. Schematic representation of components for revision TKA using the novel 3D printed augment (Left) and fully cemented stems (Right)

Twenty-two cadaveric proximal tibias underwent primary and revision total knee arthroplasty. The cadaveric specimens' demographic data is shown in table 5.1 (refer to Table 5.1). The demographic data of the experimental group and the control group were identical since they were both taken from the same cadaver. There were 6 right and 5 left tibias used in the experimental group. The average age of the cadavers was 69 years. The mean height was 140 cm and the mean body mass index (BMI) was 21.2 kg/m².

Table 5.1. Eleven fresh-frozen cadaveric pairs of tibias (22 tibias) used for biomechanical testing.

Cadaveric	Age	Sex	Height	Weight	BMI	Size of	Size of 3D	Side of 3D
-----------	-----	-----	--------	--------	-----	---------	------------	------------

Specimen Number	(years)		(inches)	(lbs)	(kg/m ²)	primary tibial baseplate	printed augment	printed augment
1	79	M	72	180	24.4	5	2	Left
2	76	M	73	160	21.5	6	4	Left
3	66	F	62	130	23.8	3	1	Right
4	89	F	62	134	24.5	3	1	Right
5	89	F	63	70	12.4	6	3	Left
6	57	M	73	140	18.5	5	2	Left
7	67	M	71	152	21.2	6	3	Right
8	64	M	66	140	22.6	4	2	Left
9	46	M	70	165	23.7	5	2	Right
10	69	F	61	109	20.6	3	1	Right
11	59	F	67	126	19.7	4	2	Right

*Male (M) and Female (F) specimens.

5.3.1 Comparison of specimens prior to rTKA

5.3.1.1 Vertical Micromotion of pTKA

First, we compared the axial or vertical micromotion. The primary TKA mean post-cycle vertical micromotion was $31.7\mu\text{m} \pm 24.4\mu\text{m}$ in the control group and $38.6\mu\text{m} \pm 37.6\mu\text{m}$ in the experimental group. There was no significant difference in post-cycle vertical micromotion between the two groups ($p= 0.38$).

The primary TKA mean pre-cycle vertical micromotion was $34.5\mu\text{m} \pm 24.6\mu\text{m}$ in the control group and $44.7\mu\text{m} \pm 41.8\mu\text{m}$ in the experimental group. There was no significant difference between pre-cycle and post-cycle micromotion in the control or experimental pTKAs (Primary control: $p=0.56$, Primary experimental: $p=0.40$).

5.3.1.2 Transverse Micromotion of pTKA

The primary TKA mean post-cycle horizontal or transverse micromotion was $58.5\mu\text{m} \pm 89.5\mu\text{m}$ in the control group and $42.9\mu\text{m} \pm 42.7\mu\text{m}$ in the experimental group. There was no significant difference in post-cycle transverse micromotion between the two groups ($p= 0.54$).

The primary TKA mean pre-cycle transverse micromotion was $52.8\mu\text{m} \pm 62.2\mu\text{m}$ in the control group and $55.2\mu\text{m} \pm 52.3\mu\text{m}$ in the experimental group. There was no significant

difference between pre-cycle and post-cycle micromotion in the control or experimental pTKAs (Primary control: $p=0.81$, Primary experimental: $p=0.95$).

5.3.1.3 Bone defect after pTKA removal

The first volumetric measurement of a proximal tibial bone defect after the explantation of the pTKA served as a trial to assess the precision and repeatability of the silicone molding technique. The volume of the bone defect after removal of the pTKA was measured 5 times. The mean and standard deviation was $23.8 \text{ cm}^3 \pm 1.1 \text{ cm}^3$. The coefficient of variation or relative standard deviation was 4.5%. The data was normally distributed. The null hypothesis for the Shapiro-Wilk test was accepted. The average bone loss encountered prior to revision surgery was $31.3 \text{ cm}^3 \pm 4.5 \text{ cm}^3$ in the control group and $29.4 \text{ cm}^3 \pm 4.2 \text{ cm}^3$ in the experimental group. There were no significant differences in bone defects between the two groups ($p=0.16$).

5.3.2 Comparison of specimens after revision TKA

5.3.2.1 Vertical Micromotion of rTKA

The revision TKA mean post-cycle vertical micromotion was $28.1\mu\text{m} \pm 20.3\mu\text{m}$ in the control group and $17.5\mu\text{m} \pm 18.7\mu\text{m}$ in the experimental group. The post-cycle vertical micromotion was significantly lower in the experimental group ($p=0.009$).

The revision TKA mean pre-cycle vertical micromotion was $32.1\mu\text{m} \pm 23.4\mu\text{m}$ in the control group and $22.5\mu\text{m} \pm 23.5\mu\text{m}$ in the experimental group. The vertical micromotion prior to cyclic loading was also significantly lower in the experimental group ($p=0.04$).

There was no significant difference between pre-cycle and post-cycle micromotion in the control or experimental rTKAs (Revision control: $p=0.52$, Revision experimental: $p=0.33$).

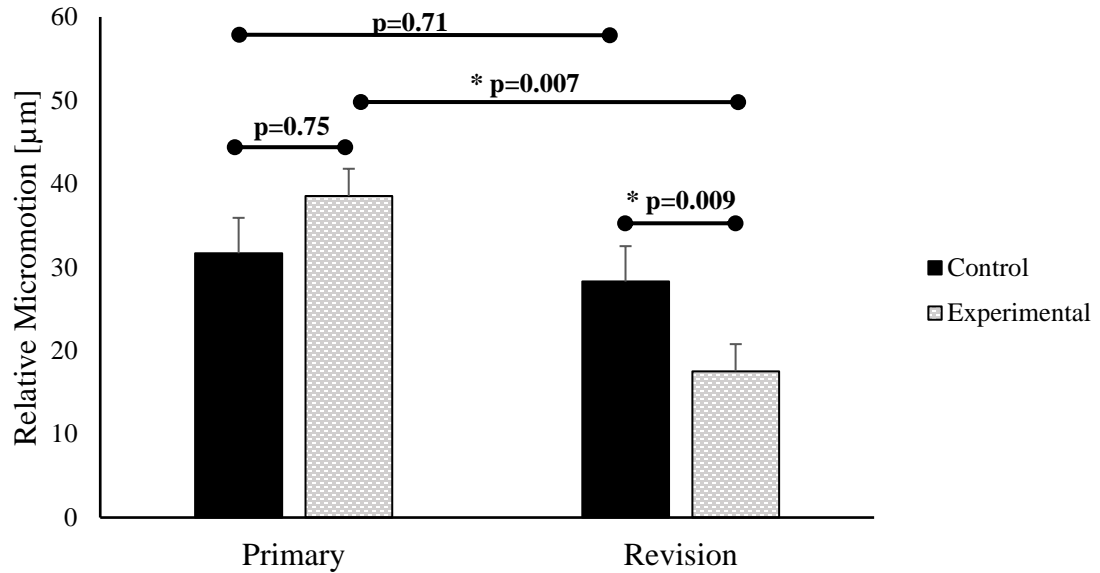


Figure 5.14. Bone-implant vertical micromotion during post-cycle loading of primary and revision TKAs. Error bars represent standard error.

Interestingly, the revision TKA with the 3D printed titanium augment outperformed the primary TKA. The experimental revision TKA had a significantly lower vertical micromotion in comparison to the pTKA ($p=0.007$).

5.3.2.2 Transverse Micromotion of rTKA

The revision TKA mean post-cycle transverse micromotion was $42.9\mu\text{m} \pm 42.7\mu\text{m}$ in the control group and $48.1\mu\text{m} \pm 37.44\mu\text{m}$ in the experimental group. There were no significant differences between the control and experimental group in terms of post-cycle transverse micromotion ($p= 0.38$).

The revision TKA mean pre-cycle transverse micromotion was $55.4\mu\text{m} \pm 63.8\mu\text{m}$ in the control group and $45.8\mu\text{m} \pm 52.6\mu\text{m}$ in the experimental group. There were no significant differences in micromotion between the control and experimental group during pre-cyclic loading ($p=0.18$). There were also no significant differences between pre-cycle and post-cycle data in both the control and experimental group (Revision control: $p=0.46$, Revision experimental: $p=0.26$).

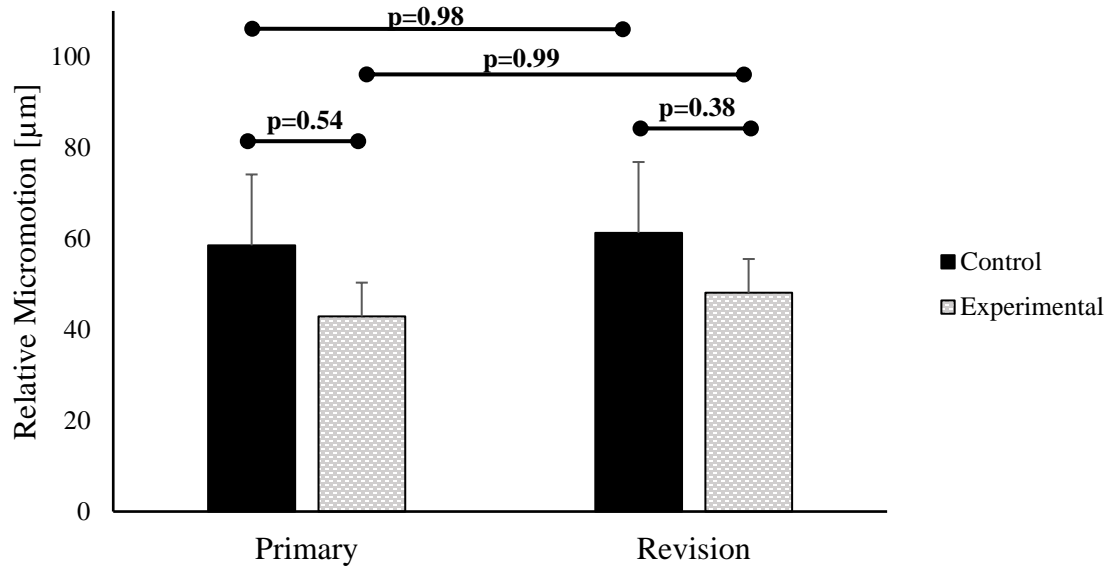


Figure 5.15. Bone-implant transverse micromotion during post-cycle loading of primary and revision TKAs. Error bars represent standard error.

5.3.2.3 Bone defect after rTKA removal and time to explantation

Once testing was completed, the bone defect was assessed after the removal of the revision implants. The mean bone defect after removing the fully cemented stem ($46.3 \text{ cm}^3 \pm 6.5 \text{ cm}^3$) was significantly lower than the mean bone defect after removing the 3D printed augment revision ($55.5 \text{ cm}^3 \pm 7.1 \text{ cm}^3$) with a p-value of 0.009. Furthermore, there were no significant differences ($p=0.06$) in the rTKA explantation time. The mean explantation time was 20.7 minutes \pm 8 minutes for the control group and 34.4 minutes \pm 16 minutes in the experimental group.

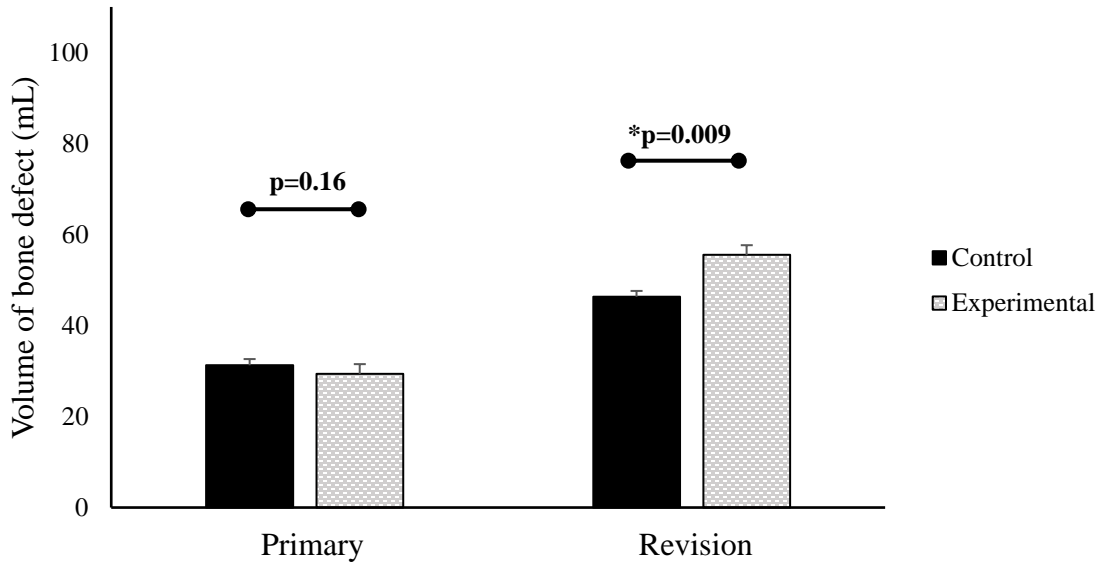


Figure 5.16. Volume of the proximal tibial bone defect after explantation of the primary and revision TKAs. **Error bars represent standard error.**

5.3.2.4 Direction of the micromotion in rTKA

The vertical and transverse micromotion was subdivided into the micromotion experienced at specific locations of the implant, based on where the markers were placed and where micromotion was measured: Medial, Anterior, Posterolateral. A summary of the location specific micromotion experienced by the revision TKA is displayed in table and schematic format (refer to Table 5.2 and 5.3, and Figure 5.17).

Table 5.2. Vertical micromotion (Post-cycle)

Location	Primary Control		Primary Exp.		Revision Control		Revision Exp.	
	Mean (μm)	SD (μm)	Mean (μm)	SD (μm)	Mean (μm)	SD (μm)	Mean (μm)	SD (μm)
Medial	38.5	± 33.0	38.6	± 39.7	32.6	± 24.4	10.9	± 31.9
Anterior	41.0	± 15.9	59.5	± 43.7	32.5	± 23.4	20.8	± 20.0
PostLat	7.9	± 17.8	14.7	± 12.6	4.1	± 21.6	6.9	± 7.2

* Note: positive values represent inferior motion (axial compression). SD: Standard deviation

Table 5.3. Transverse micromotion (Post-cycle)

Location	Primary Control		Primary Exp.		Revision Control		Revision Exp.	
	Mean (μm)	SD (μm)	Mean (μm)	SD (μm)	Mean (μm)	SD (μm)	Mean (μm)	SD (μm)
Medial	42.0	± 98.5	40.5	± 142.4	-34.9	± 64.3	-6.3	± 75.1
Anterior	1.4	± 61.0	1.65	± 55.8	-13.1	± 47.8	-12.4	± 59.6
PostLat	56.3	± 134.5	-12.8	± 47.0	-13.2	± 61.3	-17.1	± 48.6

* Note: positive values represent medial translation for the anterior marker/location and anterior translation for the medial and posterolateral marker/location. SD: Standard deviation

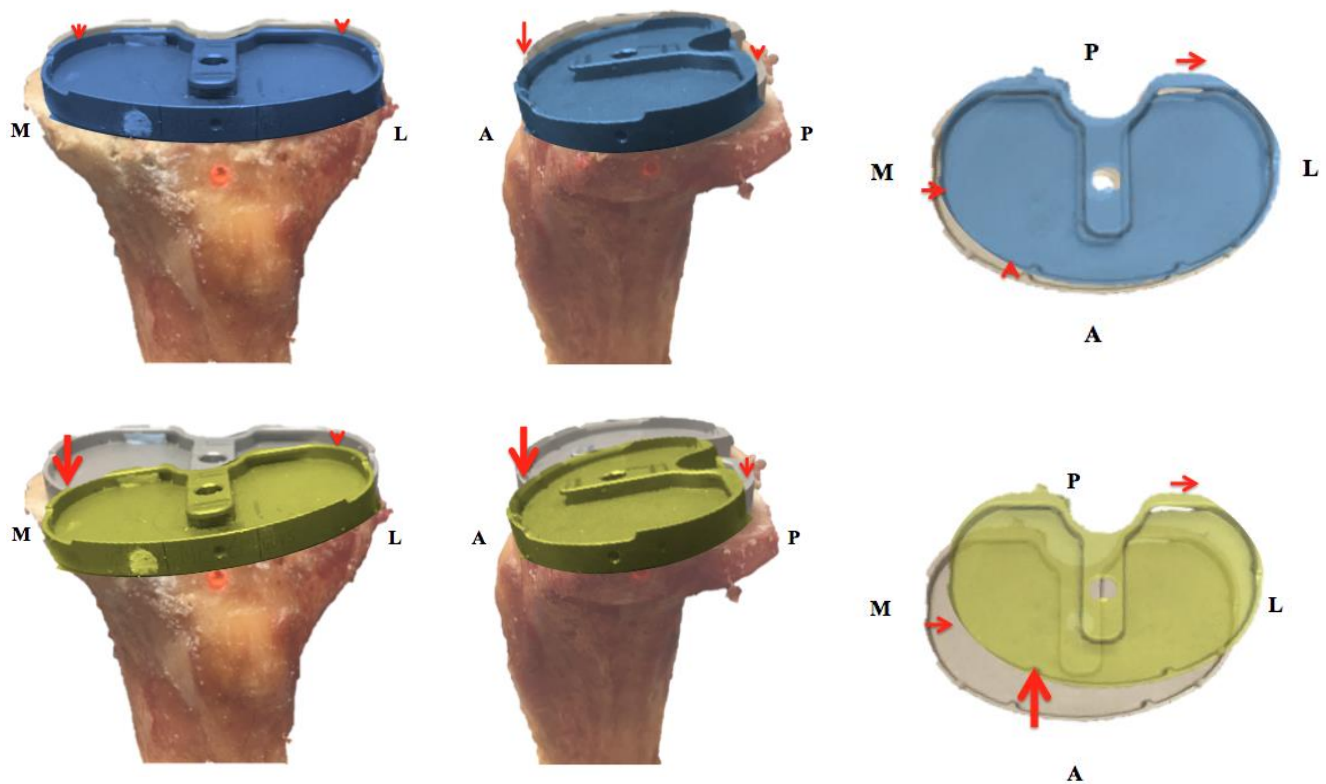


Figure 5.17. Schematic representation of the magnitude and vector of the micromotion experienced by the TKA under loading conditions. Top: Experimental group (BLUE) with the 3D printed augment, Bottom: Control group (YELLOW) with the fully cemented revision stem. The red arrows are to scale (20:1).

5.4 Discussion

The present study was the initial testing of a new 3D printed titanium augment with an anatomic shape designed to fit into the proximal tibia during revision TKA surgery. The first step was to test it in a cadaveric model with AORI type 1 bone defects. These defects are present with the iatrogenic bone loss encountered when explanting the primary TKA. Therefore, the standard of care for AORI type 1 bone defect reconstruction, a fully cement revision stem, was used as a comparison for the 3D printed titanium augment (Daines & Dennis, 2012; Haidukewych et al., 2011; Panegrossi et al., 2014; Whittaker et al., 2008). Cemented stems provide immediate fixation; however, they can be challenging to remove and may increase stress shielding of the metaphyseal bone (Sheth et al., 2017). Cement also has been shown to deform and degrade over time, resulting in debris, infection and implant loosening (Efe et al., 2011). Nevertheless, the immediate fixation acquired by cement fixation is a clear advantage during cadaveric testing. The experimental group with the novel cementless 3D printed augment used hybrid fixation. In the cadaveric model, the hybrid fixation was made up of the press-fit fixation of the 3D printed augment and the cement fixation of the distal aspect of the revision stem. In an in-vivo model, we would expect biologic fixation of the 3D augment creating additional long-term fixation of the revision implant.

Higher bone-implant micromotion has been associated with implant failure and revision surgery. Ryd et al. found that implants that show continuous migration ($> 200\mu\text{m}$) between 1 and 2 years after surgery are considered being at a higher risk for future aseptic loosening (Jensen et al., 2012; Ryd et al., 1995). Hence, we tested the micromotion of both the conventional fully cemented stem and the 3D printed augment revision implant under loading conditions as a predictor of fixation-stability and a measure of implant survivorship. A significantly lower vertical micromotion was seen in the experimental group with the use of the 3D printed augment ($p=0.009$). The vertical micromotion of the 3D printed augment was $17.5\mu\text{m} \pm 18.7\mu\text{m}$ compared to $28.3\mu\text{m} \pm 20.3\mu\text{m}$ in the control. There were no significant differences in transverse micromotion between the experimental ($48.1\mu\text{m} \pm 37.44\mu\text{m}$) and control ($42.9\mu\text{m} \pm 42.7\mu\text{m}$) group ($p=0.38$).

Interestingly, the experimental revision TKA with the 3D printed augment had significantly less overall vertical micromotion in comparison to the primary TKA ($p=0.007$). The largest difference was the significantly higher micromotion of the anterior aspect of the pTKA ($p=0.02$). The 3D printed augment group was also seen to be rotationally stable with similar transverse micromotions seen at the posterolateral and anterior aspects of the impact. Conversely, the primary TKA was not rotationally stable. The 3D printed implant's lower micromotion and better fixation-stability is based on its press-fit fixation without the help of bony ingrowth that would be present in an in-vivo model. Its superior fixation-stability is attributable to a multitude of factors.

Previous studies showed that 3D printed implants have inherent advantages. Additive manufacturing can create an implant with a highly organized microstructure with a uniform porosity making it resistant to compressive forces. The custom porosity and microstructure is also tapered to match the host bone's stiffness. By having a lower stiffness mismatch, the implant evenly transfers the surrounding stresses to the bone, decreasing stress shielding and preventing future bone loss that would result in implant subsidence (Fan et al., 2015; Hsu & Ellington, 2015; Xu et al., 2016). Additionally, the anatomic shape matches the shape of the proximal tibial bone; therefore, producing a better fit and increases the bone-implant contact area, which decreases stress shielding as well as stress risers that would be at risk for periprosthetic fractures (D. Kim et al., 2017). Note that some studies quote that stress shielding is due to the mismatch in elastic moduli (Young's modulus) between the host bone and the implant (Barrack et al., 2004; Kimpton et al., 2013; Morgan-Jones et al., 2015). The elastic modulus is a material property. The combination of the elastic modulus and the structure of the object (shape, porosity, etc.) determine the object's overall stiffness. To clarify, stress shielding is actually the mismatch in stiffness of the host bone and the implant. Furthermore, unlike cones, which are known for tissue irritation (Haidukewych et al., 2011), the anatomic 3D printed implant avoids this by having a lower profile or less prominent shape (E.-K. Park et al., 2016). It also eliminates the need for bone graft by replacing the bone defect found in revision surgery.

Another key feature that might explain why the implant might achieve better fixation is its capability for cementless biologic fixation in vivo, which could not be testing due to the

cadaveric nature of this study. While cementless biologic fixation has the advantage of better long-term fixation, osseointegration needs to occur first for this to happen. In the earlier literature, cementless TKA had higher earlier failure rates secondary to aseptic loosening (Fehring & Griffin, 1998). This can be explained by insufficient early fixation-stability of the implant leading to elevated bone-implant micromotion above the 50µm osseointegrative threshold (Chong et al., 2010; Jasty et al., 1997; Udofia et al., 2007). Thus, bony ingrowth does not occur and a weak fibrous union is established at the bone-implant interface. In the current study, we have established that the early fixation-stability created by the hybrid fixation (distal cement and proximal press-fit) of the novel 3D printed implant is well within the osseointegration threshold of 50µm. Therefore, the early fixation-stability is adequate to prevent early loosening and ensure bony ingrowth and thus ensures long-term fixation. Achieving proper bony integration in cementless implants is crucial especially in obese patients. In obese patients, cementless fixation has demonstrated to have better post-surgical outcomes and significantly less revisions in comparison to cemented TKAs (Bagsby et al., 2016).

During the study, the bone defect after removal of the revision TKAs using cement filling versus the novel 3D printed augment, were significantly different ($p=0.009$). The experimental group ($55.5 \text{ cm}^3 \pm 7.1 \text{ cm}^3$) had a larger bone defect compared to the control ($46.3 \text{ cm}^3 \pm 6.5 \text{ cm}^3$). However, the fact that the implant sits closer to the cortical bone has its advantages. The fit is tighter and the proximity of the cortical bone results in less bone deformation that you would see in trabecular bone since cortical bone is stiffer and stronger. The higher bone-implant contact achieved with the anatomic shape also enhances its potential for bony ingrowth. It increases the surface area where bony ingrowth can occur and distributes the stresses (reverse of stress shielding) and stimulating bone growth and remodeling (Shinya et al., 2011). Studies have also shown that maximal bone ingrowth usually occurs along surfaces that are relatively close to cortical bone; therefore, by having a implant occupy a larger space and be closer to the cortical bone, while maintaining the more metabolically active surrounding trabecular bone is advantageous to ensure good bony ingrowth (Bauer & Schils, 1999; Franchi et al., 2005).

During testing, the tibial components of the primary TKA were fully cemented into the proximal tibia. Two techniques exist for cementing the tibial tray. The tibial component can be

cemented by applying cement to the cut bony surface perpendicular to the axis of the tibia horizontally (only the baseplate) or it can be fully cemented (including the keel). Efe et al. demonstrated that both cementing techniques had similar degrees of bone loss (Efe et al., 2011). Therefore, the bone loss experienced during testing of this study is valid for both cementing techniques.

Furthermore, the fully cemented tibial component was used in this experiment since Sharkey et al. reported a significantly higher loosening rate of 10.5% of surface cemented components in comparison to fully cemented stems. This is controversial since some studies showed higher loosening rate and some proved that the loosening rate is equivalent granted that the cement mantle or cement penetration under the tibial tray is at least 3mm (Bert & Mcshane, 1998; Cawley, Kelly, Simpkin, Shannon, & McGarry, 2012; Schlegel et al., 2014; Vanlommel et al., 2011).

5.4.1 Limitations of the study

Earlier in the study, the 3D printed titanium augment was loaded on its own in the host bone prior to cementing the tibial tray in order to determine the press-fit fixation achieved by the augment by itself. The augment was loaded with 1400N (2BW) for 5 minutes. Micromotion was measured with the FARO arm, which was deemed inaccurate; therefore, the data was not presented in this study. Unfortunately, two tibias sustained fractures at the medial border of the medial tibial plateau. One fractured during the insertion of the augment and the specimen had a revision TKA with no fracture fixation. The other fractured during the loading of the augment by itself and went on to have osteosynthesis of the fracture with two custom made aluminum plates and screws prior to revision TKA. This could have affected the results by compromising the fixation-stability of the experimental revision TKA.

Therefore, the significantly lower micromotion seen with the 3D printed titanium augment could actually be even lower if there had not been fractures. Nevertheless, this shows that porous/3D printed revision augments have a risk of intraoperative fractures, which has been

quoted by other papers studying proximal tibial cementless press fit implants (Alexander et al., 2013; Barnett et al., 2014).

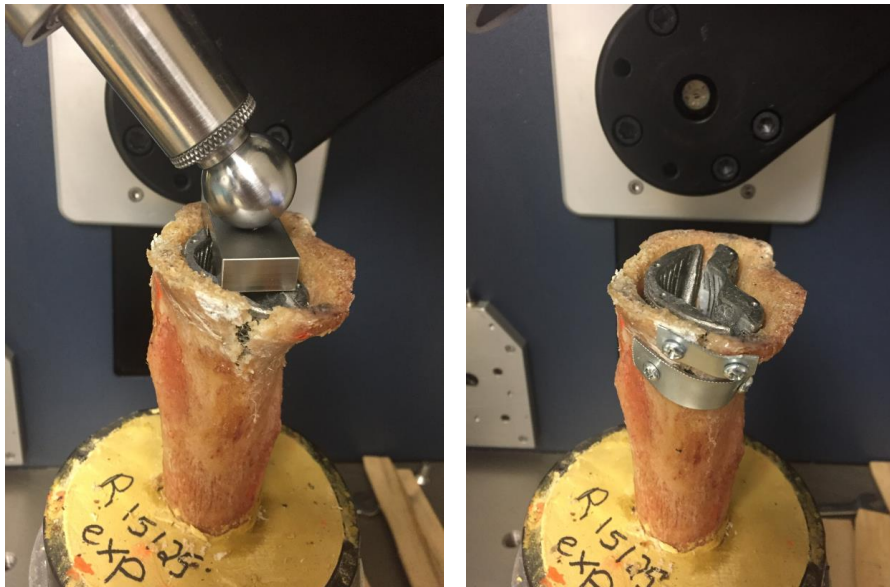


Figure 5.18. Photographs of the proximal tibial fracture during isolated augment loading (left) and resultant open reduction internal fixation.

A limitation of the study was the markers used for the optical system. A dot of fluorescent pain was placed on the bone and on the implant. The fact that the marker dots were not perfect circles affected the accuracy of the centroid calculation by the software. Therefore, this could have affected the precision and accuracy of the measurements. This could explain the large variation or standard deviations seen in the results. Similarly, the bone's plastic or elastic deformation during loading can deform the marker and again affect the accuracy of the centroid calculation. Another limitation is the fact that the actual bone-implant contact was not measured. Further studies would be needed to evaluate this.

This study was the first study to test the novel 3D printed tibial augment. We opted to test the 3D printed augment in an AORI type 1 contained tibial metaphyseal defect. Nevertheless, theoretically, the augment would be of greater benefit if it was tested in AORI type 2 and 3 defects with uncontained metaphyseal bone defects. Therefore, this study might not be reflective of the true advantage of using the 3D printed augment during revision total knee arthroplasty.

5.5 Conclusions

This study suggests that early fixation stability of revision TKA with the novel 3D printed titanium augment is significantly better than the conventional fully cemented rTKA. The early press-fit fixation of the augment is likely sufficient for promoting bony ingrowth of the augment in vivo. Further studies are needed to investigate the long-term in-vivo fixation of the novel 3D printed augment.

5.6 References

- Alexander, G. E., Bernasek, T. L., Crank, R. L., & Haidukewych, G. J. (2013). Cementless Metaphyseal Sleeves Used for Large Tibial Defects in Revision Total Knee Arthroplasty. *Journal of Arthroplasty*, 28(4), 604–607. <http://doi.org/10.1016/j.arth.2012.08.006>
- Arima, J., Whiteside, L. A., Martin, J. W., Miura, H., White, S. E., & McCarthy, D. S. (1998). Effect of partial release of the posterior cruciate ligament in total knee arthroplasty. *Clinical Orthopaedics and Related Research*, (353), 194–202. Retrieved from <http://www.ncbi.nlm.nih.gov/pubmed/9728174>
- Bagsby, D. T., Issa, K., Smith, L. S., Elmallah, R. K., Mast, L. E., Harwin, S. F., ... Malkani, A. L. (2016). Cemented vs Cementless Total Knee Arthroplasty in Morbidly Obese Patients. *Journal of Arthroplasty*, 31(8), 1727–1731. <http://doi.org/10.1016/j.arth.2016.01.025>
- Barnett, S. L., Mayer, R. R., Gondusky, J. S., Choi, L., Patel, J. J., & Gorab, R. S. (2014). Use of stepped porous titanium metaphyseal sleeves for tibial defects in revision total knee arthroplasty: Short term results. *Journal of Arthroplasty*, 29(6), 1219–1224. <http://doi.org/10.1016/j.arth.2013.12.026>
- Barrack, R. L., Stanley, T., Burt, M., & Hopkins, S. (2004). The effect of stem design on end-of-stem pain in revision total knee arthroplasty. *Journal of Arthroplasty*, 19(7 SUPPL.), 119–124. <http://doi.org/10.1016/j.arth.2004.06.009>

- Bauer, T. W., & Schils, J. (1999). The pathology of total joint arthroplasty. *Skeletal Radiology*, 28, 483–497. <http://doi.org/10.1007/s002560050552>
- Beckmann, J., Lüring, C., Springorum, R., Köck, F. X., Grifka, J., & Tingart, M. (2011). Fixation of revision TKA: A review of the literature. *Knee Surgery, Sports Traumatology, Arthroscopy*, 19(6), 872–879. <http://doi.org/10.1007/s00167-010-1249-3>
- Bert, J. M., & Mcshane, M. (1998). Is It Necessary to Cement the Tibial Stem in Cemented Total Knee Arthroplasty ?, (356), 73–78.
- Bole, M., Teeter, M., Lanting, B. A., & Howard, J. L. (2018). Correlation of tibial bone defect shape with patient demographics following total knee revision. *Journal of Orthopaedics*, 15(2), 490–494. <http://doi.org/10.1016/j.jor.2018.03.025>
- Cawley, D. T., Kelly, N., Simpkin, A., Shannon, F. J., & McGarry, J. P. (2012). Full and surface tibial cementation in total knee arthroplasty: A biomechanical investigation of stress distribution and remodeling in the tibia. *Clinical Biomechanics*, 27(4), 390–397. <http://doi.org/10.1016/j.clinbiomech.2011.10.011>
- Chambers, I. R., Fender, D., McCaskie, A. W., Reeves, B. C., & Gregg, P. J. (2001). Radiological features predictive of aseptic loosening in cemented Charnley femoral stems. *The Journal of Bone and Joint Surgery. British Volume*, 83(6), 838–42. <http://doi.org/10.1302/0301-620x.83b6.11659>
- Chen, X., Xu, L., Wang, Y., Hao, Y., & Wang, L. (2015). Image-guided installation of 3D-printed patient-specific implant and its application in pelvic tumor resection and reconstruction surgery, 5, 66–78.
- Cherian, J., Bhave, A., Harwin, S., & Mont, M. (2016). Outcomes and Aseptic Survivorship of Revision Total Knee Arthroplasty. *The American Journal of Orthopedics*, 45((2)), 79–85.
- Chong, D. Y. R., Hansen, U. N., & Amis, A. A. (2010). Analysis of bone-prosthesis interface micromotion for cementless tibial prosthesis fixation and the influence of loading conditions. *Journal of Biomechanics*, 43(6), 1074–1080. <http://doi.org/10.1016/j.jbiomech.2009.12.006>

- Daines, B. k., & Dennis, D. A. (2012). Management of Bone Defects in Revision Total Knee Arthroplasty. *Journal of Bone and Joint Surgery American*, 94(March 2013), 1131–1139.
- De Martino, I., De Santis, V., Sculco, P. K., D'Apolito, R., Assini, J. B., & Gasparini, G. (2015). Tantalum Cones Provide Durable Mid-term Fixation in Revision TKA. *Clinical Orthopaedics and Related Research*, 473(10), 3176–3182. <http://doi.org/10.1007/s11999-015-4338-2>
- Dennis, D. A., Berry, D. J., Engh, G., Fehring, T., Macdonald, S. J., Rosenberg, A. G., & Scuderi, G. (2008). Revision Total Knee Arthroplasty. *Journal of the American Academy of Orthopaedic Surgeons*, 16(8), 442–454.
- DiSilvestro, M. R., Sherman, J. T., & Dietz, T. L. (2004). A new position measurement system for micro-measurements in orthopaedics. *Conference Proceedings : ... Annual International Conference of the IEEE Engineering in Medicine and Biology Society. IEEE Engineering in Medicine and Biology Society. Conference*, 4, 2438–2441. <http://doi.org/10.1109/IEMBS.2004.1403705>
- Efe, T., Figiel, J., Sibbert, D., Fuchs-Winkelmann, S., Tibesku, C. O., Timmesfeld, N., ... Skwara, a. (2011). Revision of tibial TKA components: bone loss is independent of cementing type and technique: an in vitro cadaver study. *BMC Musculoskeletal Disord*, 12, 6. <http://doi.org/10.1186/1471-2474-12-6>
- Egloff, C., Hügler, T., & Valderrabano, V. (2012). Biomechanics and pathomechanisms of osteoarthritis. *Swiss Medical Weekly*, 142(JULY), 1–14. <http://doi.org/10.4414/smw.2012.13583>
- Eitner, U., Köntges, M., & Brendel, R. (2010). Use of digital image correlation technique to determine thermomechanical deformations in photovoltaic laminates: Measurements and accuracy. *Solar Energy Materials and Solar Cells*, 94(8), 1346–1351. <http://doi.org/10.1016/j.solmat.2010.03.028>
- Fan, H., Fu, J., Li, X., Pei, Y., Li, X., Pei, G., & Guo, Z. (2015). Implantation of customized 3-D printed titanium prosthesis in limb salvage surgery : a case series and review of the

literature. *World Journal of Surgical Oncology*, 13(308), 1–10.
<http://doi.org/10.1186/s12957-015-0723-2>

Favre, P., Perala, S., Vogel, P., Fucntese, S. F., Goff, J. R., Gerber, C., & Snedeker, J. G. (2011). In vitro assessments of reverse glenoid stability using displacement gages are misleading - Recommendations for accurate measurements of interface micromotion. *Clinical Biomechanics*, 26(9), 917–922. <http://doi.org/10.1016/j.clinbiomech.2011.05.002>

Fehring, T. K., & Griffin, W. L. (1998). Revision of failed cementless total knee implants with cement. *Clinical Orthopaedics and Related Research*, (356), 34–38.
<http://doi.org/10.1097/00003086-199811000-00007>

Franchi, M., Fini, M., Martini, D., Orsini, E., Leonardi, L., Ruggeri, A., ... Ottani, V. (2005). Biological fixation of endosseous implants. *Micron*, 36(7–8), 665–671.
<http://doi.org/10.1016/j.micron.2005.05.010>

Gandhi, R., Tsvetkov, D., Davey, J. R., & Mahomed, N. N. (2009). Survival and clinical function of cemented and uncemented prostheses in total knee replacement: A META-ANALYSIS. *Journal of Bone and Joint Surgery - British Volume*, 91–B(7), 889–895.
<http://doi.org/10.1302/0301-620X.91B7.21702>

Glenn, J. C., Sokoloski, S. N., Damer, B. M., & Tabit, J. M. (2010). Tibia pain at end of stem With stemmed revision total knee arthroplasty. Treatment with cortical strut graft technique. *Journal of Arthroplasty*, 25(3), 497.e1-497.e5.
<http://doi.org/10.1016/j.arth.2009.02.020>

Goodheart, J. R., Miller, M. A., & Mann, K. A. (2014). In vivo loss of cement-bone interlock reduces fixation strength in total knee arthroplasties. *Journal of Orthopaedic Research*, 32(8), 1052–1060. <http://doi.org/10.1002/jor.22634>

Haidukewych, G. J., Hanssen, A. D., & Jones, R. (2011). Metaphyseal Fixation in Revision Total Knee Arthroplasty: Indications and Techniques. *J Am Acad Orthop Surg*, 19(6), 311–318.

- Hosein, Y. K. (2013). The Effect of Stem Surface Treatment and Substrate Material on Joint Replacement Stability: An In-Vitro Investigation into the Stem-Cement Interface Mechanics under Various Loading Modes. Retrieved from <http://ir.lib.uwo.ca/etd/1479>
- Hsu, A., & Ellington, J. K. (2015). Evolving Techniques } 3-Dimensional Printed Titanium Truss Cage With Tibiototalcaneal Arthrodesis for Salvage of Persistent Distal Tibia Nonunion. *Foot & Ankle SPecialist*, 8(6), 483–489.
<http://doi.org/10.1177/1938640015593079>.
- Jacobs, W. C. H., Clement, D. J., & Wymenga, A. B. (2005). Retention versus removal of the posterior cruciate ligament in total knee replacement: a systematic literature review within the Cochrane framework. *Acta Orthopaedica*, 76(6), 757–768.
<http://doi.org/10.1080/17453670510045345>
- Jasty, M., Bragdon, C., Burke, D., O'Connor, D., Lowenstein, J., & Harris, W. H. (1997). In vivo skeletal responses to porous-surfaced implants subjected to small induced motions. *Journal of Bone and Joint Surgery - Series A*, 79(5), 707–714.
<http://doi.org/10.2106/00004623-199705000-00010>
- Jeffers, J. R. T., Browne, M., & Taylor, M. (2005). Damage accumulation, fatigue and creep behaviour of vacuum mixed bone cement. *Biomaterials*, 26(27), 5532–5541.
<http://doi.org/10.1016/j.biomaterials.2005.02.009>
- Jensen, C. L., Petersen, M. M., Schrøder, H. M., Flivik, G., & Lund, B. (2012). Revision Total Knee Arthroplasty With the Use of Trabecular Metal Cones. A Randomized Radiostereometric Analysis With 2 Years of Follow-Up. *Journal of Arthroplasty*, 27(10), 1820–1826.e2. <http://doi.org/10.1016/j.arth.2012.04.036>
- Julin, J., Jämsen, E., Puolakka, T., Konttinen, Y. T., & Moilanen, T. (2010). Younger age increases the risk of early prosthesis failure following primary total knee replacement for osteoarthritis: A follow-up study of 32,019 total knee replacements in the Finnish Arthroplasty Register. *Acta Orthopaedica*, 81(4), 413–419.
<http://doi.org/10.3109/17453674.2010.501747>

- Khan, M., Osman, K., Green, G., & Haddad, F. S. (2016). The epidemiology of failure in total knee arthroplasty. *Bone & Joint Journal*, 98–B(1 Supple A), 105–112.
<http://doi.org/10.1302/0301-620X.98B1.36293>
- Kim, D., Lim, J. Y., Shim, K. W., Han, J. W., Yi, S., Yoon, D. H., ... Shin, D. A. (2017). Sacral reconstruction with a 3D-printed implant after hemisacrectomy in a patient with sacral osteosarcoma: 1-year follow-up result. *Yonsei Medical Journal*, 58(2), 453–457.
<http://doi.org/10.3349/ymj.2017.58.2.453>
- Kimpton, C. I., Crocombe, A. D., Bradley, W. N., & Gavin Huw Owen, B. (2013). Analysis of stem tip pain in revision total knee arthroplasty. *Journal of Arthroplasty*, 28(6), 971–977.
<http://doi.org/10.1016/j.arth.2012.10.007>
- Kurtz, S. M., Ong, K. L., Lau, E., Widmer, M., Maravic, M., Gómez-Barrena, E., ... Röder, C. (2011). International survey of primary and revision total knee replacement. *International Orthopaedics*, 35(12), 1783–1789. <http://doi.org/10.1007/s00264-011-1235-5>
- Kurtz, S., Ong, K., Lau, E., Mowat, F., & Halpern, M. (2007). Projections of primary and revision hip and knee arthroplasty in the United States from 2005 to 2030. *Journal of Bone and Joint Surgery - Series A*, 89(4), 780–785. <http://doi.org/10.2106/JBJS.F.00222>
- Long, W. J., & Scuderi, G. R. (2009). Porous Tantalum Cones for Large Metaphyseal Tibial Defects in Revision Total Knee Arthroplasty. A Minimum 2-Year Follow-up. *Journal of Arthroplasty*, 24(7), 1086–1092. <http://doi.org/10.1016/j.arth.2008.08.011>
- Mann, K. A., Miller, M. A., Goodheart, J. R., Izant, T. H., & Cleary, R. J. (2014). Peri-implant bone strains and micro-motion following in vivo service: A postmortem retrieval study of 22 tibial components from total knee replacements. *Journal of Orthopaedic Research*, 32(3), 355–361. <http://doi.org/10.1002/jor.22534>
- Maradit Kremers, H., Larson, D. R., Crowson, C. S., Kremers, W. K., Washington, R. E., Steiner, C. A., ... Berry, D. J. (2015). Prevalence of Total Hip and Knee Replacement in the United States. *The Journal of Bone and Joint Surgery. American Volume*, 97(17), 1386–97. <http://doi.org/10.2106/JBJS.N.01141>

- Meneghini, R. M., Lewallen, D. G., & Hanssen, A. D. (2008). Use of porous tantalum metaphyseal cones for severe tibial bone loss during revision total knee replacement. *Journal of Bone and Joint Surgery - Series A*, 90(1), 78–84.
<http://doi.org/10.2106/JBJS.F.01495>
- Morgan-Jones, R., Oussedik, S. I. S., Graichen, H., & Haddad, F. S. (2015). Zonal fixation in revision total knee arthroplasty. *The Bone & Joint Journal*, 97–B(2), 147–149.
<http://doi.org/10.1302/0301-620X.97B2.34144>
- Panegrossi, G., Ceretti, M., Papalia, M., Casella, F., Favetti, F., & Falez, F. (2014). Bone loss management in total knee revision surgery. *International Orthopaedics*, 38(2), 419–427.
<http://doi.org/10.1007/s00264-013-2262-1>
- Park, E.-K., Lim, J.-Y., Yun, I.-S., Kim, J.-S., Woo, S.-H., Kim, D.-S., & Shim, K.-W. (2016). Cranioplasty Enhanced by Three-Dimensional Printing. *Journal of Craniofacial Surgery*, 27(4), 943–949. <http://doi.org/10.1097/SCS.0000000000002656>
- Peters, C. L., Mohr, R. A., Craig, M. A., & Bachus, K. N. (2001). Tibial component fixation with cement: full versus surface cementation techniques, 84132.
- Race, A., Miller, M. A., & Mann, K. A. (2010). Novel methods to study functional loading micromechanics at the stem-cement and cement-bone interface in cemented femoral hip replacements. *Journal of Biomechanics*, 43(4), 788–791.
<http://doi.org/10.1016/j.jbiomech.2009.10.021>
- Ranawat, V. S., Atkinson, H. D., & Paterson, R. S. (2012). Tibial Stem Tip Pain in Stemmed Revision Total Knee Arthroplasty. Treatment with Tension Band Plating. *Journal of Arthroplasty*, 27(8), 1580.e5-1580.e7. <http://doi.org/10.1016/j.arth.2011.12.032>
- Ro, D. H., Cho, Y., Lee, S., Chung, K. Y., Kim, S. H., Lee, Y. M., ... Lee, M. C. (2016). Extent of vertical cementing as a predictive factor for radiolucency in revision total knee arthroplasty. *Knee Surgery, Sports Traumatology, Arthroscopy*, 24(8), 2710–2717.
<http://doi.org/10.1007/s00167-016-4011-7>

- Ryd, L., Albrektsson, B. E., Carlsson, L., Dansgard, F., Herberts, P., Lindstrand, A., ... Toksvig-Larsen, S. (1995). Roentgen stereophotogrammetric analysis as a predictor of mechanical loosening of knee prostheses. *J Bone Joint Surg Br*, 77(3), 377–383. <http://doi.org/0301-620X/95/3974>
- Saleh, K. J., Macaulay, A., Radosevich, D. M., Clark, C. R., Engh, G., Gross, A., ... Windsor, R. (2001). The Knee Society Index of Severity for failed total knee arthroplasty: Practical application. *Clinical Orthopaedics and Related Research*, (392), 166–173. <http://doi.org/10.1097/00003086-200111000-00020>
- Schlegel, U. J., Bishop, N. E., Püschel, K., Morlock, M. M., & Nagel, K. (2014). Comparison of different cement application techniques for tibial component fixation in TKA. *International Orthopaedics*, 39(1), 47–54. <http://doi.org/10.1007/s00264-014-2468-x>
- Sheth, N. P., Bonadio, M. B., & Demange, M. K. (2017). Bone Loss in Revision Total Knee Arthroplasty. *Journal of the American Academy of Orthopaedic Surgeons*, 25(5), 348–357. <http://doi.org/10.5435/JAAOS-D-15-00660>
- Shinya, A., Ballo, A. M., Lassila, L. V. J., Shinya, A., Närhi, T. O., & Vallittu, P. K. (2011). Stress and Strain Analysis of the Bone-Implant Interface: A Comparison of Fiber-Reinforced Composite and Titanium Implants Utilizing 3-Dimensional Finite Element Study. *Journal of Oral Implantology*, 37(sp1), 133–140. <http://doi.org/10.1563/AAID-JOI-D-09-00046>
- Stryker. (2017). Simplex P Bone Cements. *Bone*, 5. Retrieved from www.stryker.com
- Tomlinson, M., & Harrison, M. (2012). The New Zealand Joint Registry. *Foot and Ankle Clinics*, 17(January 1999), 719–723. <http://doi.org/10.1016/j.fcl.2012.08.011>
- Udofia, I., Liu, F., Jin, Z., Roberts, P., & Grigoris, P. (2007). The initial stability and contact mechanics of a press-fit resurfacing arthroplasty of the hip. *Journal of Bone and Joint Surgery - British Volume*, 89-B(4), 549–556. <http://doi.org/10.1302/0301-620X.89B4.18055>

- Vanlommel, J., Luyckx, J. P., Labey, L., Innocenti, B., De Corte, R., & Bellemans, J. (2011). Cementing the Tibial Component in Total Knee Arthroplasty. Which Technique is the Best? *Journal of Arthroplasty*, 26(3), 492–496. <http://doi.org/10.1016/j.arth.2010.01.107>
- Whaley, A. L., Trousdale, R. T., Rand, J. A., & Hanssen, A. D. (2003). Cemented long-stem revision total knee arthroplasty. *Journal of Arthroplasty*, 18(5), 592–599. [http://doi.org/10.1016/S0883-5403\(03\)00200-6](http://doi.org/10.1016/S0883-5403(03)00200-6)
- Whiteside, L. A. (1998). Morselized allografting in revision total knee arthroplasty. *Orthopedics*, 21(9), 1041–3. Retrieved from <http://www.ncbi.nlm.nih.gov/pubmed/9769056>
- Whittaker, J. P., Dharmarajan, R., & Toms, A. D. (2008). The management of bone loss in revision total knee replacement. *Journal of Bone and Joint Surgery - British Volume*, 90–B(8), 981–987. <http://doi.org/10.1302/0301-620X.90B8.19948>
- Xu, N., Wei, F., Liu, X., Jiang, L., Cai, H., Li, Z., ... Liu, Z. (2016). Reconstruction of the Upper Cervical Spine Using a Personalized 3D-Printed Vertebral Body in an Adolescent With Ewing Sarcoma. *SPINE*, 41(1), E50–E54. <http://doi.org/10.1097/BRS.0000000000001179>
- Yuan, X., Broberg, J. S., Naudie, D. D., Holdsworth, D. W., & Teeter, M. G. (2018). Radiostereometric analysis using clinical radiographic views: Validation with model-based radiostereometric analysis for the knee. *Journal of Engineering in Medicine*, 232(8), 759–767. <http://doi.org/10.1177/0954411918785662>

CHAPTER 6

6 Conclusion

Overview: This chapter summarizes the main findings of the thesis and suggests future research that can be done related to this field of study.

6.1 Conclusion

In conclusion, the FARO Gage arm was compared to the digital image correlation system, the standard in bone-implant micromotion measurement tools. The FARO Gage arm had a low degree of correlation with the DIC and lacked accuracy and thus was not an adequate measurement system for bone-implant micromotion.

Primary TKA micromotion was examined and significantly greater implant subsidence was seen in the anterior and medial regions of the bone-implant interface.

Furthermore, the early fixation-stability of revision TKA with the novel 3D printed titanium augment is significantly better than the conventional fully cemented rTKA. The hybrid fixation achieved by the combination of the distal cemented stem and the press-fit of the porous/3D printed augment produced significantly less micromotion than the fully cemented rTKA stem. The early press-fit fixation of the augment is likely sufficient for promoting bony ingrowth of the augment in vivo.

6.2 Future Directions

Further research is needed to analyze, in detail, the magnitude and direction of bone-implant micromotion in other types of primary TKAs. This data would be helpful to see if there are pTKA implants that experience less micromotion and/or whether a common motion

tendency is experienced in all pTKA implants, which could be used as key information for improvements in pTKA design.

The next step in testing the novel 3D printed titanium revision augment would be to evaluate the early fixation-stability it can achieve with larger bone defects such as AORI II's and AORI III's. Future studies will also have to examine its osseointegrative capabilities in vivo and eventually determine if its long-term in vivo fixation is superior to the current standard of care.

Bibliography

- Abramson, S. B., & Attur, M. (2009). Developments in the scientific understanding of osteoarthritis. *Arthritis Research and Therapy*, *11*(3). <http://doi.org/10.1186/ar2655>
- Ackland, D. C., Robinson, D., Redhead, M., Lee, P. V. S., Moskaljuk, A., & Dimitroulis, G. (2017). A personalized 3D-printed prosthetic joint replacement for the human temporomandibular joint: From implant design to implantation. *Journal of the Mechanical Behavior of Biomedical Materials*, *69*(September 2016), 404–411. <http://doi.org/10.1016/j.jmbbm.2017.01.048>
- Ahmad, R., Patel, A., Mandalia, V., & Toms, A. (2016). Posterior Tibial Slope: Effect on, and Interaction with, Knee Kinematics. *JBJS Reviews*, *4*(4), e3–e3. <http://doi.org/10.2106/JBJS.RVW.O.00057>
- Alexander, G. E., Bernasek, T. L., Crank, R. L., & Haidukewych, G. J. (2013). Cementless Metaphyseal Sleeves Used for Large Tibial Defects in Revision Total Knee Arthroplasty. *Journal of Arthroplasty*, *28*(4), 604–607. <http://doi.org/10.1016/j.arth.2012.08.006>
- Almeida e Silva, J. S., Erdelt, K., Edelhoff, D., Araújo, É., Stimmelmayer, M., Vieira, L. C. C., & Güth, J. F. (2014). Marginal and internal fit of four-unit zirconia fixed dental prostheses based on digital and conventional impression techniques. *Clinical Oral Investigations*, *18*(2), 515–523. <http://doi.org/10.1007/s00784-013-0987-2>
- Aranda, J. L., Jiménez, M. F., Rodríguez, M., & Varela, G. (2017). Tridimensional titanium-printed custom-made prosthesis for sternocostal reconstruction. *European Journal of Cardio-Thoracic Surgery*, *48*(August 2015), e92-294. <http://doi.org/10.1093/ejcts/ezv265>
- Arden, N., & Nevitt, M. C. (2006). Osteoarthritis: Epidemiology. *Best Practice and Research: Clinical Rheumatology*, *20*(1), 3–25. <http://doi.org/10.1016/j.berh.2005.09.007>
- Arima, J., Whiteside, L. A., Martin, J. W., Miura, H., White, S. E., & McCarthy, D. S. (1998). Effect of partial release of the posterior cruciate ligament in total knee arthroplasty. *Clinical Orthopaedics and Related Research*, (353), 194–202. Retrieved from

<http://www.ncbi.nlm.nih.gov/pubmed/9728174>

Australian Orthopaedic Association. (2017). Australian Orthopaedic Association National Joint Replacement Registry; Hip, Knee & Shoulder Arthroplasty: Annual Report 2017. *National Joint Replacement Registry*, 1–380. Retrieved from <https://aoanjrr.sahmri.com/documents/10180/397736/Hip%2C Knee %26 Shoulder Arthroplasty>

Bagsby, D. T., Issa, K., Smith, L. S., Elmallah, R. K., Mast, L. E., Harwin, S. F., ... Malkani, A. L. (2016). Cemented vs Cementless Total Knee Arthroplasty in Morbidly Obese Patients. *Journal of Arthroplasty*, *31*(8), 1727–1731. <http://doi.org/10.1016/j.arth.2016.01.025>

Baker, P. N., Khaw, F. M., Kirk, L. M. G., Esler, C. N. A., & Gregg, P. J. (2007). A randomised controlled trial of cemented versus cementless press-fit condylar total knee replacement: 15-YEAR SURVIVAL ANALYSIS. *Journal of Bone and Joint Surgery - British Volume*, *89-B*(12), 1608–1614. <http://doi.org/10.1302/0301-620X.89B12.19363>

Barazanchi, A., Li, K. C., Hons, B., Al-amleh, B., Lyons, K., Waddell, J. N., & Denttech, M. (2017). Additive Technology : Update on Current Materials and Applications in Dentistry, *26*, 156–163. <http://doi.org/10.1111/jopr.12510>

Barnett, S. L., Mayer, R. R., Gondusky, J. S., Choi, L., Patel, J. J., & Gorab, R. S. (2014). Use of stepped porous titanium metaphyseal sleeves for tibial defects in revision total knee arthroplasty: Short term results. *Journal of Arthroplasty*, *29*(6), 1219–1224. <http://doi.org/10.1016/j.arth.2013.12.026>

Barrack, R. L., Stanley, T., Burt, M., & Hopkins, S. (2004). The effect of stem design on end-of-stem pain in revision total knee arthroplasty. *Journal of Arthroplasty*, *19*(7 SUPPL.), 119–124. <http://doi.org/10.1016/j.arth.2004.06.009>

Bauer, T. W., & Schils, J. (1999). The pathology of total joint arthroplasty. *Skeletal Radiology*, *28*, 483–497. <http://doi.org/10.1007/s002560050552>

Bauermeister, A. J., Zuriarrain, A., & Newman, M. I. (2016). Three-dimensional printing in

- plastic and reconstructive surgery a systematic review. *Annals of Plastic Surgery*, 77(5), 569–576. <http://doi.org/10.1097/SAP.0000000000000671>
- Beckmann, J., Lüring, C., Springorum, R., Köck, F. X., Grifka, J., & Tingart, M. (2011). Fixation of revision TKA: A review of the literature. *Knee Surgery, Sports Traumatology, Arthroscopy*, 19(6), 872–879. <http://doi.org/10.1007/s00167-010-1249-3>
- Bedson, J., & Croft, P. R. (2008). The discordance between clinical and radiographic knee osteoarthritis: A systematic search and summary of the literature. *BMC Musculoskeletal Disorders*, 9, 1–11. <http://doi.org/10.1186/1471-2474-9-116>
- Bellemans, J., Colyn, W., Vandenuecker, H., & Victor, J. (2012). Is Neutral Mechanical Alignment Normal for All Patients? The Concept of Constitutional Varus. *Clinical Orthopaedics and Related Research*, 470(1), 45–53. <http://doi.org/10.1007/s11999-011-1936-5>
- Bert, J. M., & Mcshane, M. (1998). Is It Necessary to Cement the Tibial Stem in Cemented Total Knee Arthroplasty ?, (356), 73–78.
- Bierma-Zeinstra, S. M. A., & Koes, B. W. (2007). Risk factors and prognostic factors of hip and knee osteoarthritis. *Nature Clinical Practice Rheumatology*, 3(2), 78–85. <http://doi.org/10.1038/ncprheum0423>
- Blasioli, D. J., & Kaplan, D. L. (2014). The Roles of Catabolic Factors in the Development of Osteoarthritis. *Tissue Engineering Part B: Reviews*, 20(4), 355–363. <http://doi.org/10.1089/ten.teb.2013.0377>
- Bole, M., Teeter, M., Lanting, B. A., & Howard, J. L. (2018). Correlation of tibial bone defect shape with patient demographics following total knee revision. *Journal of Orthopaedics*, 15(2), 490–494. <http://doi.org/10.1016/j.jor.2018.03.025>
- Brånemark, R., Brånemark, P.-I., Rydevik, B., & Myers, R. R. (2001). Osseointegration in skeletal reconstruction and rehabilitation. *J Rehabil Res Dev*, 38(2), 1–4.
- Brouwer, R., Huizinga, M., Duivenvoorden, T., van Raaij, T., Verhagen, A., Bierma-Zeinstra,

- S., & Verhaar, J. (2005). Osteotomy for treating knee osteoarthritis. *Cochrane Database of Systematic Reviews*, (1), CD004019. <http://doi.org/10.1002/14651858.CD004019.pub3>
- Canadian Institute for Health Information. (2015). Hip and Knee Replacements in Canada: Canadian Joint Replacement Registry 2015 Annual Report, (September), 1–63. Retrieved from https://se-cure.cihi.ca/free_products/CJRR_2015_Annual_Report_EN.pdf
- Cavanaugh, P. K., Mounts, T., & Vaccaro, A. R. (2015). Use of 3-Dimensional Printing in Spine Care. *Contemporary Spine Surgery*, 16(1), 1–6.
- Cawley, D. T., Kelly, N., Simpkin, A., Shannon, F. J., & McGarry, J. P. (2012). Full and surface tibial cementation in total knee arthroplasty: A biomechanical investigation of stress distribution and remodeling in the tibia. *Clinical Biomechanics*, 27(4), 390–397. <http://doi.org/10.1016/j.clinbiomech.2011.10.011>
- Chambers, I. R., Fender, D., McCaskie, A. W., Reeves, B. C., & Gregg, P. J. (2001). Radiological features predictive of aseptic loosening in cemented Charnley femoral stems. *The Journal of Bone and Joint Surgery. British Volume*, 83(6), 838–42. <http://doi.org/10.1302/0301-620x.83b6.11659>
- Chen, X., Xu, L., Wang, Y., Hao, Y., & Wang, L. (2015). Image-guided installation of 3D-printed patient-specific implant and its application in pelvic tumor resection and reconstruction surgery, 5, 66–78.
- Cherian, J., Bhave, A., Harwin, S., & Mont, M. (2016). Outcomes and Aseptic Survivorship of Revision Total Knee Arthroplasty. *The American Journal of Orthopedics*, 45((2)), 79–85.
- Cherian, J. J., Kapadia, B. H., Banerjee, S., Jauregui, J. J., Issa, K., & Mont, M. A. (2014). Mechanical, anatomical, and kinematic axis in TKA: Concepts and practical applications. *Current Reviews in Musculoskeletal Medicine*, 7(2), 89–95. <http://doi.org/10.1007/s12178-014-9218-y>
- Chong, D. Y. R., Hansen, U. N., & Amis, A. A. (2010). Analysis of bone-prosthesis interface micromotion for cementless tibial prosthesis fixation and the influence of loading conditions. *Journal of Biomechanics*, 43(6), 1074–1080.

<http://doi.org/10.1016/j.jbiomech.2009.12.006>

- Conlisk, N., Howie, C. R., & Pankaj, P. (2018). Quantification of interfacial motions following primary and revision total knee arthroplasty: A verification study versus experimental data. *Journal of Orthopaedic Research*, 36(1), 387–396. <http://doi.org/10.1002/jor.23653>
- Crause, L. a., O'Donoghue, D. E., O'Connor, J. E., & Strümpfer, F. (2010). Use of a Faro Arm for optical alignment, 7739(July 2010), 77392S. <http://doi.org/10.1117/12.856810>
- Daines, B. k, & Dennis, D. A. (2012). Management of Bone Defects in Revision Total Knee Arthroplasty. *Journal of Bone and Joint Surgery American*, 94(March 2013), 1131–1139.
- De Martino, I., De Santis, V., Sculco, P. K., D'Apolito, R., Assini, J. B., & Gasparini, G. (2015). Tantalum Cones Provide Durable Mid-term Fixation in Revision TKA. *Clinical Orthopaedics and Related Research*, 473(10), 3176–3182. <http://doi.org/10.1007/s11999-015-4338-2>
- Dennis, D. A., Berry, D. J., Engh, G., Fehring, T., Macdonald, S. J., Rosenberg, A. G., & Scuderi, G. (2008). Revision Total Knee Arthroplasty. *Journal of the American Academy of Orthopaedic Surgeons*, 16(8), 442–454.
- DiSilvestro, M. R., Sherman, J. T., & Dietz, T. L. (2004). A new position measurement system for micro-measurements in orthopaedics. *Conference Proceedings : ... Annual International Conference of the IEEE Engineering in Medicine and Biology Society. IEEE Engineering in Medicine and Biology Society. Conference*, 4, 2438–2441. <http://doi.org/10.1109/IEMBS.2004.1403705>
- Drake, R., Vogl, A., & Mitchell, A. (Eds.). (2015). *Gray's Anatomy for Students* (3rd Editio). Philadelphia: Churchill Livingstone, Elsevier.
- Efe, T., Figiel, J., Sibbert, D., Fuchs-Winkelmann, S., Tibesku, C. O., Timmesfeld, N., ... Skwara, a. (2011). Revision of tibial TKA components: bone loss is independent of cementing type and technique: an in vitro cadaver study. *BMC Musculoskelet Disord*, 12, 6. <http://doi.org/10.1186/1471-2474-12-6>

- Egloff, C., Hügle, T., & Valderrabano, V. (2012). Biomechanics and pathomechanisms of osteoarthritis. *Swiss Medical Weekly*, *142*(JULY), 1–14.
<http://doi.org/10.4414/smw.2012.13583>
- Eitner, U., Köntges, M., & Brendel, R. (2010). Use of digital image correlation technique to determine thermomechanical deformations in photovoltaic laminates: Measurements and accuracy. *Solar Energy Materials and Solar Cells*, *94*(8), 1346–1351.
<http://doi.org/10.1016/j.solmat.2010.03.028>
- Eskandari, H. (1993). *Bone-Prosthesis interface relative displacement of the knee tibial component: Finite element analysis and measurement.*
- Fan, H., Fu, J., Li, X., Pei, Y., Li, X., Pei, G., & Guo, Z. (2015). Implantation of customized 3-D printed titanium prosthesis in limb salvage surgery : a case series and review of the literature. *World Journal of Surgical Oncology*, *13*(308), 1–10.
<http://doi.org/10.1186/s12957-015-0723-2>
- Favre, P., Perala, S., Vogel, P., Fucntese, S. F., Goff, J. R., Gerber, C., & Snedeker, J. G. (2011). In vitro assessments of reverse glenoid stability using displacement gages are misleading - Recommendations for accurate measurements of interface micromotion. *Clinical Biomechanics*, *26*(9), 917–922. <http://doi.org/10.1016/j.clinbiomech.2011.05.002>
- Favre, P., Seebeck, J., Thistlethwaite, P. A. E., Obrist, M., Steffens, J. G., Hopkins, A. R., & Hulme, P. A. (2016). In vitro initial stability of a stemless humeral implant. *Clinical Biomechanics*, *32*, 113–117. <http://doi.org/10.1016/j.clinbiomech.2015.12.004>
- Fehring, T. K., & Griffin, W. L. (1998). Revision of failed cementless total knee implants with cement. *Clinical Orthopaedics and Related Research*, (356), 34–38.
<http://doi.org/10.1097/00003086-199811000-00007>
- Franchi, M., Fini, M., Martini, D., Orsini, E., Leonardi, L., Ruggeri, A., ... Ottani, V. (2005). Biological fixation of endosseous implants. *Micron*, *36*(7–8), 665–671.
<http://doi.org/10.1016/j.micron.2005.05.010>
- Gandhi, R., Tsvetkov, D., Davey, J. R., & Mahomed, N. N. (2009). Survival and clinical

function of cemented and uncemented prostheses in total knee replacement: A META-ANALYSIS. *Journal of Bone and Joint Surgery - British Volume*, 91–B(7), 889–895.
<http://doi.org/10.1302/0301-620X.91B7.21702>

Glenn, J. C., Sokoloski, S. N., Damer, B. M., & Tabit, J. M. (2010). Tibia pain at end of stem With stemmed revision total knee arthroplasty. Treatment with cortical strut graft technique. *Journal of Arthroplasty*, 25(3), 497.e1-497.e5.
<http://doi.org/10.1016/j.arth.2009.02.020>

Goldring, M. B., & Marcu, K. B. (2009). Cartilage homeostasis in health and rheumatic diseases. *Arthritis Research and Therapy*, 11(3). <http://doi.org/10.1186/ar2592>

Goodheart, J. R., Miller, M. A., & Mann, K. A. (2014). In vivo loss of cement-bone interlock reduces fixation strength in total knee arthroplasties. *Journal of Orthopaedic Research*, 32(8), 1052–1060. <http://doi.org/10.1002/jor.22634>

Guccione, A., Felson, D., Anderson, J. J., Anthony, J. M., Zhang, Y., Wilson, P. W. F., ... Kannel, W. B. (1994). The Effects of Specific Medical Conditions on the Functional Limitations of Elders in the Framingham Study. *American Journal of Public Health*, 85, 351–358.

Haidukewych, G. J., Hanssen, A. D., & Jones, R. (2011). Metaphyseal Fixation in Revision Total Knee Arthroplasty: Indications and Techniques. *J Am Acad Orthop Surg*, 19(6), 311–318.

Hamid, K. S., Parekh, S. G., & Adams, S. B. (2016). Salvage of Severe Foot and Ankle Trauma With a 3D Printed Scaffold. *Foot & Ankle International*, 37(4), 433 –439.
<http://doi.org/10.1177/1071100715620895>

Hatamleh, M. M., Bhamrah, G., Ryba, F., Mack, G., & Huppa, C. (2016). Simultaneous Computer-Aided Design/Computer-Aided Manufacture Bimaxillary Orthognathic Surgery and Mandibular Reconstruction Using Selective-Laser Sintered Titanium Implant. *Journal of Craniofacial Surgery*, 27(7), 1810–1814.
<http://doi.org/10.1097/SCS.0000000000003039>

- Helmy, N., Dao Trong, M. L., & Kühnel, S. P. (2014). Accuracy of Patient Specific Cutting Blocks in Total Knee Arthroplasty. *BioMed Research International*, 2014(October 2009). <http://doi.org/10.1155/2014/562919>
- Hirschmann, M. T., & Müller, W. (2015). Complex function of the knee joint: the current understanding of the knee. *Knee Surgery, Sports Traumatology, Arthroscopy*, 23(10), 2780–2788. <http://doi.org/10.1007/s00167-015-3619-3>
- Hoang, D., Perrault, D., Stevanovic, M., & Ghiassi, A. (2016). Surgical applications of three-dimensional printing : a review of the current literature & how to get started, 4(23). <http://doi.org/10.21037/atm.2016.12.18>
- Hood, B., Blum, L., Holcombe, S. A., Wang, S. C., Urquhart, A. G., Goulet, J. A., & Maratt, J. D. (2017). Variation in Optimal Sagittal Alignment of the Femoral Component in Total Knee Arthroplasty. *Orthopedics*, 40(2), 102–106. <http://doi.org/10.3928/01477447-20161108-04>
- Hosein, Y. K. (2013). *The Effect of Stem Surface Treatment and Substrate Material on Joint Replacement Stability: An In-Vitro Investigation into the Stem-Cement Interface Mechanics under Various Loading Modes*. Retrieved from <http://ir.lib.uwo.ca/etd/1479>
- Hsu, A., & Ellington, J. K. (2015). Evolving Techniques } 3-Dimensional Printed Titanium Truss Cage With Tibiotalocalcaneal Arthrodesis for Salvage of Persistent Distal Tibia Nonunion. *Foot & Ankle Specialist*, 8(6), 483–489. <http://doi.org/10.1177/1938640015593079>.
- Hungerford, D. S., & Krackow, K. A. (1985). Total Joint Arthroplasty of the Knee. *Clinical Orthopaedics and Related Research*, 192, 23–33. <http://doi.org/10.1097/00003086-198501000-00004>
- Imanishi, J., & Choong, P. F. M. (2015). CASE REPORT – OPEN ACCESS International Journal of Surgery Case Reports Three-dimensional printed calcaneal prosthesis following total CASE REPORT – OPEN ACCESS. *International Journal of Surgery Case Reports*, 10, 83–87. <http://doi.org/10.1016/j.ijscr.2015.02.037>

- Insall, J., Hood, R., Flawn, L., & Sullivan, D. (1983). The total condylar knee prosthesis in gonarthrosis. A five to nine-year follow-up of the first one hundred consecutive replacements. *J Bone Joint Surg*, *65-A*, 619–628. <http://doi.org/10.1302/0301-620X.96B7.33946>
- Iseki, Y., Takahashi, T., Takeda, H., Tsuboi, I., Imai, H., Mashima, N., ... Yamamoto, H. (2009). Defining the load bearing axis of the lower extremity obtained from anterior-posterior digital radiographs of the whole limb in stance. *Osteoarthritis and Cartilage*, *17*(5), 586–591. <http://doi.org/10.1016/j.joca.2008.10.001>
- Jacobs, W. C. H., Clement, D. J., & Wymenga, A. B. (2005). Retention versus removal of the posterior cruciate ligament in total knee replacement: a systematic literature review within the Cochrane framework. *Acta Orthopaedica*, *76*(6), 757–768. <http://doi.org/10.1080/17453670510045345>
- Jasty, M., Bragdon, C., Burke, D., O'Connor, D., Lowenstein, J., & Harris, W. H. (1997). In vivo skeletal responses to porous-surfaced implants subjected to small induced motions. *Journal of Bone and Joint Surgery - Series A*, *79*(5), 707–714. <http://doi.org/10.2106/00004623-199705000-00010>
- Jeffers, J. R. T., Browne, M., & Taylor, M. (2005). Damage accumulation, fatigue and creep behaviour of vacuum mixed bone cement. *Biomaterials*, *26*(27), 5532–5541. <http://doi.org/10.1016/j.biomaterials.2005.02.009>
- Jensen, C. L., Petersen, M. M., Schrøder, H. M., Flivik, G., & Lund, B. (2012). Revision Total Knee Arthroplasty With the Use of Trabecular Metal Cones. A Randomized Radiostereometric Analysis With 2 Years of Follow-Up. *Journal of Arthroplasty*, *27*(10), 1820–1826.e2. <http://doi.org/10.1016/j.arth.2012.04.036>
- Jevsevar, D. (2013). AAOS Clinical Guideline Summary: Treatment of Osteoarthritis of the Knee: Evidence-Based Guideline, 2nd Edition. *J Am Acad Orthop Surg*, *21*(9), 571–576.
- Julin, J., Jämsen, E., Puolakka, T., Konttinen, Y. T., & Moilanen, T. (2010). Younger age increases the risk of early prosthesis failure following primary total knee replacement for

- osteoarthritis: A follow-up study of 32,019 total knee replacements in the Finnish Arthroplasty Register. *Acta Orthopaedica*, 81(4), 413–419.
<http://doi.org/10.3109/17453674.2010.501747>
- Khan, M., Osman, K., Green, G., & Haddad, F. S. (2016). The epidemiology of failure in total knee arthroplasty. *Bone & Joint Journal*, 98–B(1 Supple A), 105–112.
<http://doi.org/10.1302/0301-620X.98B1.36293>
- Khan, W. S., Rayan, F., Dhinsa, B. S., & Marsh, D. (2012). An osteoconductive, osteoinductive, and osteogenic tissue-engineered product for trauma and orthopaedic surgery: How far are we? *Stem Cells International*, 2012.
<http://doi.org/10.1155/2012/236231>
- Kharb, A., Saini, V., Jain, Y., & Dhiman, S. (2011). A review of gait cycle and its parameters. *IJCEM Int J Comput Eng Manag*, 13(July), 78–83. http://doi.org/10.1007/3-540-49384-0_1
- Kim, D., Lim, J. Y., Shim, K. W., Han, J. W., Yi, S., Yoon, D. H., ... Shin, D. A. (2017). Sacral reconstruction with a 3D-printed implant after hemisacrectomy in a patient with sacral osteosarcoma: 1-year follow-up result. *Yonsei Medical Journal*, 58(2), 453–457.
<http://doi.org/10.3349/ymj.2017.58.2.453>
- Kim, G. B., Lee, S., Kim, H., Yang, D. H., Kim, Y., Kyung, Y. S., & Kim, C. (2016). Three-Dimensional Printing : Basic Principles and Applications in Medicine and Radiology, 17(2), 182–197.
- Kimpton, C. I., Crocombe, A. D., Bradley, W. N., & Gavin Huw Owen, B. (2013). Analysis of stem tip pain in revision total knee arthroplasty. *Journal of Arthroplasty*, 28(6), 971–977.
<http://doi.org/10.1016/j.arth.2012.10.007>
- Kirkley, A., Birmingham, T., Litchfield, R., Giffin, R., Willits, K., Wong, C., ... Fowler, P. (2017). A Randomized Trial of Arthroscopic Surgery for. *New England Journal of Medicine*, 359(11), 1097–1107. <http://doi.org/10.1056/NEJMoa1602615>
- Kurtz, S. M., Ong, K. L., Lau, E., Widmer, M., Maravic, M., Gómez-Barrena, E., ... Röder, C.

- (2011). International survey of primary and revision total knee replacement. *International Orthopaedics*, 35(12), 1783–1789. <http://doi.org/10.1007/s00264-011-1235-5>
- Kurtz, S., Ong, K., Lau, E., Mowat, F., & Halpern, M. (2007). Projections of primary and revision hip and knee arthroplasty in the United States from 2005 to 2030. *Journal of Bone and Joint Surgery - Series A*, 89(4), 780–785. <http://doi.org/10.2106/JBJS.F.00222>
- Laupattarakasem, W., Laopaiboon, M., Laupattarakasem, P., & Sumananont, C. (2008). Arthroscopic debridement for knee osteoarthritis. *Cochrane Database of Systematic Reviews*, (1). <http://doi.org/10.1002/14651858.CD005118.pub2>
- Lee, S. M., Seong, S. C., Lee, S., Choi, W. C., & Lee, M. C. (2012). Outcomes of the different types of total knee arthroplasty with the identical femoral geometry. *Knee Surgery & Related Research*, 24(4), 214–20. <http://doi.org/10.5792/ksrr.2012.24.4.214>
- Lee, U. L., Kwon, J. S., Woo, S. H., & Choi, Y. J. (2016). Simultaneous Bimaxillary Surgery and Mandibular Reconstruction With a 3-Dimensional Printed Titanium Implant Fabricated by Electron Beam Melting: A Preliminary Mechanical Testing of the Printed Mandible. *Journal of Oral and Maxillofacial Surgery*, 74(7), 1501.e1-1501.e15. <http://doi.org/10.1016/j.joms.2016.02.031>
- Leighton, R., Fitzpatrick, J., Smith, H., Crandall, D., Flannery, C. R., & Conrozier, T. (2018). Systematic clinical evidence review of NASHA (Durolane hyaluronic acid) for the treatment of knee osteoarthritis. *Open Access Rheumatology: Research and Reviews*, Volume 10, 43–54. <http://doi.org/10.2147/OARRR.S162127>
- Leiser, Y., Shilo, A. D., & Wolff, A. A. (2016). Functional Reconstruction in Mandibular Avulsion Injuries, 27(8), 2113–2116. <http://doi.org/10.1097/SCS.00000000000003104>
- Leopold, S. S. (2009). Minimally Invasive Total Knee Arthroplasty for Osteoarthritis. *New England Journal of Medicine*, 360(17), 1749–1758. <http://doi.org/10.1056/NEJMct0806027>
- Li, H., Qu, X., Mao, Y., Dai, K., & Zhu, Z. (2016). Custom Acetabular Cages Offer Stable Fixation and Improved Hip Scores for Revision THA With Severe Bone Defects. *Clinical*

Orthopaedics and Related Research, 474(3), 731–740. <http://doi.org/10.1007/s11999-015-4587-0>

Li, X., Wang, Y., Zhao, Y., Liu, J., Xiao, S., & Mao, K. (2017). Multi-level 3D printing implant for reconstructing cervical spine with metastatic papillary thyroid carcinoma. *SPINE*, (May), 1.

Liang, H., Ji, T., Zhang, Y., Wang, Y., & Guo, W. (2017). Reconstruction with 3D-printed pelvic endoprostheses after resection of a pelvic tumour. *Bone and Joint Journal*, 99–B(2), 267–275. <http://doi.org/10.1302/0301620X.99B2.BJJ20160654.R1>

Logan, L., Hickman, R., Harris, S., & Heriza, C. (2008). Review research design : recommendations for levels of evidence and quality rating. *Developmental Medicine & Child Neurology* 2008, 50, 99–103. <http://doi.org/10.1111/j.1469-8749.2007.02005.x>

Long, W. J., & Scuderi, G. R. (2009). Porous Tantalum Cones for Large Metaphyseal Tibial Defects in Revision Total Knee Arthroplasty. A Minimum 2-Year Follow-up. *Journal of Arthroplasty*, 24(7), 1086–1092. <http://doi.org/10.1016/j.arth.2008.08.011>

Loughlin, J. (2005). The genetic epidemiology of human primary osteoarthritis: Current status. *Expert Reviews in Molecular Medicine*, 7(9), 1–12. <http://doi.org/10.1017/S1462399405009257>

Luring, C., Perlick, L., Trepte, C., Linhardt, O., Perlick, C., Plitz, W., & Grifka, J. (2006). Micromotion in cemented rotating platform total knee arthroplasty: Cemented tibial stem versus hybrid fixation. *Archives of Orthopaedic and Trauma Surgery*, 126(1), 45–48. <http://doi.org/10.1007/s00402-005-0082-5>

Macdonald, K. V., Sanmartin, C., Langlois, K., & Marshall, D. A. (2014). Symptom onset , diagnosis and management of osteoarthritis, 25(9), 10–17.

Man, G. S., & Mologhianu, G. (2014). Osteoarthritis pathogenesis - a complex process that involves the entire joint. *Journal of Medicine and Life*, 7(1), 37–41. Retrieved from [/pmc/articles/PMC3956093/?report=abstract](http://pmc/articles/PMC3956093/?report=abstract)

- Mann, K. A., Miller, M. A., Goodheart, J. R., Izant, T. H., & Cleary, R. J. (2014). Peri-implant bone strains and micro-motion following in vivo service: A postmortem retrieval study of 22 tibial components from total knee replacements. *Journal of Orthopaedic Research*, 32(3), 355–361. <http://doi.org/10.1002/jor.22534>
- Mao, Y., Xu, C., Xu, J., Li, H., Liu, F., Yu, D., & Zhu, Z. (2015). The use of customized cages in revision total hip arthroplasty for Paprosky type III acetabular bone defects. *International Orthopaedics*, 39(10), 2023–2030. <http://doi.org/10.1007/s00264-015-2965-6>
- Maradit Kremers, H., Larson, D. R., Crowson, C. S., Kremers, W. K., Washington, R. E., Steiner, C. A., ... Berry, D. J. (2015). Prevalence of Total Hip and Knee Replacement in the United States. *The Journal of Bone and Joint Surgery. American Volume*, 97(17), 1386–97. <http://doi.org/10.2106/JBJS.N.01141>
- Martelli, S. (2003). New method for simultaneous anatomical and functional studies of articular joints and its application to the human knee. *Computer Methods and Programs in Biomedicine*, 70(3), 223–240. [http://doi.org/10.1016/S0169-2607\(02\)00028-7](http://doi.org/10.1016/S0169-2607(02)00028-7)
- Masouros, S. D., Bull, A. M. J., & Amis, A. A. (2010). (i) Biomechanics of the knee joint. *Orthopaedics and Trauma*, 24(2), 84–91. <http://doi.org/10.1016/j.mporth.2010.03.005>
- McCalden, R. W., Robert, C. E., Howard, J. L., Naudie, D. D., McAuley, J. P., & MacDonald, S. J. (2013). Comparison of outcomes and survivorship between patients of different age groups following TKA. *Journal of Arthroplasty*, 28(8 SUPPL), 83–86. <http://doi.org/10.1016/j.arth.2013.03.034>
- Meftah, M., White, P. B., Ranawat, A. S., & Ranawat, C. S. (2016). Long-term results of total knee arthroplasty in young and active patients with posterior stabilized design. *Knee*, 23(2), 318–321. <http://doi.org/10.1016/j.knee.2015.10.008>
- Meneghini, R. M., Lewallen, D. G., & Hanssen, A. D. (2008). Use of porous tantalum metaphyseal cones for severe tibial bone loss during revision total knee replacement. *Journal of Bone and Joint Surgery - Series A*, 90(1), 78–84.

<http://doi.org/10.2106/JBJS.F.01495>

Mihalko, W. M. (2013). *Campbell's Operative Orthopaedics*. (S. Canale & J. Beaty, Eds.) (12th ed.). Philadelphia: Elsevier. <http://doi.org/10.1177/003591573102400728>

Mobbs, R. J., Coughlan, M., Thompson, R., Sutterlin, C. E., & Phan, K. (2017). The utility of 3D printing for surgical planning and patient-specific implant design for complex spinal pathologies: case report. *Journal of Neurosurgery: Spine*, *26*(4), 513–518.
<http://doi.org/10.3171/2016.9.SPINE16371>

Moiduddin, K., Al-Ahmari, A., Kindi, M. Al, Nasr, E. S. A., Mohammad, A., & Ramalingam, S. (2016). Customized porous implants by additive manufacturing for zygomatic reconstruction. *Biocybernetics and Biomedical Engineering*, *36*(4), 719–730.
<http://doi.org/10.1016/j.bbe.2016.07.005>

Morgan-Jones, R., Oussedik, S. I. S., Graichen, H., & Haddad, F. S. (2015). Zonal fixation in revision total knee arthroplasty. *The Bone & Joint Journal*, *97-B*(2), 147–149.
<http://doi.org/10.1302/0301-620X.97B2.34144>

Morgan, H., Battista, V., & Leopold, S. S. (2005). Constraint in Primary Total Knee Arthroplasty. *J Am Acad Orthop Surg*, *13*(8), 515–524.

Murphy, L., Schwartz, T. A., Helmick, C. G., Renner, J. B., Tudor, G., Koch, G., ... Jordan, J. M. (2015). Lifetime Risk of Symptomatic Knee Osteoarthritis. *Arthritis Rheum.*, *59*(9), 1207–1213. <http://doi.org/10.1002/art.24021.Lifetime>

Nilsson, K. G., Kärrholm, J., Carlsson, L., & Dalén, T. (1999). Hydroxyapatite coating versus cemented fixation of the tibial component in total knee arthroplasty: prospective randomized comparison of hydroxyapatite-coated and cemented tibial components with 5-year follow-up using radiostereometry. *The Journal of Arthroplasty*, *14*(1), 9–20.
[http://doi.org/10.1016/S0883-5403\(99\)90196-1](http://doi.org/10.1016/S0883-5403(99)90196-1)

Panegrossi, G., Ceretti, M., Papalia, M., Casella, F., Favetti, F., & Falez, F. (2014). Bone loss management in total knee revision surgery. *International Orthopaedics*, *38*(2), 419–427.
<http://doi.org/10.1007/s00264-013-2262-1>

- Park, E.-K., Lim, J.-Y., Yun, I.-S., Kim, J.-S., Woo, S.-H., Kim, D.-S., & Shim, K.-W. (2016). Cranioplasty Enhanced by Three-Dimensional Printing. *Journal of Craniofacial Surgery*, 27(4), 943–949. <http://doi.org/10.1097/SCS.0000000000002656>
- Park, J. B. (1992). Orthopedic prosthesis fixation. *Annals of Biomedical Engineering*, 20(6), 583–594. <http://doi.org/10.1007/BF02368607>
- Pereira, D., Ramos, E., & Branco, J. (2015). Osteoarthritis. *Acta Médica Portuguesa*, 28(1), 99–106.
- Peters, C. L., Mohr, R. A., Craig, M. A., & Bachus, K. N. (2001). Tibial component fixation with cement: full versus surface cementation techniques, 84132.
- Phan, K., Sgro, A., Maharaj, M. M., D’Urso, P., & Mobbs, R. J. (2016). Application of a 3D custom printed patient specific spinal implant for C1/2 arthrodesis. *Journal of Spine Surgery (Hong Kong)*, 2(4), 314–318. <http://doi.org/10.21037/jss.2016.12.06>
- Prabhakar, P., Sames, W. J., Dehoff, R., & Babu, S. S. (2015). Computational modeling of residual stress formation during the electron beam melting process for Inconel 718. *Additive Manufacturing*, 7, 83–91. <http://doi.org/10.1016/j.addma.2015.03.003>
- Quilez, M. P., Seral, B., & Pérez, M. A. (2017). Biomechanical evaluation of tibial bone adaptation after revision total knee arthroplasty: A comparison of different implant systems. *PLoS ONE*, 12(9), 1–14. <http://doi.org/10.1371/journal.pone.0184361>
- Race, A., Miller, M. A., & Mann, K. A. (2010). Novel methods to study functional loading micromechanics at the stem-cement and cement-bone interface in cemented femoral hip replacements. *Journal of Biomechanics*, 43(4), 788–791. <http://doi.org/10.1016/j.jbiomech.2009.10.021>
- Ranawat, V. S., Atkinson, H. D., & Paterson, R. S. (2012). Tibial Stem Tip Pain in Stemmed Revision Total Knee Arthroplasty. Treatment with Tension Band Plating. *Journal of Arthroplasty*, 27(8), 1580.e5-1580.e7. <http://doi.org/10.1016/j.arth.2011.12.032>
- Ritter, M. A., Davis, K. E., Meding, J. B., Pierson, J. L., Berend, M. E., & Malinzak, R. A.

- (2011). The Effect of Alignment and EMI on Failure of Total Knee Replacement, 1588–1596.
- Ro, D. H., Cho, Y., Lee, S., Chung, K. Y., Kim, S. H., Lee, Y. M., ... Lee, M. C. (2016). Extent of vertical cementing as a predictive factor for radiolucency in revision total knee arthroplasty. *Knee Surgery, Sports Traumatology, Arthroscopy*, 24(8), 2710–2717. <http://doi.org/10.1007/s00167-016-4011-7>
- Rohling, R., Munger, P., Hollerbach, J. M., & Peters, T. (1995). Comparison of relative accuracy between a mechanical and an optical position tracker for image-guided neurosurgery. *Computer Aided Surgery*, 1(1), 30–34. <http://doi.org/10.3109/10929089509106823>
- Ryd, L., Albrektsson, B. E., Carlsson, L., Dansgard, F., Herberts, P., Lindstrand, A., ... Toksvig-Larsen, S. (1995). Roentgen stereophotogrammetric analysis as a predictor of mechanical loosening of knee prostheses. *J Bone Joint Surg Br*, 77(3), 377–383. <http://doi.org/0301-620X/95/3974>
- Saleh, K. J., Macaulay, A., Radosevich, D. M., Clark, C. R., Engh, G., Gross, A., ... Windsor, R. (2001). The Knee Society Index of Severity for failed total knee arthroplasty: Practical application. *Clinical Orthopaedics and Related Research*, (392), 166–173. <http://doi.org/10.1097/00003086-200111000-00020>
- Samiezadeh, S., Bougherara, H., Abolghasemian, M., D’Lima, D., & Backstein, D. (2018). Rotating hinge knee causes lower bone–implant interface stress compared to constrained condylar knee replacement. *Knee Surgery, Sports Traumatology, Arthroscopy*, 0(0), 0. <http://doi.org/10.1007/s00167-018-5054-8>
- Schlegel, U. J., Bishop, N. E., Püschel, K., Morlock, M. M., & Nagel, K. (2014). Comparison of different cement application techniques for tibial component fixation in TKA. *International Orthopaedics*, 39(1), 47–54. <http://doi.org/10.1007/s00264-014-2468-x>
- Shan, X. F., Chen, H. M., Liang, J., Huang, J. W., & Cai, Z. G. (2015). Surgical Reconstruction of Maxillary and Mandibular Defects Using a Printed Titanium Mesh. *Journal of Oral and*

Maxillofacial Surgery, 73(7), 1437.e1-1437.e9. <http://doi.org/10.1016/j.joms.2015.02.025>

Sheth, N. P., Bonadio, M. B., & Demange, M. K. (2017). Bone Loss in Revision Total Knee Arthroplasty. *Journal of the American Academy of Orthopaedic Surgeons*, 25(5), 348–357. <http://doi.org/10.5435/JAAOS-D-15-00660>

Shinya, A., Ballo, A. M., Lassila, L. V. J., Shinya, A., Närhi, T. O., & Vallittu, P. K. (2011). Stress and Strain Analysis of the Bone-Implant Interface: A Comparison of Fiber-Reinforced Composite and Titanium Implants Utilizing 3-Dimensional Finite Element Study. *Journal of Oral Implantology*, 37(sp1), 133–140. <http://doi.org/10.1563/AAID-JOI-D-09-00046>

Simoneau, C., Terriault, P., Jetté, B., Dumas, M., & Brailovski, V. (2017). Development of a porous metallic femoral stem: Design, manufacturing, simulation and mechanical testing. *Materials and Design*, 114, 546–556. <http://doi.org/10.1016/j.matdes.2016.10.064>

Skwara, A., Figiel, J., Knott, T., Paletta, J. R. J., Fuchs-Winkelmann, S., & Tibesku, C. O. (2009). Primary stability of tibial components in TKA: In vitro comparison of two cementing techniques. *Knee Surgery, Sports Traumatology, Arthroscopy*, 17(10), 1199–1205. <http://doi.org/10.1007/s00167-009-0849-2>

Small, S. R., Rogge, R. D., Malinzak, R. A., Reyes, E. M., Cook, P. L., Farley, K. A., & Ritter, M. A. (2016). Micromotion at the tibial plateau in primary and revision total knee arthroplasty: fixed versus rotating platform designs. *Bone and Joint Research*, 5(4), 122–129. <http://doi.org/10.1302/2046-3758.54.2000481>

Smith, K. E., Dupont, K. M., Safranski, D. L., Blair, J. W., Buratti, D. R., Zeetser, V., ... Gall, K. (2016). Use of 3D printed bone plate in novel technique to surgically correct hallux valgus deformities. *Techniques in Orthopaedics*, 31(3), 181–189. <http://doi.org/10.1097/BTO.0000000000000189>

Stoffelen, D. V. C., Eraly, K., & Debeer, P. (2015). The use of 3D printing technology in reconstruction of a severe glenoid defect : a case report with 2 . 5 years of follow-up. *Journal of Shoulder and Elbow Surgery*, 24(8), e218–e222.

<http://doi.org/10.1016/j.jse.2015.04.006>

- Stoor, P., Suomalainen, A., Mesimäki, K., & Kontio, R. (2017). Rapid prototyped patient specific guiding implants in critical mandibular reconstruction. *Journal of Cranio-Maxillo-Facial Surgery*, *45*, 63–70. <http://doi.org/10.1016/j.jcms.2016.10.021>
- Stryker. (2017). Simplex P Bone Cements. *Bone*, *5*. Retrieved from www.stryker.com
- Tack, P., Victor, J., Gemmel, P., & Annemans, L. (2016). 3D - printing techniques in a medical setting : a systematic literature review, 1–21. <http://doi.org/10.1186/s12938-016-0236-4>
- Taniguchi, N., Fujibayashi, S., Takemoto, M., Sasaki, K., Otsuki, B., Nakamura, T., ... Matsuda, S. (2016). Effect of pore size on bone ingrowth into porous titanium implants fabricated by additive manufacturing: An in vivo experiment. *Materials Science and Engineering C*, *59*, 690–701. <http://doi.org/10.1016/j.msec.2015.10.069>
- Technologies, F. (2014). CAM2 ® SmartInspect Basic v1.2 FaroArm/FARO Gage Training Workbook.
- Tomlinson, M., & Harrison, M. (2012). The New Zealand Joint Registry. *Foot and Ankle Clinics*, *17*(January 1999), 719–723. <http://doi.org/10.1016/j.fcl.2012.08.011>
- Udofia, I., Liu, F., Jin, Z., Roberts, P., & Grigoris, P. (2007). The initial stability and contact mechanics of a press-fit resurfacing arthroplasty of the hip. *Journal of Bone and Joint Surgery - British Volume*, *89-B*(4), 549–556. <http://doi.org/10.1302/0301-620X.89B4.18055>
- Vandekerckhove, P. J. T. K., Matlovich, N., Teeter, M. G., MacDonald, S. J., Howard, J. L., & Lanting, B. A. (2017). The relationship between constitutional alignment and varus osteoarthritis of the knee. *Knee Surgery, Sports Traumatology, Arthroscopy*, *25*(9), 2873–2879. <http://doi.org/10.1007/s00167-016-3994-4>
- Vanlommel, J., Luyckx, J. P., Labey, L., Innocenti, B., De Corte, R., & Bellemans, J. (2011). Cementing the Tibial Component in Total Knee Arthroplasty. Which Technique is the Best? *Journal of Arthroplasty*, *26*(3), 492–496. <http://doi.org/10.1016/j.arth.2010.01.107>

- Viera, A. J., & Garrett, J. M. (2005). Understanding Interobserver Agreement : The Kappa Statistic. *Family Medicine*, 37(5), 360–363.
- Wang, L., Cao, T., Li, X., & Huang, L. (2016). Three-dimensional printing titanium ribs for complex reconstruction after extensive posterolateral chest wall resection in lung cancer. *Journal of Thoracic and Cardiovascular Surgery*, 152(1), e5–e7.
<http://doi.org/10.1016/j.jtcvs.2016.02.064>
- Wang, X., Xu, S., Zhou, S., Xu, W., Leary, M., Choong, P., ... Min, Y. (2016). Biomaterials Topological design and additive manufacturing of porous metals for bone scaffolds and orthopaedic implants : A review. *Biomaterials*, 83, 127–141.
<http://doi.org/10.1016/j.biomaterials.2016.01.012>
- Wei, R., Guo, W., Ji, T., Zhang, Y., & Liang, H. (2017). One-step reconstruction with a 3D-printed, custom-made prosthesis after total en bloc sacrectomy: a technical note. *European Spine Journal*, 26(7), 1902–1909. <http://doi.org/10.1007/s00586-016-4871-z>
- Whaley, A. L., Trousdale, R. T., Rand, J. A., & Hanssen, A. D. (2003). Cemented long-stem revision total knee arthroplasty. *Journal of Arthroplasty*, 18(5), 592–599.
[http://doi.org/10.1016/S0883-5403\(03\)00200-6](http://doi.org/10.1016/S0883-5403(03)00200-6)
- Whiteside, L. A. (1998). Morselized allografting in revision total knee arthroplasty. *Orthopedics*, 21(9), 1041–3. Retrieved from
<http://www.ncbi.nlm.nih.gov/pubmed/9769056>
- Whittaker, J. P., Dharmarajan, R., & Toms, A. D. (2008a). The management of bone loss in revision total knee replacement. *The Journal of Bone and Joint Surgery*, 90(8), 981–987.
<http://doi.org/10.1302/0301-620X.90B8.19948>
- Whittaker, J. P., Dharmarajan, R., & Toms, A. D. (2008b). The management of bone loss in revision total knee replacement. *Journal of Bone and Joint Surgery - British Volume*, 90–B(8), 981–987. <http://doi.org/10.1302/0301-620X.90B8.19948>
- Wong, I., Hiemstra, L., Ayeni, O. R., Getgood, A., Beavis, C., Volesky, M., ... MacDonald, P. B. (2018). Position Statement of the Arthroscopy Association of Canada (AAC)

Concerning Arthroscopy of the Knee Joint—September 2017. *Orthopaedic Journal of Sports Medicine*, 6(2), 1–4. <http://doi.org/10.1177/2325967118756597>

Wong, K. C., Kumta, S. M., Geel, N. V., & Demol, J. (2015). One-step reconstruction with a 3D-printed, biomechanically evaluated custom implant after complex pelvic tumor resection. *Computer Aided Surgery*, 20(1), 14–23. <http://doi.org/10.3109/10929088.2015.1076039>

Xie, F., Thumboo, J., & Li, S. C. (2007). True Difference or Something Else? Problems in Cost of Osteoarthritis Studies. *Seminars in Arthritis and Rheumatism*, 37(2), 127–132. <http://doi.org/10.1016/j.semarthrit.2007.01.001>

Xie, H., & Kang, Y. (2014). Digital image correlation technique. *Optics and Lasers in Engineering*, 65, 1–2. <http://doi.org/10.1016/j.optlaseng.2014.07.010>

Xu, N., Wei, F., Liu, X., Jiang, L., Cai, H., Li, Z., ... Liu, Z. (2016). Reconstruction of the Upper Cervical Spine Using a Personalized 3D-Printed Vertebral Body in an Adolescent With Ewing Sarcoma. *SPINE*, 41(1), E50–E54. <http://doi.org/10.1097/BRS.0000000000001179>

Yuan, X., Broberg, J. S., Naudie, D. D., Holdsworth, D. W., & Teeter, M. G. (2018). Radiostereometric analysis using clinical radiographic views: Validation with model-based radiostereometric analysis for the knee. *Journal of Engineering in Medicine*, 232(8), 759–767. <http://doi.org/10.1177/0954411918785662>

Zampagni, M. L., Dona, G., Motta, M., Martelli, S., Benelli, P., & Marcacci, M. (2006). a New Method for Anthropometric Acquisition of the Upper Extremity Parameters in Elite Master Swimmers. *Journal of Mechanics in Medicine and Biology*, 06(01), 1–11. <http://doi.org/10.1142/S0219519406001741>

Zhang, W., Nuki, G., Moskowitz, R. W., Abramson, S., Altman, R. D., Arden, N. K., ... Tugwell, P. (2010). OARSI recommendations for the management of hip and knee osteoarthritis. Part III: Changes in evidence following systematic cumulative update of research published through January 2009. *Osteoarthritis and Cartilage*, 18(4), 476–499.

<http://doi.org/10.1016/j.joca.2010.01.013>

Zingde, S. M., & Slamin, J. (2017). Biomechanics of the knee joint, as they relate to arthroplasty. *Orthopaedics and Trauma*, 31(1), 1–7.

<http://doi.org/10.1016/j.mporth.2016.10.001>

Appendices

Appendix 1. REB approval

LAWSON APPROVAL

LAWSON APPROVAL NUMBER: R-18-261

PROJECT TITLE: A novel approach to revision TKA using 3D printed titanium implants:
A biomechanical cadaveric study

PRINCIPAL INVESTIGATOR: Dr. Brent Lanting

LAWSON APPROVAL DATE: Tuesday, 15 May 2018

ReDA ID: 4590

Overall Study Status: Active

Please be advised the above project was reviewed by Lawson Administration and the project was approved. Your official approval document can be found in the documents section of your study in ReDA.

Appendix 2. Chapter 2 Search Strategy

Table A2. Search Strategy based on individual bibliographical databases

	OVID Medline	OVID Embase	Scopus	CINAHL	Cochrane
1	3D printing.mp. or Printing, Three-Dimensional/	3D printing.mp. or Printing, Three-Dimensional/	(3D printing) OR	S1"3d printing" OR (MH "Printing, Three-Dimensional")	3D printing
2	Bioprinting.mp. or Bioprinting/	Bioprinting.mp. or Bioprinting/	(additive manufacturing) AND	S2(MH "Printing, Three-Dimensional") OR "additive manufacturing"	additive manufacturing
3	3D printed.mp.	3D printed.mp.	(implant) AND	S3"3d bioprinting"	implant
4	custom printing.mp.	custom printing.mp.	(plastic OR	S4"implant"	insert
6	additive manufacturing.mp.	additive manufacturing.mp.	(neurology or Otorhinolaryngology or spine) AND	S5"insert"	graft
7	stereoscopic printing.mp.	stereoscopic printing.mp.	(surgery) AND (LIMIT-TO (SUBJAREA,"MED I")))	S6"graft"	prosthesis
8	implant.mp. or Bone Transplantation/ or "Prostheses and Implants"/	implant.mp. or Bone Transplantation/ or "Prostheses and Implants"/	(LIMIT-TO (LANGUAGE,"English") OR LIMIT-TO (LANGUAGE,"French"	S7(MH "Prostheses and Implants") OR "prostheses and implants"	musculoskeletal
9	implantation.mp.	implantation.mp.		S8(MH "Musculoskeletal System") OR "musculoskeletal"	bone
10	insert.mp.	insert.mp.		S9(MH "Joints") OR (MH "Bone and Bones")	joint
11	graft.mp. or Transplants/	graft.mp. or Transplants/		S10(MH "Arthroplasty") OR "arthroplasty" OR (MH "Arthroplasty, Replacement")	articulation
12	prosthesis.mp.	prosthesis.mp.		S11"reconstruction" OR (MH "American Society of Plastic Surgical Nurses")	surgery
13	musculoskeletal.mp. or Musculoskeletal System/	musculoskeletal.mp. or Musculoskeletal System/		S12(MH "Orthopedic Surgery") OR (MH "Surgery, Otorhinolaryngologic") OR "orthopaedic surgery"	orthopaedic surgery
14	bone.mp. or "Bone and Bones"/	bone.mp. or "Bone and Bones"/		S13(MH "Surgery, Plastic") OR "plastic surgery"	plastic surgery
15	joint.mp. or Joints/	joint.mp. or Joints/		S14(MH "Neurosurgery") OR "neurosurgery"	maxillofacial surgery

16	articulation.mp.	articulation.mp.	h "))	S1 OR S2 OR S3	neurosurgery
17	Orthopedics/ or Arthroplasty, Replacement, Hip/ or orthopaedic surgery.mp. or Orthopedic Procedures/	Orthopedics/ or Arthroplasty, Replacement, Hip/ or orthopaedic surgery.mp. or Orthopedic Procedures/		S4 OR S5 OR S6 OR S7	#1 or #2
18	plastic surgery.mp. or Surgery, Plastic/	plastic surgery.mp. or Surgery, Plastic/		S8 OR S9 OR S10 OR S11 OR S12 OR S13 OR S14 OR S15 OR S16 OR S17	#3 or #4 or #5 or #6
19	reconstructive surgery.mp. or Reconstructive Surgical Procedures/	reconstructive surgery.mp. or Reconstructive Surgical Procedures/		S18 AND S19 AND	#7 or #8 or #9 or #10
20	joint replacement.mp. or Arthroplasty, Replacement/	joint replacement.mp. or Arthroplasty, Replacement/		S1"3d printing" OR (MH "Printing, Three-Dimensional")	#18 and #11
21	Surgery, Oral/ or oromaxillofacial surgery.mp.	Surgery, Oral/ or oromaxillofacial surgery.mp.		S2(MH "Printing, Three-Dimensional") OR "additive manufacturing"	#12 or #13 or 14 or #15
22	Oral Surgical Procedures/ or dental surgery.mp.	Oral Surgical Procedures/ or dental surgery.mp.			#19 or #20
23	Neurosurgical Procedures/ or cranial surgery.mp. or Skull/	Neurosurgical Procedures/ or cranial surgery.mp. or Skull/			
24	neurosurgery.mp. or Neurosurgery/	neurosurgery.mp. or Neurosurgery/			
25	otorhinolaryngology.mp. or Otolaryngology/	otorhinolaryngology.mp. or Otolaryngology/			
26	ear nose throat surgery.mp. or Otorhinolaryngologic Diseases/ or Otorhinolaryngologic Surgical Procedures/	ear nose throat surgery.mp. or Otorhinolaryngologic Diseases/ or Otorhinolaryngologic Surgical Procedures/			
27	ENT.mp.	ENT.mp.			
28	Spinal Diseases/ or spine surgery.mp.	Spinal Diseases/ or spine surgery.mp.			
29	surgery/ or surgery.mp.	surgery/ or surgery.mp.			
30	1 or 2 or 3 or 4 or 5 or 6	1 or 2 or 3 or 4 or 5 or 6			
31	7 or 8 or 9 or 10 or 11	7 or 8 or 9 or 10 or 11			
32	12 or 13 or 14 or 15	12 or 13 or 14 or 15			
33	28 and 31	28 and 31			

34	16 or 17 or 18 or 19 or 20 or 21 or 22 or 23 or 24 or 25 or 26 or 27 or 32	16 or 17 or 18 or 19 or 20 or 21 or 22 or 23 or 24 or 25 or 26 or 27 or 32			
-----------	--	--	--	--	--

Appendix 3. Chapter 2 Article Summary

Table 3.1 Summary of spine articles

Authors	Indication for Surgical Procedure	Surgical Outcomes	Complications
Li et al.	Reconstruction of bone defects (Excision of C2-4 Papillary thyroid carcinoma)	<ul style="list-style-type: none"> – 11/17 on the Japanese Orthopedic Association scale – X-rays and CT revealed no implant displacement or subsidence at the 12-month follow-up 	none
Xu et al.	Reconstruction of bone defects (Excision of C2 Ewing sarcoma)	<ul style="list-style-type: none"> – Walking on postoperative day 7 – Normal neurovascular exam 	none
Phan et al.	Decompression and fusion of nerve impingement (C1-C2 spinal fusion)	<ul style="list-style-type: none"> – Significant reduction in occipital neuralgia and sub-occipital pain – Reduced operative time in comparison to standard decompression/fusion 	none
Mobbs et al.	Reconstruction of bone defects (Excision of C1-2 chordoma/ lumbar congenital spinal defect, L5 hemivertebra)	<ul style="list-style-type: none"> – Successful C1-2 fusion – Facilitated the surgery and shortened the procedure time, – Eliminates the need for rib or fibular grafts (less complication/ pain) 	none
Kim et al.	Reconstruction of bone defects (Excision of sacral osteosarcoma - hemisacrectomy)	<ul style="list-style-type: none"> – Postoperative pain was minimal and the patient recovered sufficiently – Walking at 2 weeks postoperatively. – CT at 1-year follow-up showed excellent bony fusion – No rectal sphincter tone loss 	Expected foot drop (part of excision)
Wei et al.	Reconstruction of bone defects (Excision of sacral chordoma – en bloc sacrectomy)	<ul style="list-style-type: none"> – CT showed some new bone formation around the prosthesis–ilium interface – Spinopelvic joint stable – Osseointegration achieved 	Two fractured screws in bilateral ilia, no functional effect

Table 3.2. Summary of pelvis/hip articles

Authors	Indication for Surgical Procedure	Surgical Outcomes	Complications
Liang et al.	Reconstruction of bone defects (Excision of pelvic tumour, 11 osteosarcoma, 9 chondrosarcoma, 6 Ewing sarcoma, 9 other)	<ul style="list-style-type: none"> - Mean Musculoskeletal Tumour Society 93 (MSTS-93) score was 22.7 (20 to 25) for patients with iliac prosthesis - MSTS-93 of 19.8 (15 to 26) for those with a standard prosthesis - MSTS-93 of 17.7 (9 to 25) for those with a screwrod connected prosthesis 	<ul style="list-style-type: none"> - 7 delayed wound healing - 2 hip dislocations
Li et al.	Reconstruction of bone defects (Massive acetabular bone defects during revision THA)	<ul style="list-style-type: none"> - Mean Harris hip score improved from 36 +/- 8 to 82 +/- 18 (p< 0.001). - Reliable restoration of the hip center. - No re-revisions - None of the cups showed radiographic migration, but one cage was believed to be loose, based on a circumferential 2-mm radiolucent line. 	<ul style="list-style-type: none"> - 1 deep infection and 1 superficial infection - 1 hip dislocation - 1 suspected injury of the superior gluteal nerve (large exposure)
Wong et al.	Reconstruction of bone defects (Excision of left pelvis chondrosarcoma - partial acetabular resection)	<ul style="list-style-type: none"> - Precise tumor margin excision - Adequate reduction in stress shielding (FEA) 	<ul style="list-style-type: none"> - 2 months to plan, not appropriate for fast growing tumors
Chen et al.	Reconstruction of bone defects (Excision of right pelvis sarcoma)	<ul style="list-style-type: none"> - Increased precision of the tumor resection and implant installation with the use of navigation 	<ul style="list-style-type: none"> - none

Table 3.3. Summary of hand and upper limbs articles

Authors	Indication for Surgical Procedure	Surgical Outcomes	Complications
Fan et al.	Reconstruction of bone defects (Excision of clavicle Ewing's sarcoma, scapular ES, pelvic chondrosarcoma)	<ul style="list-style-type: none"> - MSTS 93 scores were 93, 73, and 90 % in patients with clavicle ES, scapular ES, and pelvic CS - Satisfactory shoulder ROM - No recurrences of tumor - No limb length discrepancy, screw loosening, implant breakage or joint collapse 	<ul style="list-style-type: none"> - none
Stoffelen et al.	Reconstruction of bone defects (Total shoulder replacement with severe glenoid bone loss requiring revision total shoulder replacement)	<ul style="list-style-type: none"> - Constant score had improved to 51 points. (pre-op 37) at 2.5 year follow up. - Shoulder Pain and Disability Index and shortened Disabilities of the Arm, Shoulder, and Hand score improved to 28% and 40.9 	<ul style="list-style-type: none"> - none

Table 3.4. Summary of foot and ankle articles

Authors	Indication for Surgical Procedure	Surgical Outcomes	Complications
Hsu et al.	Reconstruction of bone defects (Limb salvage with 3D Printed Titanium Truss Cage and Tibiotalocalcaneal Arthrodesis)	<ul style="list-style-type: none"> – Stable alignment and ankle fusion at 5 months – Minimal pain at 1 year follow up – Return to ADLs 	none
Smith et al.	Realignment (Hallux valgus/ MT primus varus with Fast Forward procedure/ 3D printed low profile tethering plate)	<ul style="list-style-type: none"> – Comparable, and in some instances superior, fatigue strength compared with traditional plate manufacturing methods. – Hallux valgus angle and Intermetatarsal angle corrected 	none
Imanishi et al.	Reconstruction of bone defects (Total calcaneotomy and calcaneus replacement for Right calcaneus chondrosarcoma)	<ul style="list-style-type: none"> – Pain free and walking unsupported on bare feet. – American Orthopaedic Foot and Ankle Society (AOFAS) Ankle–Hindfoot Scale score of 82 	none
Hamid et al.	Reconstruction of bone defects (Severe bone defect from open distal intra-articular tibial fracture requiring arthrodesis/ limb salvage)	<ul style="list-style-type: none"> – Pain-free with a visual analog score of 0 of 10 for pain. – Successful bone incorporation of the talus, calcaneus, and 3 of 4 cortices of the tibia on CT 	none

Table 3.5. Summary of skull articles

Authors	Indication for Surgical Procedure	Surgical Outcomes	Complications
Park et al.	Reconstruction of bone defects (Head trauma with partial craniectomy)	<ul style="list-style-type: none"> – Good fixation of titanium implants and satisfactory skull-shape symmetry on CT/ physical exam 	Skin flap infection
Ackland et al.	Joint replacement (TMJ Osteoarthritis)	<ul style="list-style-type: none"> – Normal jaw opening distance (40.0 mm) 	none
Leiser et al.	Osteosynthesis (Maxillofacial trauma/ comminution of mandible)	<ul style="list-style-type: none"> – Normal mouth opening of 40 mm and complete anteroposterior and lateral mandibular movements – Good functional and aesthetic results. – Proper lower facial height was achieved 	none

Hatamleh et al.	Osteosynthesis (Maxillofacial trauma in childhood/ mandibular defect requiring osteotomy and ORIF)	– The patient was pleased with his improved appearance	none
Shan et al.	Reconstruction of bone defects (Excision of 2 mandibular osteosarcoma, and 2 maxilla ossifying fibroma)	– Good reproducibility of procedure, less than 2 mm deviation for maxilla – 1-mm-thick 3D printed individualized titanium mesh was strong enough to restore the zygomaticomaxillary buttress	none
Stoor et al.	Reconstruction of bone defects (Excision of mandible due to squamous cell carcinoma (10), ameloblastoma (3) or drug induced osteonecrosis (1))	– Obtained symmetry and continuity of the mandibular border	Perforation of lingual mucosa
Lee et al.	Reconstruction of bone defects (Tumour removed during childhood)	– Mandibular opening was 38 mm, and the patient has had no problems with food consumption – Symmetrical face – 3D printed mandible had adequate strength that would withstand bite force	none

Table 3.6. Summary of thorax articles

Authors	Indication for Surgical Procedure	Surgical Outcomes	Complications
Wang et al.	Reconstruction of bone defects (Excision of non-small cell lung cancer with rib defect)	– Stable reconstruction, with preservation of thoracic morphology on CT – Excellent cosmetic results	none
Aranda et al.	Reconstruction of bone defects (Excision of para-sternal sarcoma/ liposarcoma)	– Stable reconstruction, with preservation of thoracic morphology on CT – Excellent cosmetic results	none

Curriculum Vitae

NAME: Charles-Antoine Dion

EDUCATION:

2015 - 2020 Orthopaedic Surgery Residency, Western University, London, ON
2017 - 2018 Master of Science in Surgery (Candidate), Western University, London, ON
2011 – 2015 Doctor of Medicine, University of Ottawa, Ottawa, ON
2008- 2011 Honours BSc. in Human Kinetics, University of Ottawa, Ottawa, ON

ACADEMIC HIGHLIGHTS AND ACHIEVEMENTS:

2018 W. Bailey Resident Teaching Award (2nd consecutive year), London, ON
2018 Top Orthopaedic Resident Teacher, 2017-2018 academic year, London, ON.
2017 W. Bailey Resident Teaching Award, London, ON
2016 James Roth Award for best orthopaedic poster presentation, London, ON
2016 Licentiate of the Medical Council of Canada
2015 AHC Interprofessional Champion Award, Academic Health Council, ON
2013 Dr. J. MacGregor Steele and Dr. John M. Steele Scholarship
2013 Medical Student Scholarship, University of Ottawa, ON
2012 CHEO Paediatric Surgery Scholarship
2012 John F. Seely Scholarship
2012 Recognition of Academic Excellence, University of Ottawa, ON
2011 Volunteer Youth Award, Ottawa, ON
2011 NSERC Undergraduate Student Research Award
2011 Médéric Montpetit Award, University of Ottawa, ON
2011 Undergraduate Research Opportunity Program Scholarship, Ottawa, ON
2009 - 2011 Dean's Honour List, University of Ottawa, ON
2008 - 2011 Bryistol-Myers Squibb Canada Scholarship (\$8000)
2008 - 2011 President's Scholarship, University of Ottawa, ON (\$30,000)

RESEARCH PUBLICATIONS:

- 2018 Podium Presentation
8th World Congress of Biomechanics, Dublin, Ireland.
Revision total knee arthroplasty using a novel 3D printed titanium augment: A biomechanical cadaveric study.
- 2018 Podium Presentation
Canadian Bone and Joint Conference, London, ON
Revision total knee arthroplasty using a novel 3D printed titanium augment: A biomechanical cadaveric study
- 2018 Poster Presentation
COA/ CORA, Victoria, BC
Surgical outcomes of 3D printed musculoskeletal metal implants: A systematic review
- 2018 Podium Presentation
COA/ CORA, Victoria, BC
Does recession of the posterior cruciate ligament influence outcome in total knee arthroplasty?
- 2017 E-Poster Presentation
92e Congrès de la Société Française de Chirurgie Orthopédique et Traumatologique (SOFECOT), Paris, France
La résection du ligament croisé postérieur influence-t-elle les résultats cliniques lors d'arthroplastie totale du genou?
- 2017 Podium Presentation
Resident Research Day, London, ON
Surgical outcomes of 3D printed musculoskeletal metal implants: A

systematic review

- 2010 Poster Presentation
UROF Research Symposium, Ottawa, ON (2010)
Improving the non-invasive monitoring of core temperature in infants during elective surgeries.

RESEARCH PRESENTATIONS:

- 2018 **Dion, C.**, Pollock, M., Howard, J. Somerville, L., Lanting, B. (2018). Surgical outcomes of 3D printed musculoskeletal metal implants: A systematic review. Submitted to the *Journal of Musculoskeletal Research (JMR)*.
- 2016 Chen, S., Roffey, D., **Dion, C.**, Arab, A., & Wai, E. (2016). Effect of Perioperative Vitamin C Supplementation on Postoperative Pain and the Incidence of Chronic Regional Pain Syndrome: A Systematic Review and Meta-Analysis. *The Clinical Journal of Pain*, 32(2), 179-185. doi:10.1097/AJP.0000000000000218

PROFESSIONAL DEVELOPMENT AND ADDITIONAL TRAINING:

- 2017 AAHKS Resident Course, Dallas, TX
- 2017 AO Advanced Principles of Fracture Management, Toronto, ON
- 2017 AO Basic Principles of Fracture Management, Chicago, IL
- 2016 Licentiate of the Medical Council of Canada
- 2016 Resident Teacher Bootcamp – nominated by program director, London, ON
- 2016 Surgical Foundations/ Principles of Surgery, London, ON
- 2015 Advanced Trauma Life Support, London, ON
- 2015 Advanced Cardiac Life Support, London, ON
- 2014 Canadian Conference on Medical Education (CCME), Ottawa, ON
- 2013 PPL - Private Pilot License (C-150, C-172, Fuel injected, Night Rating)
- 2013 Restricted Radio Operator's License
- 2013 PADI Advanced Open Water Diver
- 2012 Canadian Sport Parachuting Association – Solo certified skydiver

- 2010 National Lifeguard Service Award – Pool and Waterfront
- 2007 Canadian Ski Instructor Alliance – Freestyle & Level 1
- 2007 Pleasure Craft Operator License

COMMUNITY INVOLVEMENT AND CONTRIBUTIONS TO THE FACULTY:

- 2018 PARO General Council Representative
- 2018 London Executive ePractice Committee Member
- 2018 Surgical Anatomy Teacher – 4th year medical students
- 2018 Resident Mentor – Western Surgery Interest Group Mentorship Program
- 2018 Skeleton Crew – Fanshawe Dragon Boat Festival Competitor
- 2017-2018 Hip Hip Hooray! Pedometer Challenge - Western Orthopaedic Chair
- 2016-2018 Western T-OSCE examiner for medical students
- 2017 - 2018 Teaching to Teach Instructor
- 2016 - 2018 Surgical Foundations Instructor
- 2015 - 2017 Transition to Residency Teacher
- 2015 Academic Health Council Representative
- 2015 Donor Emissary Representative
- 2011-2013 Anatomy and Interprofessional Interest Group Coordinator

LANGUAGES:

English and French (spoken and written)